R-8490

FINAL REPORT

REACTIVE STREAM SEPARATION PHOTOGRAPHY

Rocketdyne
North American Rockwell

6633 Canoga Avenue
Canoga Park, California 91304

R-8490

FINAL REPORT

REACTIVE STREAM SEPARATION PHOTOGRAPHY

By

W. H. Nurick
J. D. Cordill

Prepared For

National Aeronautics & Space Administration
Jet Propulsion Laboratory
Pasadena, California

Contract NAS7-720

Technical Management
National Aeronautics & Space Administration
Jet Propulsion Laboratory
Pasadena, California
J. H. Rupe

Rocketdyne
A Division of North American Rockwell Corporation
6633 Canoga Avenue, Canoga Park, California

FOREWORD

This report was prepared in compliance with NASA-JPL Contract NAS7-720 entitled "Reactive Stream Separation Photography". J. H. Rupe, Jet Propulsion Laboratory, was Project Manager. The Rocketdyne Program Manager was Mr. T. A. Coultas. The technical approach of the program was guided and directed by Mr. S. D. Clapp, and Dr. D. T. Campbell.

ABSTRACT

High-speed photographic techniques were used to study impinging streams of N_2O_4/N_2H_4; N_2O_4/50-50, IRFNA/UDMH, and ClF_5/N_2H_4 propellants in an experimental investigation of reactive stream separation. The high-resolution color motion pictures obtained show the detailed behavior of the liquid streams, spray fan, and individual droplets within the combustion zone. It was found that when reactive streams meet and form a spray fan, they may be cyclically and vigorously blown apart by a disturbance which could be a detonation or explosive deflagration, and then reform. This phenomenon was found to occur with N_2O_4/N_2H_4, N_2O_4/50-50 and IRFNA/UDMH, differing in average explosion strength according to the propellant combination. Cyclic blowapart frequencies and magnitudes were determined at variable impinging stream dynamic pressure ratio. and jet diameters. Streak movies were also taken to determine the velocity and point of initiation of the disturbance. With the propellants ClF_5/N_2H_4 no cyclic blowapart ("popping") was encountered, but rather a continuous stream separation was observed. By manipulation of orifice sizes and dynamic pressure ratio these latter propellants were made to form a mixed, or non-separated spray fan.

CONTENTS

ILLUSTRATIONS

TABLES

SUMMARY

The results of this study show conclusively that the blowapart processes are cyclical and sequentially consists of: (1) propellant "mixing" in a spray fan, (2) apparent detonation or explosive deflagration of the spray immediately downstream of stream impingement, (3) violent separation (blowapart) of the individual propellant streams, and (4) recovery of the stream impingement. As intended, the program test conditions spanned operation from "mixed" to significantly "separated" conditions. The presence of burning spray droplets was clearly shown in all regions photographed.

The cyclic blowapart process described in these results appears more likely to be responsible for "reactive stream separation" than any quasi-steady lamination within the spray fan for hydrazine NTO propellant types. The latter process, as inferred from still photographs, has been generally accepted by previous investigators. Some suggestion of color lamination along the edge of the spray fan was seen (in the present program) between incidence of blowapart. The scale of this lamination, if real, was relatively small and its quantitative significance is questionable. On the other hand, for the ClF_5/N_2H_4 combination, a distinct continuous separation was observed. This phenomenon was observed with both 0.173-inch and 0.030-inch orifice diameters, but was eliminated at the smaller orifice size by operation at high (~1.6) dynamic pressure ratio.

The experimental procedures used in the program provided an excellent description of the spray field characteristics and afford an established experimental technique for further studies of the "blowapart" phenomenon.

The propellant combinations used were N_2O_4/N_2H_4, N_2O_4/50-50 (N_2H_4-UDMH), IRFNA/N_2H_4 and ClF_5/N_2H_4. The primary program objective was to photographically describe the impingement process under both "mixing" and "stream separation" conditions. Secondary goals included documentation

of the presence of propellant spray droplets in selected regions for comparison with existing holographic data and identification of individual droplet composition by color. In addition to propellant combination, test variables included chamber pressure, jet dynamic pressure ratio, orifice diameters, injection velocities, and impingement angle.

Single element unlike-doublet injectors with orifice diameters of 0.030, 0.072, and 0.173 inch were tested with varying injection velocities with the N_2O_4/N_2H_4 propellant combination. Using a 0.173-inch orifice, tests were conducted at atmospheric and ~200 psia chamber pressure using N_2O_4/50-50 propellants. One test series was conducted at atmospheric pressure with ClF_5/N_2H_4 propellants using 0.030 and 0.173-inch orifice injectors. For the 0.030-inch tests the dynamic pressure ratio of the impinging jets was varied. Most of the other tests conducted in this study were at or near a unity dynamic pressure ratio. In order to avoid uncertainties due to variable jet hydraulic effects, smooth, long (100 L/D) orifice injection tubes were used for all tests. Both still and high-speed camera coverage were employed with special lighting and photographic techniques designed for observation of the jet and spray behavior within the combustion field. A specially modified streak camera was used to measure the speed and point of initiation of the disturbance.

Several summary descriptive comments may be made about the cyclic disturbance observed: (1) with the exception of ClF_5/N_2H_4, all propellants evaluated experienced some degree of cyclic blowapart; (2) the strong and moderate strength explosions, which visibly consume all parts of the spray, originated very close to the impingement point and seemed to propagate initially with equal force in all directions; (3) a weaker type blowapart originated approximately 1-inch downstream of the impingement point, appearing largely as a puff of dense oxidizer vapor leaving the spray-field; (4) audible popping sounds were heard only with the strong class of blowapart; (5) the disturbances do not occur at regular or periodic

intervals, that is, recorded frequencies are time averaged values; (6) as observed with N_2O_4/50-50, there was no significant change in the type or frequency of cyclic blowapart upon operation at elevated pressure (200 psia).

INTRODUCTION

Current injector design technology for unlike impinging liquid propellant rockets is predominantly based upon knowledge of propellant mixing acquired from cold-flow tests with propellant simulants. To the extent that real propellants behave in the same manner as the nonreactive liquids, rational design may be accomplished in a manner which provides both efficient combustion and compatibility with the thrust chamber and nozzle materials. As first reported (1959) by Elverum and Standhammer at JPL (Ref. 1), however, impinging hypergolic liquid streams may, under certain conditions, tend to separate or be blown apart rather than achieving the intended degree of mixing. These effects were observed, specifically, with the N_2O_4/N_2H_4 propellant system. Continued JPL experimental investigation by Johnson, Riebling, et al. (Ref. 2 through 7), of injecting impinging jets or sheets of N_2O_4 and N_2H_4 in baffled, or divided chambers, confirmed Elverum's photographic indication of fuel/oxidizer stratification. By auxiliary injection of fuel and oxidizer downstream of the chamber divider, performance changes could be used to monitor the presence of unmixed propellants from the main injection element. This work showed that the incidence of separation was dependent upon orifice sizes; mixing was obtained with the smaller streams; but separation occurred with jets larger than about 0.040 to 0.060 inch.

Since 1966, continued and expanded interest in "blowapart" or "reactive stream separation," as it has alternately been called, is evidenced by both in-house and contractual work by NASA-JPL, NASA-Lewis Research Center, and by the Air Force (AFRPL). Most of the experimental methods have involved photography. These include Burrow's study of an impinging-quadlet N_2O_4/N_2H_4 injector (Ref. 8), several investigations by Dynamic Science (Ref. 9 and 10) and in-house work at Rocketdyne (Ref. 11). Current alternate methods for study of reactive stream separation include use by Houseman (Ref. 12) of a probe to obtain samples for an on-line mass spectrometer.

Kushida and Houseman (Ref. 14) made a first attempt to develop an analytical model to predict that separation would or would not occur. This model included two regimes, depending upon the pressure of the environment. At low to moderate pressures, separation was presumed to result from liquid/liquid interfacial reaction and was thus dependent upon a "residence time" as indexed by the jet diameter divided by the injection velocity (D/V) and upon the propellant injection temperature. At some higher pressure, the value of which depended upon D/V, a gas phase reaction was presumed to sustain the liquid stream separation. Lawver, Breen, et al (Ref. 9) obtained data which seemed to verify the significance of D/V and propellant temperature, and further suggested that pressure effects were of limited importance. Their semi-empirical model, developed somewhat differently from that of Kushida, emphasized the strong effect of liquid temperatures through an Arhenius reaction rate expression. Furthermore, their performance data with a micro-rocket, using four unlike doublets to inject N_2O_4/N_2H_4 showed a dramatic, almost discontinuous decrease in performance as the propellant temperature was raised, which was attributed to the onset of blowapart. Thus, it appeared that, at least with unlike doublets using N_2O_4/N_2H_4, zones of "separation" and of "mixing" had been mapped out. Unfortunately, however, as reported by Zung (Ref. 10) in September 1969, much of the Ref. 9 data is now considered questionable due to oxidizer boiling as it was injected, and the propellant reaction with lucite windows of the experimental apparatus. Boiling probably presented liquid-liquid impingement and photographic interpretation was severely impaired by the lucite burning. More recent work by Dynamic Science (Ref. 10) suggests that separation is more prevalent at elevated pressures and also that propellant temperatures play an insignificant role. This conclusion is also questionable since the dynamic pressure ratio did not remain constant.

In summary, by the summer of 1969, blowapart was widely recognized as a phenomenon which should be characterized for the injector designer. However, design and operating conditions conducive to separation had not been adequately delineated, even for the much-studied N_2O_4/N_2H_4 system. Data

of N_2O_4 with other hydrazine-type fuels was sparse. Techniques had not yet been demonstrated which could provide uncontroversial data on separation. The physical nature of the separation process, when it did occur, was generally presumed to involve a quasi-steady lamination of the spray fans with fuel on one side and oxidizer on the other.

In Campbell's investigation, extremely detailed color photographs had been obtained of atmospheric pressure firings of N_2O_4 and 50% N_2H_4-50% UDMH. Individual burning fuel and oxidizer droplets were not only discernible but could be distinguished by their color. Fuel and oxidizer could also be distinguished on the edge of the spray fan. Good intermixing of the propellants was obvious for the limited number of test conditions. The present study was undertaken with the primary aim of applying these same photographic techniques to several hypergolic propellant combustions under conditions where (1) mixing occurs, and (2) where separation (or blowapart) took place. As a secondary goal, it was desired to verify the existence of a field of spray droplets in the combustion zone downstream of a large unlike-doublet injector which was subject to blowapart. Previous photographic studies in open air tests with N_2O_4/50% N_2H_4-50% UDMH (Ref. 15) had failed to reveal droplets with such an injector.

Following completion of the initial phase of the subject work, an Interim Report (R-8110) was published which described a distinct cyclic type of blowapart with N_2O_4/N_2H_4. The subsequent work in this program was directed toward determining whether this phenomenon occurred with other hypergolic liquid propellant combinations and toward ascertaining the effect of operating pressure. Selected tests were also planned in which orifice sizes, injection velocities and jet dynamic pressure ratios were varied. This report covers all phases of the subject program including the results contained in R-8110.

It should be noted that this report covers a two-year period and since the publication of the Interim Report other investigators including Houseman (Ref. 16) and Clayton (Ref. 17) have published experimental results relating cyclic (pop) rates to various injection, and propellant operating conditions. The results from these latter studies are compared to our results where appropriate.

EXPERIMENTAL APPARATUS, FACILITIES, AND PROCEDURES

The primary objective of the program was to photographically observe impinging NTO/hydrazine streams under conditions where they mix and under conditions where stream separation occurs. Additionally, photographic documentation of propellant droplets in the spray field was desired. The experimental approach employed to obtain these photographs included both still and motion picture film coverage of injector elements under hot fire conditions. Various camera settings and lighting adjustments were used to obtain the desired results. Because coverage of condensed phase phenomena was sought, combinations of backlighting, light filtering, and film exposure were selected to minimize the flame light and to silhouette the jets and spray. Color contrast between individual propellant streams and spray was also sought for aid in distinguishing between fuel and oxidizer in the spray fan.

A description of the experimental apparatus and procedures required to fulfill the program objectives is presented in the following sections.

APPARATUS

Experimental hardware for the program included a series of bipropellant-type injectors and a combustion chamber with photographic viewing ports.

Injector Design

Criteria for injector design was based on the attainment of a set of injectors which would permit operation under conditions ranging from those in which good propellant mixing occurs to those which result in stream separation. An injector design parameter, orifice diameter/injection velocity (D/V),which represents an index of relative contact residence time between impinging streams, had been previously correlated with the presence or absence of stream separation. Large D/V values imply long contact times, which, in turn, have been associated with stream separation.

Conversely, small D/V values represent short contact times, which are generally considered conducive to stream mixing. The D/V parameter was used to design injector elements for the subject study.

Three injector configurations were selected. Design parameters for the injectors are listed in Table I. A schematic diagram of a typical setup is shown in Figs. 1 and 2. All injectors were single-element, unlike-doublet, impinging-stream-type configurations having equal diameter fuel and oxidizer orifices. The impinging stream included angle was either 45 or 60 degrees. The orifice diameters were 0.030, 0.072, and 0.173-inch, which permitted evaluation of a large D/V range. These design conditions for the series of injectors permit spanning of the mix/separate combustion transition as defined in previous studies*, Ref. 9.

The orifices for the three injector configurations were formed by smooth stainless-steel tubes with L/D values of 100. Large orifice L/D were employed to eliminate uncertainties with regard to hydraulic effects by providing fully developed turbulent flow and uniform, well-formed jets. The orifice tubes were attached to an aluminum block with swedge-lock fittings. The block served as a common mount for all orifice pairs. The swedge-lock arrangement allowed each tube to be set at the free stream liquid jet length to the impingement point of five times the jet diameter.

All elements were initially cold-flowed with water to verify impingement alignment.

*Although the Ref. 9 data is now under question, it was concluded that use of the three indicated orifice sizes together with pressure throttling allowed a comfortable margin for operating in both "mix" and "separate" regions.

TABLE I

SUMMARY OF DESIRED INJECTOR CONDITIONS

Orifice Dia. D_o-D_f	L_{fs}/D_j	L_{or}/D_j	θ
.030	5.0	100	60
.060	5.0	100	60
.173	5.0	100	45
.173	5.0	100	60

where:

L_{fs} = Free stream jet length to the impingent point

D_j = Orifice jet diameter

θ = Impingement angle

o = Oxidizer

f = Fuel

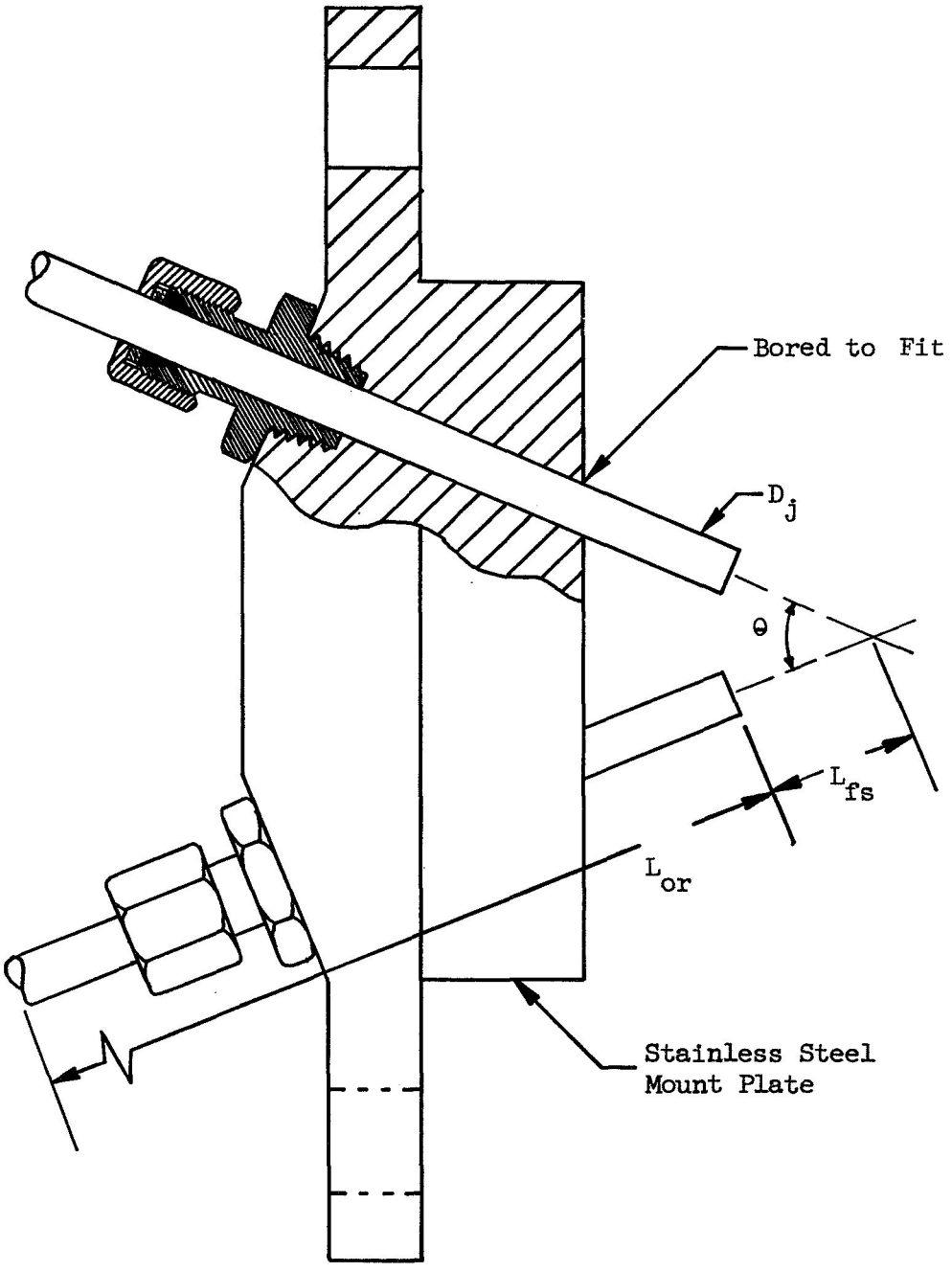

Figure 1. Schematic of 0.173 or 0.072 Inch Orifice Configuration Single Element Injector.

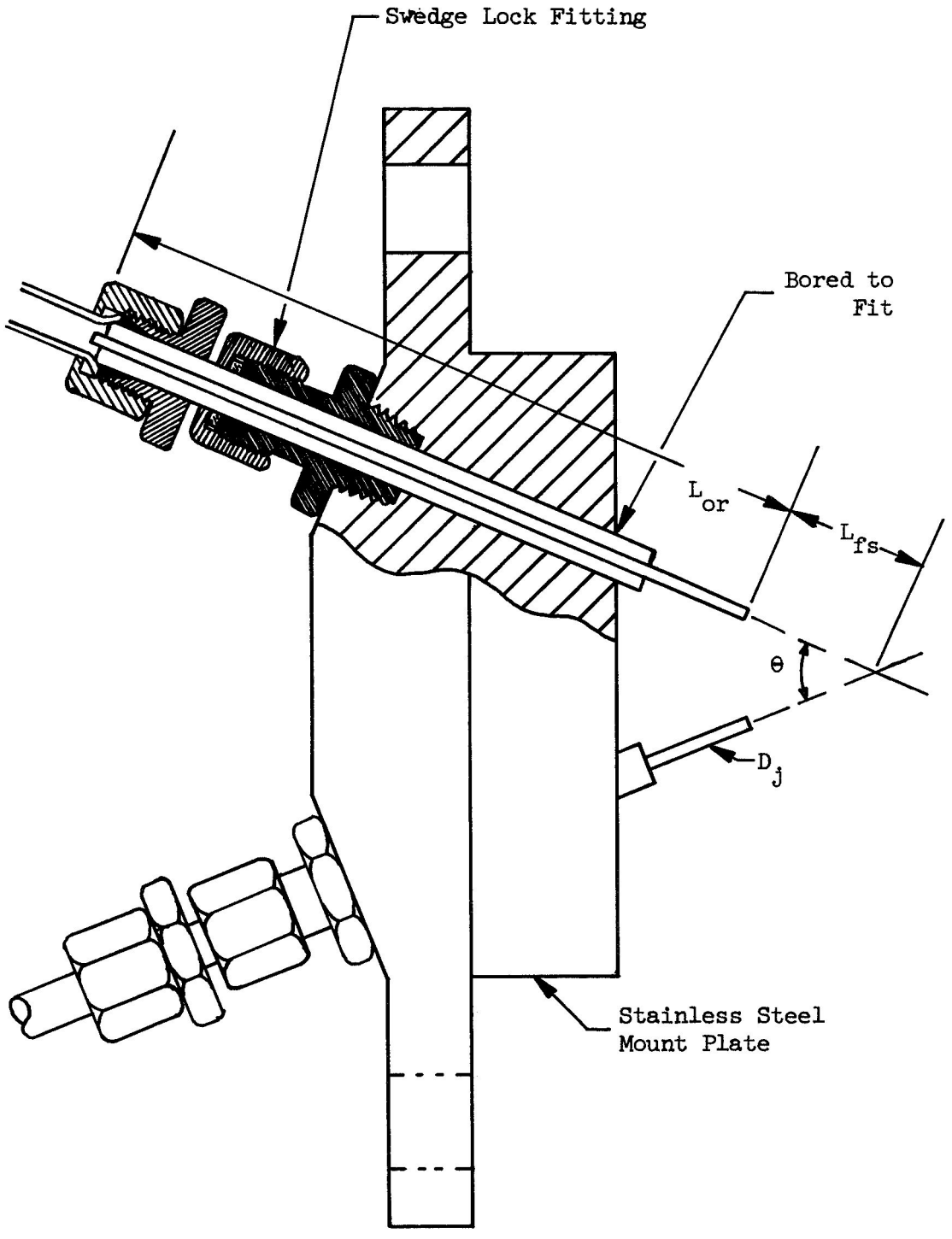

Figure 2. Schematic of 0.030 or 0.026 Inch Orifice Configuration Single Element Injector.

Water flow calibrations of each orifice size were also conducted to determine orifice discharge coefficient. Orifice discharge coefficients for the 0.030-, 0.072-, and 0.173-inch orifice injectors were 0.453, 0.606, and 0.596, respectively.

Windowed Chamber

Reactive stream separation tests were also conducted in a variable pressure chamber wherein the ambient pressure is controlled by injection of gaseous nitrogen. The chamber has transparent sides to allow visual observation of a single element reacting spray. A schematic drawing of the chamber is shown in Fig. 3. The chamber consists of a cylindrical steel shell (18-inches in diameter by 24-inches in length) with plexiglas view windows on each of two sides (one for camera view and one for backlighting) and an injector mount plate and nozzle plate at respective ends of the chamber. The chamber is pre-pressurized by gaseous nitrogen introduced through an annular ring of orifices in the injector mount plate. The gaseous nitrogen orifices encircle the injector to contain the injected spray thereby reducing spray impingement on the view windows. Additionally, separate gaseous nitrogen window purges, introduced through orifices located around the window periphery and directed to impinge on the window, are employed to further inhibit spray impingement on the window from occluding the camera view of the reacting spray.

TEST FACILITY

The experimental hot firings were conducted at the Propellant Engineering (PEL) and the Combustion and Heat Transfer (CHTL) laboratories of the Santa Susana Field Test Site.

Schematic flow diagrams of the overall test stand at PEL are shown in Figs. 4 through 6, respectively. These include schematics of the NTO tankage and supply, and hydrazine tankage and supply systems. Test

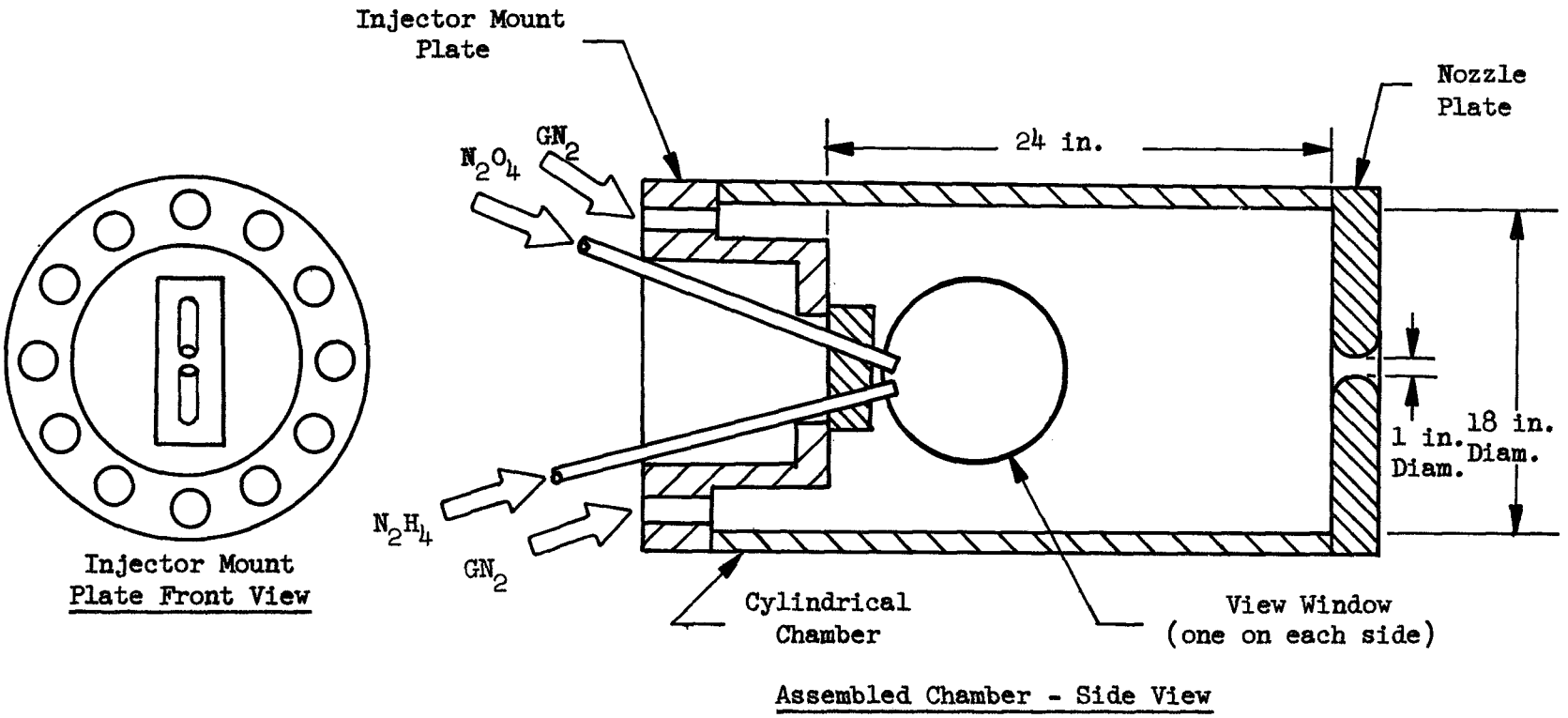

Figure 3. Schematic Drawing of Variable Pressure Test Chamber

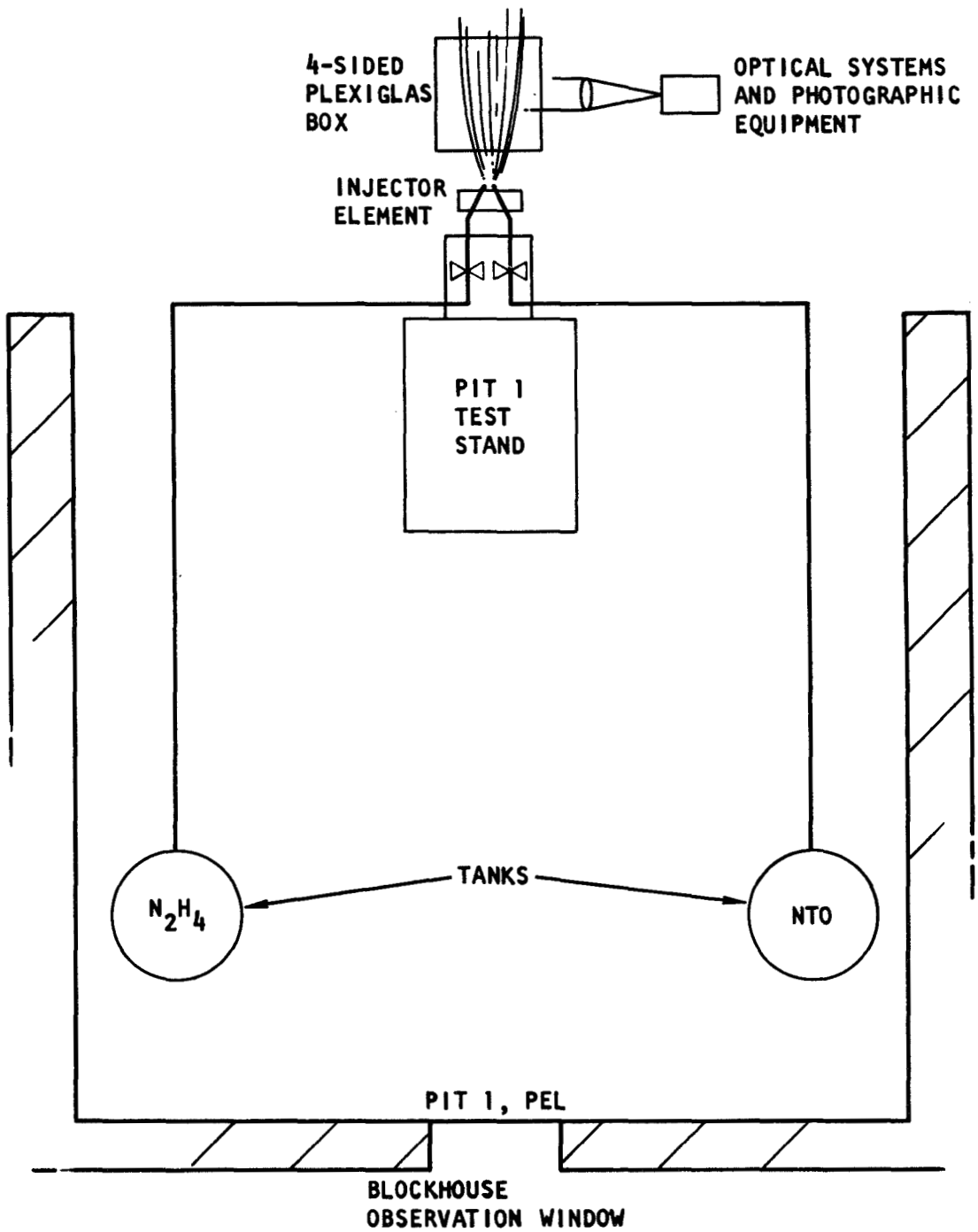

Figure 4. Overall Blowapart Facility Schematic

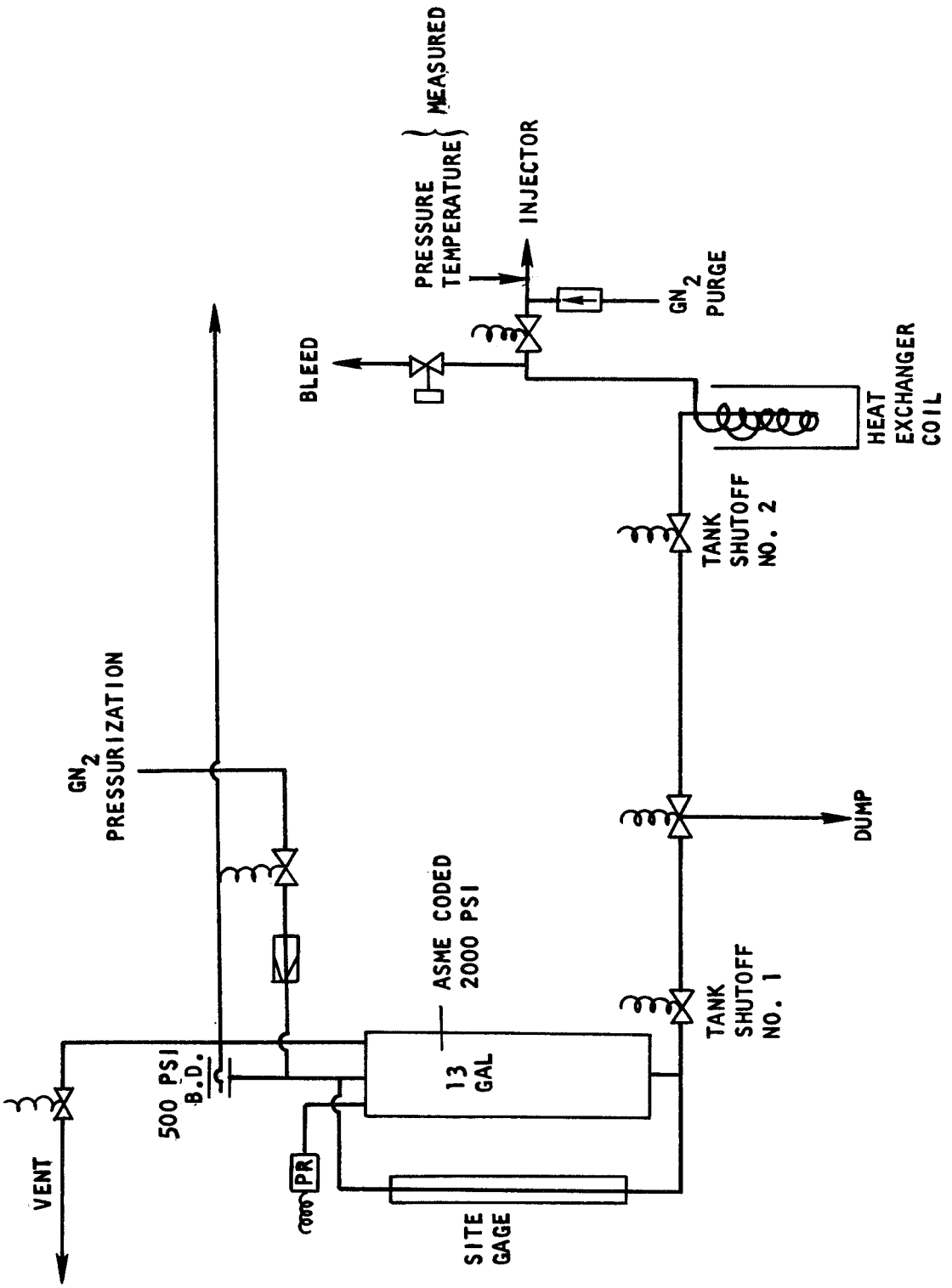

Figure 5. NTO Tankage and Supply

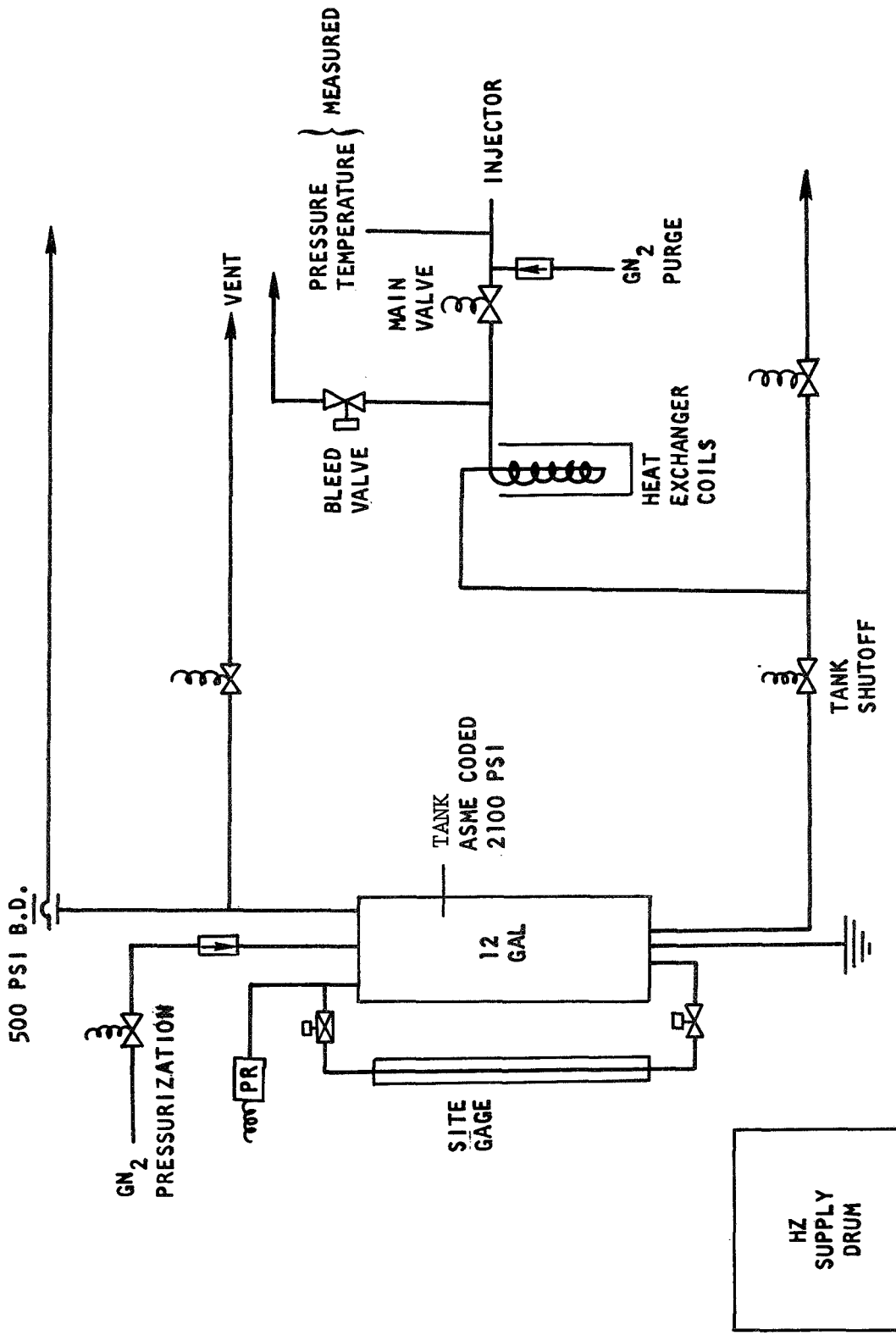

Figure 6. Hydrazine Tankage and Supply

equipment includes propellant run tanks, propellant feed system plumbing and an enclosure mount for the injector. All tests at this facility were conducted with the NTO/hydrazine propellant combination.

The N_2H_4 system consists of a 12.0 gallon, 2100-psig rating stainless-steel tank with associated pressurization, vent, and outlet controls and valves. The N_2H_4 tank shutoff valve was a 1/2-inch Annin (Model 4520). Tubing connecting the N_2H_4 tank shutoff valve and tank main valve was 1/2-inch diameter by 0.049-inch wall seamless 321 stainless steel. The N_2H_4 main valve was a 1/2-inch (Model 9420) Annin.

The N_2O_4 system consists of a 13-gallon, 2000-psig rating stainless-steel tank with its separate pressurization, vent, and outlet controls and valves. The nitrogen tetroxide system had three valves, a 1/2-inch Annin (Model 3420) shutoff, a 1/2-inch Vacco (Model 403) prevalve, and a 1/2-inch (Model 9420) Annin main valve. The N_2O_4 propellant line was mainly 1/2-inch diameter by 0.049-inch wall seamless 321 stainless-steel tubing. One-quarter-inch Marotta purge valves with check valves were teed into the main feed lines downstream of each main valve.

Early in the program effort, it became evident that temperature conditioning of the oxidizer was required to prevent flash vaporization of the oxidizer stream and thereby improve oxidizer stream collimation. Accordingly, an ice-cooled temperature bath was installed in the oxidizer line upstream of the main valve. A similar ice bath was also installed in the fuel line to provide approximately equal injection temperatures for each propellant.

The CHTL facility is shown in Fig. 7. Basically it consists of three liquid propellant storage and delivery systems, separate heat exchangers for temperature conditioning of each propellant.

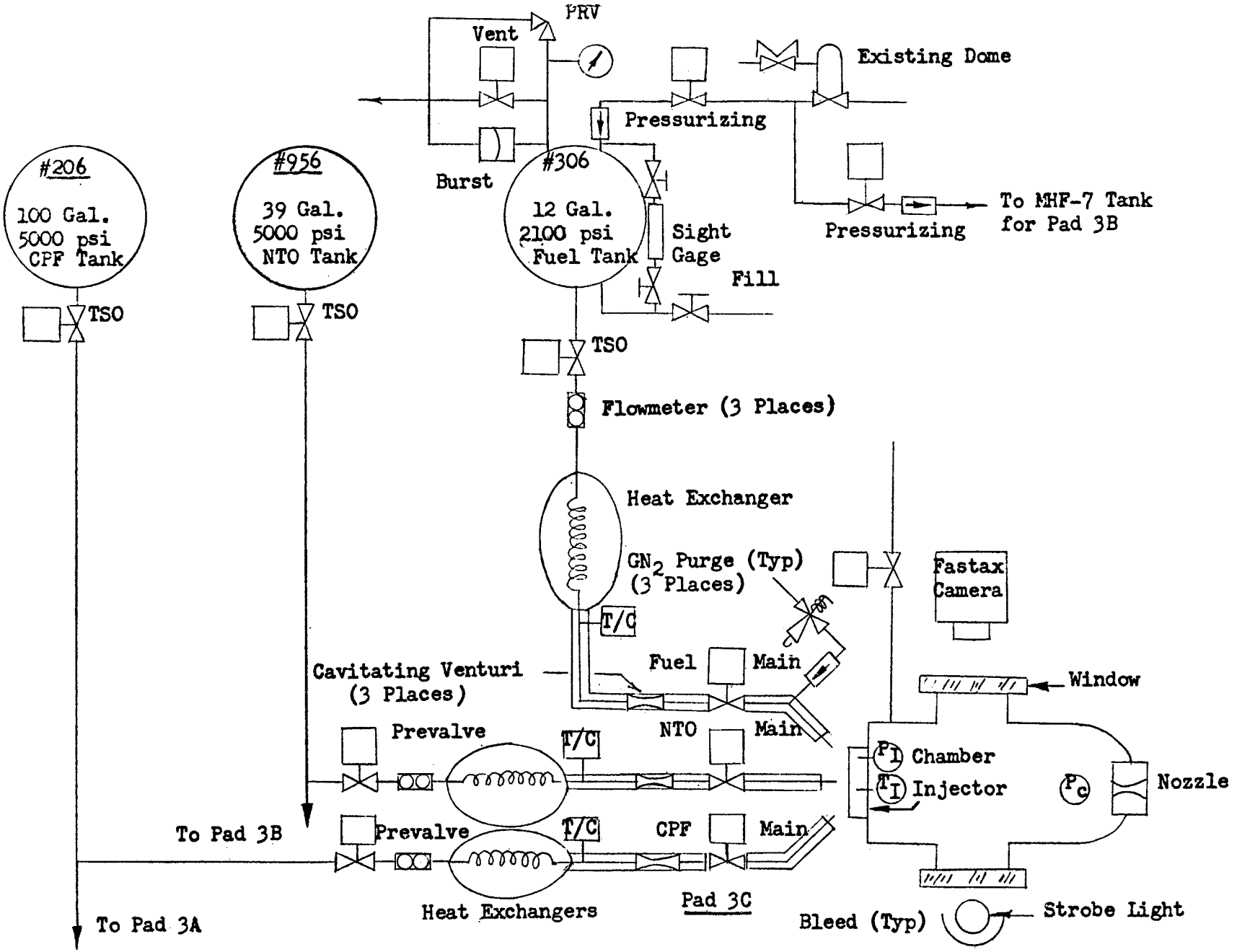

Figure 7. Reactive Stream Separation Test Facility

Propellant Systems

Two oxidizer systems and one fuel system (refer to Fig. 7)were provided to accommodate the several propellant combinations planned for study in Task A-1. One of the oxidizer systems will supply either NTO or IRFNA from a 5000-psi, 30-gallon run tank. The other delivers chlorine pentafluoride (CPF) from a 5000-psi, 100-gallon run tank. The fuel system supplies the various propellants (N_2H_4, UDMH, 50-50) from a 2100-psi, 12-gallon tank. Each system is provided with appropriate valves for safe, controlled test operations. Pressure reliefs are set at 1500-psi for the NTO/IRFNA system, 2586-psi for the CPF system and 1000-psi for the fuel system.

Propellant conditioning is necessary to assure single-phase liquid flow from the injector elements. The heat exchangers used for propellant conditioning consist of 18-foot coils of 1/2-inch stainless steel tubing immersed in 5-gallon containers. In addition, the chilled coolant is pump-fed through propellant line jackets down to the injector element. Ice water is used to cool the NTO, IRFNA and hydrazine fuels to approximately 40°F. The CPF is chilled below 0°F by a trichloroethylene/dry ice slush.

System instrumentation is basic and uncomplicated since the bulk of the experimental results come from photographic coverage. Tank pressure instrumentation is used to set the run conditions. Turbine flowmeters monitor the propellant flowrates. Iron-constantan thermocouples monitor the coolant bath temperatures and the propellant line temperature in the jacketed sections. Cavitating venturis are provided to eliminate propellant surge and flowrate dependence on downstream transients (e.g., blowapart at injector face).

Test Procedures

The test procedure for all hot firing was essentially the same. Initially, a chilldown period was allotted to condition the propellant in the ice bath

containers. During the propellant temperature conditioning period, camera equipment was positioned for the planned test. Subsequently, the propellant main valves were electrically connected and the test area cleared.

An automatic timer, Eagle Model HM-7 was used to actuate the propellant main valves and camera equipment for the tests. The hot-firing sequence consisted of (1) pressurization of the propellant tanks, and (2) initiation of the test using the automatic timer. After completion of the test, propellant was cleared from the propellant lines and injector using manually actuated nitrogen gas purges. The test firing was completed with removal of the main valve electrical connections and opening of the test area for personnel.

PHOTOGRAPHIC APPARATUS AND TECHNIQUES

Still Photography: Single Light Source Apparatus

Figure 8 is a schematic of the optical system initially used for color photography of the spray field.

The light from an EG&G type FX-11 Xenon flash lamp is focused by a Fresnel lens (L_1) through a 4-inch by 4-inch by 4-inch spray volume. The transmitted light is then directed by three mirrors (M_1, M_2, and M_3) and refocused by Fresnel lens L_2 onto a ground glass screen. Fresnel lens L_3 images the ground glass screen onto the camera lens. The ground glass screen serves as a light diffuser and provides a more uniformly illuminated background at L_3, which the camera views. Provision was made for using a beam splitter, which would reflect approximately 60% of the light to provide bottom illumination of the spray.

With this system, the spray can be simultaneously illuminated from top and bottom and rear using a single flash lamp. The camera views the spray in silhouette against the background of lens L_3, while the top and bottom illumination is provided to bring out the color contrast between propellants.

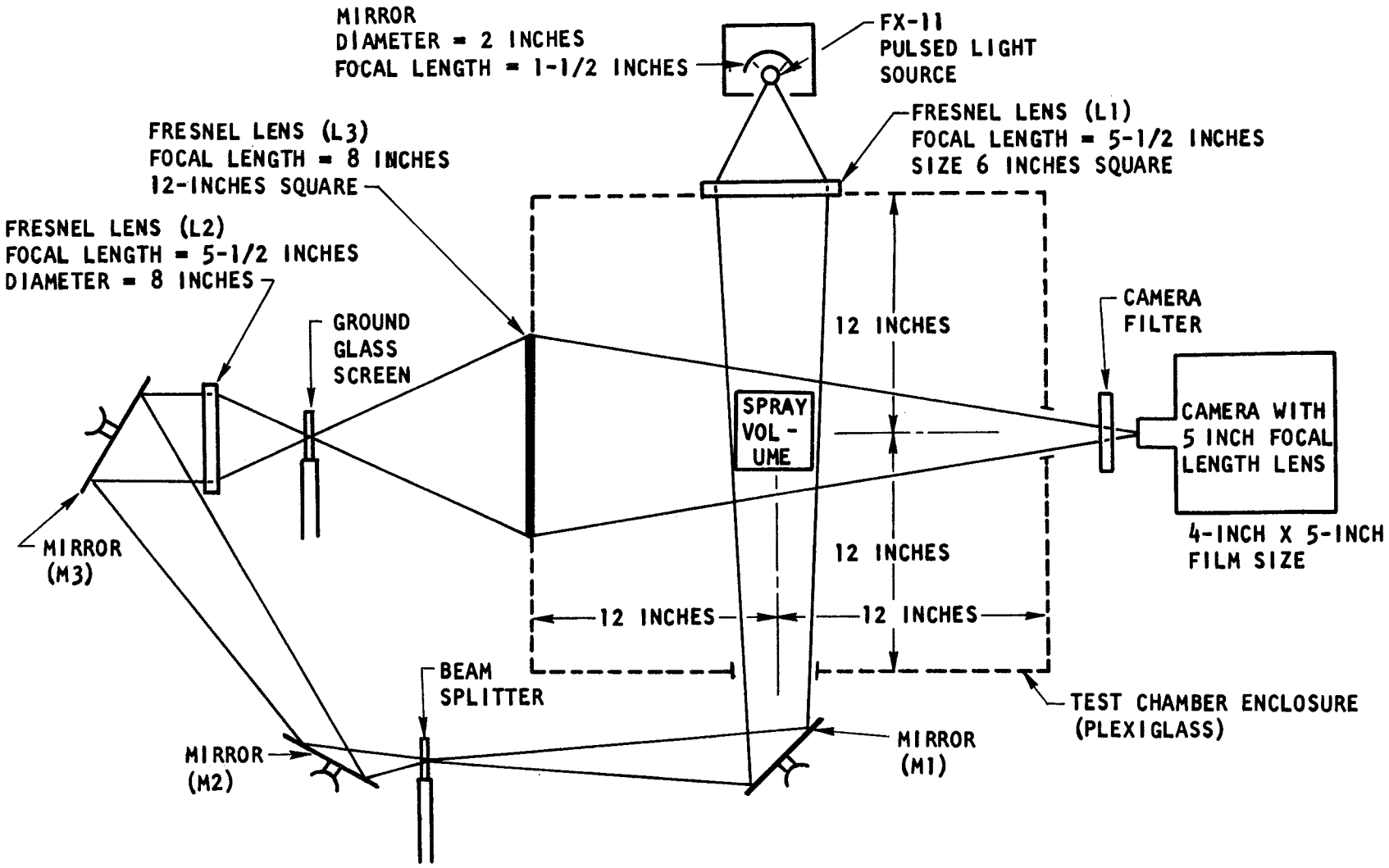

Figure 8. Single Light Source Apparatus for Blowapart Photography

The optics are protected from the propellants by a four-sided plexiglass box measuring 2-feet-square on a side. To keep the box transparent, replaceable glass or plexiglass plates are attached inside each of its four sides.

The Xenon flash lamp is driven by an EG&G Model 501 high-speed strobscope power supply which can flash the lamp up to 6000 times per second. For use with the still camera, the strobe lamp system is fired for a single flash by the flash synchronization switch on the camera shutter.

The FX-11 Xenon flash lamp has the highest radiance and energy rating of any of several flash lamp types compatible with the Model 501 power supply. The input energy per flash can be set at 0.32, 0.64, and 1.28 joules, which yield manufacturers rated light outputs per flash of 0.7, 2.0, and 4.0 millijoules per steradian, respectively. The respective flash durations were measured to be approximately 1, 2, and 3 microseconds.

The initial photographic work was carried out using the aforementioned optical system and a still camera with a 4-inch by 5-inch polaroid film pack. Color polaroid film was used, because the 1-minute development time permits immediate examination of the results of a run. It was planned that once satisfactory photographic results were obtained with polaroid film, the photographs would then be taken with a faster, higher resolution film such as Ektachrome S, Ektachrome B, or Ektachrome D.

The first series of test runs were made using a variety of camera filters to find the filter that did the best job of filtering out the flame light while at the same time providing maximum color contrast in the propellants. Test runs were made using Kodak Wratten filter types 30, 31, 32, 34, and 34A. The filter chosen as a result of the tests was filter 34. A graph of the spectral transmittance of Wratten filters used in the program is shown in Fig. 9.

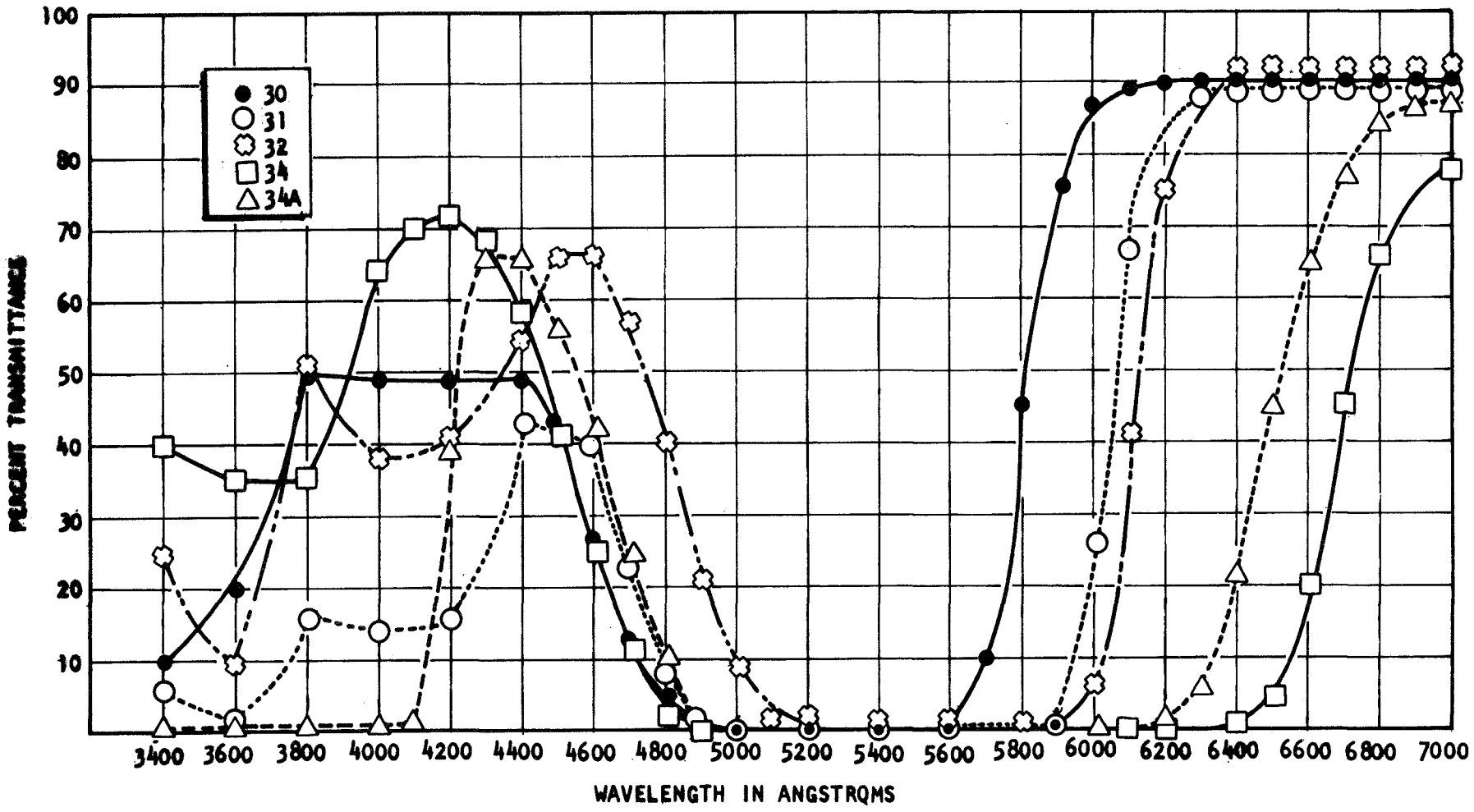

Figure 9. Spectral Transmittance of Wratten Filters 30, 31, 32, 34, and 34A

Still Photography: Multiple Light Source Apparatus

After the initial sequence of tests, attempts were made to improve color contrast by modifying the lighting system. A schematic of the modified photographic setup is shown in Fig. 10 . The top light was focused to produce a smaller diameter beam; hence, a higher irradiance, within the spray volume to be photographed. Also, the spray was simultaneously illuminated from an oblique front angle by a second Xenon flash lamp and focusing lens. A third Xenon lamp was used for simultaneously back lighting the spray. The flash lamps used for front oblique and back lighting were General Radio Stroboslave, type 1539-A. The electrical energy input per flash for these lamps was about 0.4 joule with a 3-microsecond flash duration. As before, the EG&G FX-11 lamp and Model 501 Stroboscope power supply was used for top lighting. The three flash lamps were triggered simultaneously by a trigger signal supplied by the flash synchronization switch on the camera shutter.

Tests were also carried out with oblique front lighting from the FX-11 flash lamp focused to a 1-inch-diameter spot at the injector axis. In this case, back lighting was carried out with an EG&G FX-3 spiral lamp which is further described in the following discussion of the setup used for Fastax photography. A neutral density filter was placed over this (latter) lamp so that the back lighting would be of low level and not wash out any droplet color produced by the front light.

Fastax Photography: Multiple Light Source Apparatus

Figure 11 shows the photographic arrangement used for Fastax photography. The backlight was provided by an EG&G FX-3 spiral lamp which was driven by a type 501 stroboscope power supply. The FX-3 was used because it has a much longer life-time than the FX-11. Although the radiance is an order of magnitude less than the FX-11, it is sufficiently high for back lighted photography. An FX-11 flash lamp driven by a second type 501 stroboscope power supply was used alternatively in the front oblique or top position. The motion pictures were obtained with a prismless Fastax camera, again

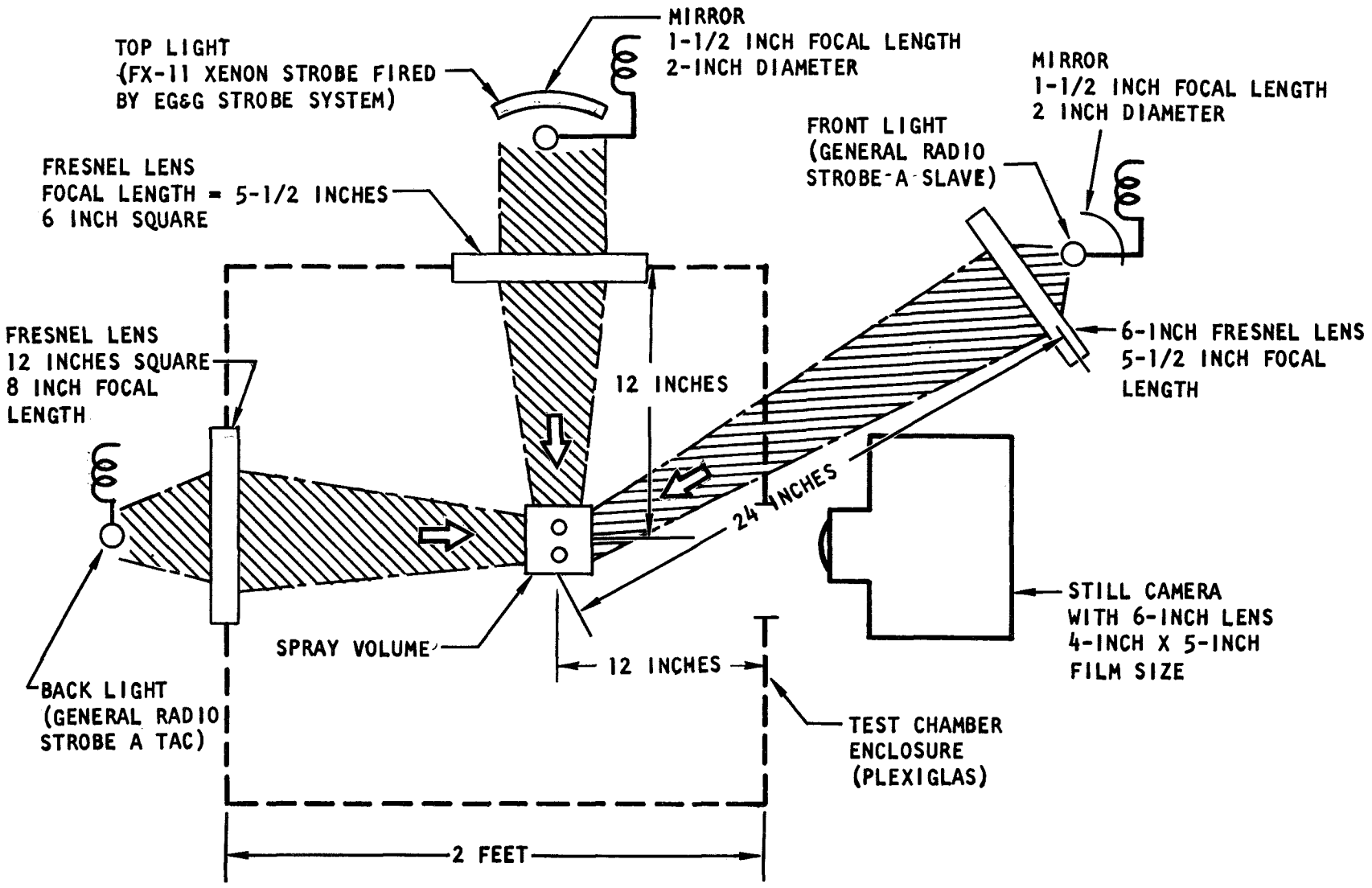

Figure 10. Multiple Light Source Photographic Apparatus Test Setup for Enhanced Top and Front Lighting

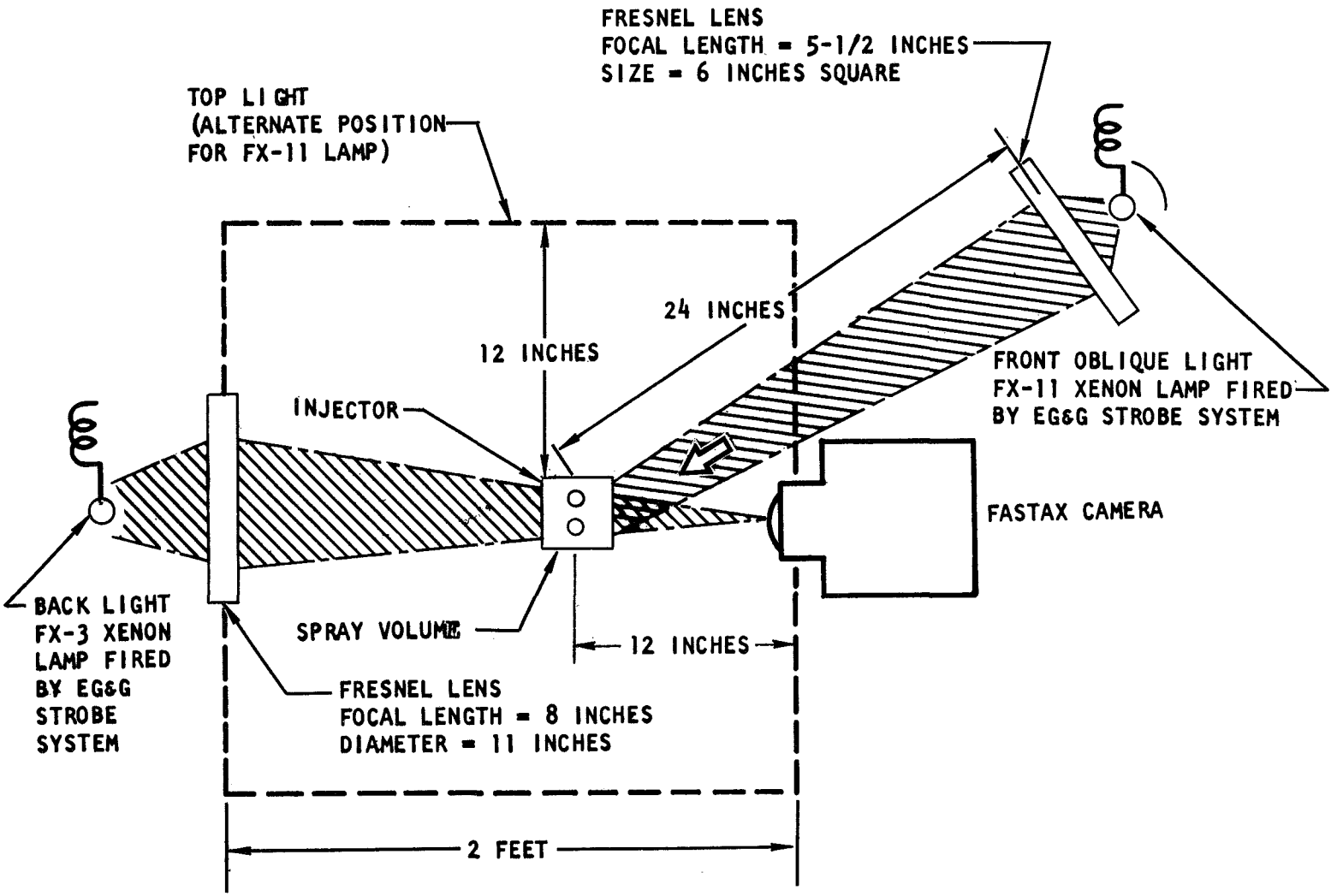

Figure 11. Photographic Apparatus for Fastax Photography

Ektachrome EF film was used to image the spray. The stroboscope was synchronized with the camera to flash once each time the film advanced one frame.

Throughout the test program the lighting technique used was varied to attempt to bring out propellant droplet color in the movies. Initially, only back lighting was employed and no attempt was made to bring out propellant color. In later efforts, propellant color contrast was enhanced with the use of front or top lighting. A ground glass light diffusion screen was placed over the FX-3 flash lamp to provide more uniform distribution of back lighting. No filter was required to eliminate the flame because actual exposure to microflash was nominally two microseconds.

Overall Film Coverage. A two-sided prism Fastax camera with Ektachrome EF film was used separately to monitor the overall burning spray from a position 30 degrees off axis and 15 feet downstream of the spray field. Magnification was about 1/100. In this case all lighting was provided by the combustion flame.

EXPERIMENTAL RESULTS

A tabulation of the hot firing test data is presented in Table II . Tests 1 through 8 were system and photographic checkout runs and yielded no usable data. Tests 9 through 12 were run in open air with the 45 degree impingement angle (included) 0.173-inch orifice unlike doublet injector. The propellant temperatures were 50°F, and the propellant type was nitrogen tetroxide (NTO) and hydrazine (Hz). Runs 22 through 33 were also at atmospheric pressure and the propellants were NTO/Hz; however, the orifice sizes were 0.030, 0.072 and 0.173 inch (all had a 60 degree included impingement angle). In tests 34 through 51 the effect of propellant combination was evaluated. The propellants were NTO/50-50 (50% Hz + 50% UDMH), IRFNA/UDMH and CPF/Hz. During tests 52 through 56 the effect of chamber pressure was studied at elevated chamber pressure of ~200 psia. For these tests the propellant combination was NTO/50-50. In all of the above experiments (9 through 56) the contact time $(D/V)_f$ was between .4 and 4 x 10^{-4} sec. Lastly, using a .026-inch orifice element the effects of dynamic pressure ratio and reduced contact time (.2 x 10^{-4} sec) were evaluated using the propellant combination CPF/Hz at atmospheric pressure.

A detailed description of these tests is contained in the following discussion. For convenience, the presentation of the results is grouped by propellant combination.

A movie depicting the data obtained in the subject program is available on a loan basis from JPL. A description of the available film record is contained in Appendix A. It should be noted that the film provides a more graphic presentation of the data than can be shown by single frame reproductions contained in this report.

TABLE II. SUMMARY OF TEST CONDITIONS

Test No.	Injector		Dynamic Pressure	Injection Velocity		P_c	Prop.Temp.		Propellants	$(D/V)_f$	Remarks
	$D_o=D_f$ in.	Impingement Angle,°	$\rho_f V_f^2/\rho_o V_o^2$	V_{ox} Ft/sec	V_f Ft/sec	psia	T_{ox} °F	T_f °F		-sec x 10^{-4}	
1*	0.030	60	1.0	35 to 60	40 to 80	13.7	30 to 80	35 to 80	NTO/Hz	.3 to .65	Initial System & Photographic Setup Checkout Tests
2*	↕	↕	↕	↕	↕	↕	↕	↕	↕	↕	
3*											
4*											
5*											
6*											
7*											
8*	0.030	60	1.0	35 to 60	40 to 80	13.7	30 to 80	35 to 80	NTO/Hz	.3 to .65	
9	0.173	45	.86	33	43	13.7	55	60	NTO/Hz	3.3	Baseline Tests with JPL Injector
10	↕	↕	.86	33	43	↕	55	62	↕	3.3	
11			.91	33	41		55	58		3.5	
12			.93	33	41		52	67		3.5	
13			1.0	30	36		50-60	50-60		4.1	
14			1.0	30	36		↕	50-60		4.1	
15			.85	30	40			50-60		3.6	
16			.69	28	41			60-70		3.5	
17			.63	28	43			↕		3.3	
18			.83	30	43					3.3	
19			.88	32	43					3.3	
20			.91	33	43					3.3	
21	0.173	45	.91	33	43	13.7	↕	↕	NTO/Hz	3.3	
22	0.072	60	.85	38	50	13.7	40-50	50-60	NTO/Hz	1.2	Effect of Orifice Size on Blowapart
23	↕	↕	.94	51	63	↕	↕	↕	↕	.95	
24	0.030	60	1.0	47	56	13.7	40-50	50-60	NTO/Hz	.45	Effect of Orifice Size on Blowapart
25	↕	↕	1.0	47	56	↕	↕	↕	↕	.45	
26			1.03	46	54					.46	
27	0.173	60	1.26	41.6	56.2	13.7	40	40	NTO/Hz	2.6	Study of the Effect of Propellant Reactivity on Blowapart
28	↕	↕	1.15	40.3	51.9	↕	↕	↕	↕	2.8	
29			1.14	40.5	51.9					2.8	
30			.90	42.3	48.5					3.0	
31*			-	-	-					-	
32			1.02	41.3	50.1					2.9	
33	0.173	60	1.09	39.2	49.2	13.7	40	40	NTO/Hz	2.9	

*No photographic data obtained during this run.

TABLE II. (Cont.)

Test No.	Injector		Dynamic Pressure $\rho_f V_v^2/\rho_o V_o^2$	Injection Velocity		P_c psia	Prop. Temp.		Propellants	$(D/V)_f$ -sec x 10^{-4}	Remarks
	$D_o=D_f$ in.	Impingement Angle, °		V_{ox} Ft/sec	V_f Ft/sec		T_{ox} °F	T_f °F			
34	0.173	60	.95	41.8	55.5	13.7	-10	40	CPF/Hz	2.6	Study of the Effect of Propellant Reactivity on Blowapart
35	↕	↕	.97	40.9	55.3	↕	↕	↕	↕	2.6	
36	↕	↕	1.09	37.7	54.6	↕	↕	↕	↕	2.6	
37	↕	↕	1.0	38.8	53.5	↕	↕	↕	↕	2.7	
38	↕	↕	.86	43.8	55.5	↕	↕	↕	↕	2.6	
39	↕	↕	.88	42.6	55.0	↕	↕	↕	↕	2.6	
40	0.173	60	1.08	37.5	54.0	13.7	-10	40	CPF/Hz	2.6	
41*	0.173	60	.53	37.3	34.4	13.7	40	50	NTO/50-50	4.1	Study of the Effect of Propellant Reactivity on Blowapart
42*	↕	↕	.63	42.5	41.2	↕	↕	↕	↕	3.4	
43*	↕	↕	2.01	37.1	63.0	↕	↕	↕	↕	2.2	
44	↕	↕	1.28	38.0	52.0	↕	↕	↕	↕	2.7	
45	↕	↕	1.04	40.2	51.3	↕	↕	↕	↕	2.7	
46	↕	↕	1.05	40.2	51.6	↕	↕	↕	↕	2.7	
47	0.173	60	1.04	40.2	51.4	13.7	40	50	NTO/50-50	2.7	
48*	0.173	60	1.1	39.4	57.0	13.7	35	50	IRFNA/ UDMH	2.5	Study of the Effect of Propellant Reactivity on Blowapart
49	↕	↕	1.1	40.0	67.0	↕	↕	↕	↓	2.1	
50	↕	↕	.97	40.9	55.1	↕	↕	↕	↓	2.6	
51	0.173	60	.95	40.9	54.5	13.7	35	50	↓	2.6	
52*	0.173	60	.25	34.4	22.3	165	40	45	NTO/50-50	6.3	Effect of Chamber Pressure on Blowapart
53	↕	↕	1.5	39.8	64.5	235	↕	↕	↓	2.2	
54	↕	↕	1.1	39.8	55.0	225	↕	↕	↓	2.6	
55	↕	↕	.99	40.4	53.0	225	↕	↕	↓	2.7	
56	0.173	60	.96	40.4	52.0	220	40	45	↓	2.7	
57	0.026	60	1.62	52	91	13.7	-10	64	CPF/Hz	.24	Effect of Dynamic Pressure Ratio on Blowapart
58*	↓	↓	-	-	-	↓	-	-	↓	-	
59*	↓	↓	.68	87	98.5	↓	-10	66	↓	.22	
60	↓	↓	.805	77	95.0	↓	-10	65	↓	.23	
61	↓	↓	1.35	74	118.0	↓	-6	67	↓	.18	

*No Fastax photographic data obtained during this run.

NITROGEN TETROXIDE/HYDRAZINE RESULTS

Experiments with the 0.030-inch Orifice Pair

Experiments with the 0.030-inch orifice pair consisted of still photographs and Fastax photography tests as described in the following paragraphs.

Still Photography Tests. The first test was conducted with ambient temperature (70 to 80°F) propellants. This test revealed that NTO flashing occurred. As a result, the NTO jet emerged from the orifice tube as a two-phase mixture. To remedy this situation, both propellants were conditioned in ice baths to reduce temperatures to approximately 40°F. This worked satisfactorily and well-collimated jets resulted.

After reducing propellant inlet temperature and some variation of the experimental photographic technique, good pictures were obtained in tests 2 through 4. These tests with the 0.030-inch-diameter orifice pair were conducted over a range of D/V values from 0.3×10^{-4} to 1.0×10^{-4} seconds. Propellant mixing was obtained during all tests. This conclusion was reached by visual examination of the photographed spray fan (edge view).

Photographs from each of the tests indicated the presence of a well-developed spray fan without any indication of stratification or separation of propellant species. Qualitatively this fan was the same as would be expected with non-reactive liquid streams. A typical photograph is presented in Fig. 12. Hydrazine and NTO velocities were 50 and 42 ft/sec, respectively, and propallent temperatures were approximately 40°F. Here droplets are clearly visible. In this picture, the NTO is injected from the bottom orifice tube.

Color photographic techniques were varied for tests 5 through 8, to improve the color contrast between NTO and hydrazine liquids. Initially, the single light source/mirror arrangement previously shown in Fig. 8 was employed. Good photographs of the burning spray were obtained which showed the droplets clearly silhouetted against the back light. However, the color contrast of propellant streams and droplets was not sufficient to identify individual

P_c = 13.7 psia

T_o = 40°F

T_F = 50°F

ϕ = 1.0

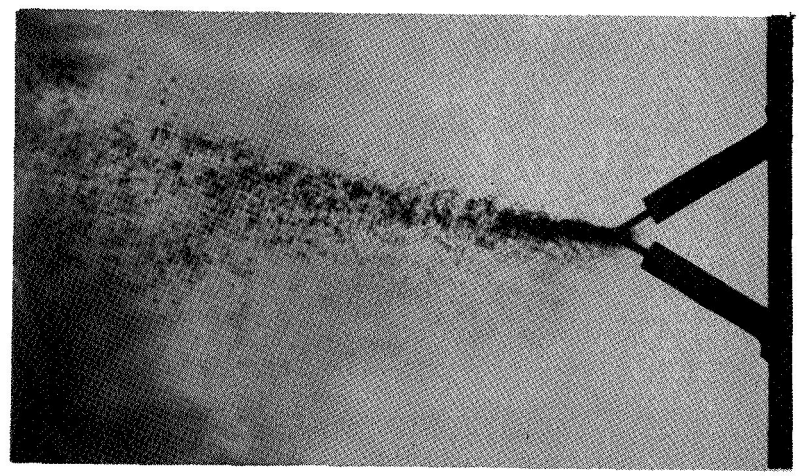

Figure 12. Burning Spray from N_2O_4/N_2H_4 Impinging Doublet, 0.030-Inch-Diameter Orifice Element, Edge View of Spray Fan from Injector Face to 4 Inches Downstream, Run 8

droplets as being either fuel or oxidizer, as was desired. Improved color contrast of the propellant streams was obtained from a multiple light source (Fig. 11). For this setup colors were discernible within the spray fan. However, distinct color contrast of individual droplets was still not achieved. Comparison with the photographs of Ref. 13 indicated that the problem was the result of an insufficient balance of top (or front) lighting to back lighting. As a result of the shift in emphasis toward use of Fastax film coverage, further development of color contrast in the spray droplets was not conducted in the subject program.

Fastax Photography Tests. Fastax film coverage was employed in tests 24 through 26 to provide a continuous record of the element spray characteristics for the 0.030-inch orifice pair. Continuous observation of the spray field affords information on transient spray field disturbances which might otherwise be missed by individual still photographs. These tests, were prompted by results (later discussed) obtained with large elements using Fastax photography.

Test results using the 0.030-inch-diameter orifices were not completely definitive, because good steady-state flow conditions were not achieved during the test series. Marginal cooling of the injector element housing resulted in partial flash vaporization of the precooled oxidizer in the injector hardware. However, steady-state flow was obtained for a period of approximately 300 milliseconds, at the end of the 1.5-second test firings. During this limited duration of steady-state operation, the injector operated in the "mixing" combustion regime. No occurrences of stream separation were noted.

Experiments With the 0.173-Inch-Diameter Orifice Pair

Experiments with the 0.173-inch orifice pair consisted of still photographs and Fastax photography tests as described in the following paragraphs.

Still Photography Tests. Tests 9 through 12 were conducted with the 0.173-inch-diameter orifice pair using still photography. The impingement angle for these tests was 45 degrees. The operating conditions, including D/V, were maintained nominally constant for all tests. Primary results of the tests were the observation of (1) violent stream separation on one test, (2) a bright flash which over-illuminates the entire photograph on another test, and (3) jet impingement to form a spray fan, on the third test. The different appearance of the propellant spray field in each of the three tests suggested different stages in a time dependent process. These photographs were the first indication that blowapart involved a periodic contact of propellant streams followed by a spray field disturbance resulting in violent stream separation. As a result of these still photo observations, the use of high-speed Fastax photography was selected for further study of the blowapart phenomenon.

Fastax Photography Tests. Two differing impingement angle 0.173-inch injector elements were evaluated using Fastax photographic coverage. Runs 13 through 21 were with a 45-degree impingement angle injector, while a 60 degree impingement angle was employed for runs 27 through 33. In the first tests conducted with the 45-degree impingement angle orifice pair, fan edge views* were obtained from the injector to about 4-inches downstream. A cyclic-type propellant blowapart phenomenon was observed on all three tests. The propellant blowapart was characterized by flashes, possibly detonations or explosive deflagrations, occurring approximately 5 to 10 milliseconds apart, although the frequency was irregular. There was no warning in the prior frames that the disturbances were about to occur. Following each detonation, most of the propellant is consumed and the propellant streams are violently separated. Subsequently, the propellant streams reimpinge, forming a spray fan, and

*"Edge views" are obtained from a direction perpendicular to the plane containing the two impinging jets and show the narrow dimension of the spray fan. Fan views are oriented 90 degrees from the edge view and show the broad side of the fan.

the process is repeated. A typical sequence of the blowapart process is shown in Fig. 13 . (Note that this figure and several following figures require two pages to show a complete sequence of events.)

To define the three-dimensional spray field behavior during incidence of blowapart, photography of "fan" views of the propellant spray at both upstream (injector face to 4 inches) and downstream (2 to 6 inches from injector face) locations were obtained, as well as additional edge views at the downstream location. This was accomplished in tests 16 through 21. Figure 14 shows a fan view of the same process shown in Fig. 10. Note the semicircular rings of concentrated spray in the first photograph. This is qualitatively the same as would be expected of nonreactive liquid streams. Proceeding to the downstream views, Fig. 15 (edge view) and Fig.16 (fan view), additional information is obtained which shows spray can actually be seen to be blown downstream by the "disturbance" prior to its gasification. Referring back to Fig. 10 one notes that spray is also blown against the injector; in other words, it appears to be blown in both directions from an apparent source somewhat downstream of the jet impingement location. The spray so affected appears to consist of a very fine mist of shattered droplets, ligaments, etc. Gasification of this mist is rapid*. Some relatively coarse spray near the injector persists and subsequently moves downstream alongside the new spray fan formed when the "blown apart" jets reimpinge. In between periods where blowapart took place, large numbers of distinct droplets could be seen in the region from 2 to 6 inches downstream of the injector.

In addition to the 45-degree impingement angle element a 60-degree 0.173-inch element was also studied. During tests 27 through 33, edge view Fastax movies were taken of the impingement/combustion process. Modification of the propellant feed system for these tests was accomplished to include cavitating venturies just upstream of the injector. This was done

*Although vaporization is achieved, mixing of the fuel and oxidizer vapors is probably quite incomplete.

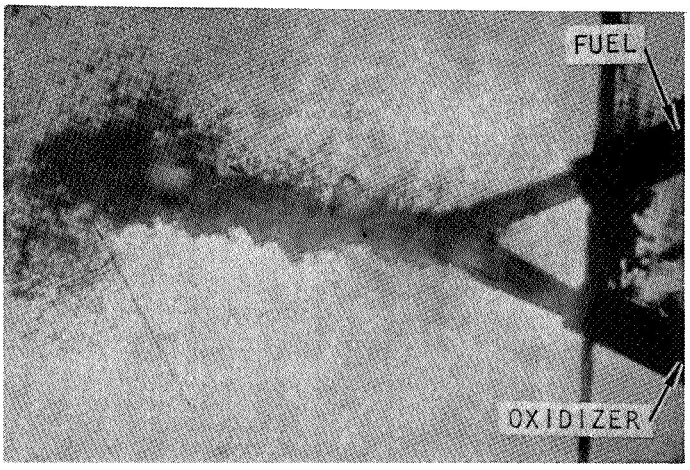

(a) Time = 0 milliseconds
(Edge of Spray Fan)

P_c = 13.7 psia

T_o = 40°F

T_F = 50°F

ϕ = 1.0

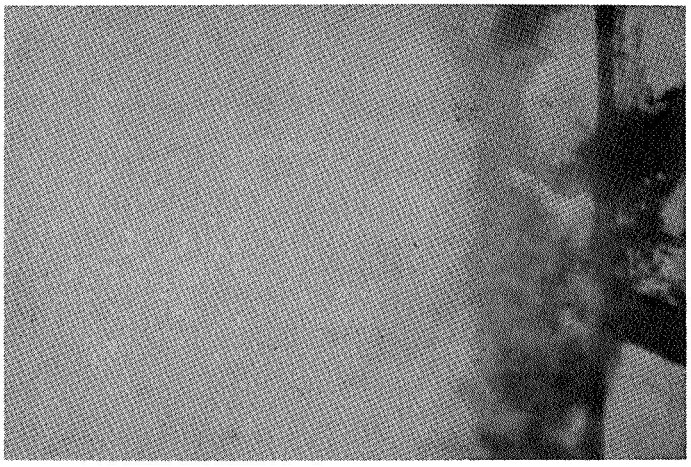

(b) Time = 1.5 milliseconds
(Reactive Stream
"Blowapart")

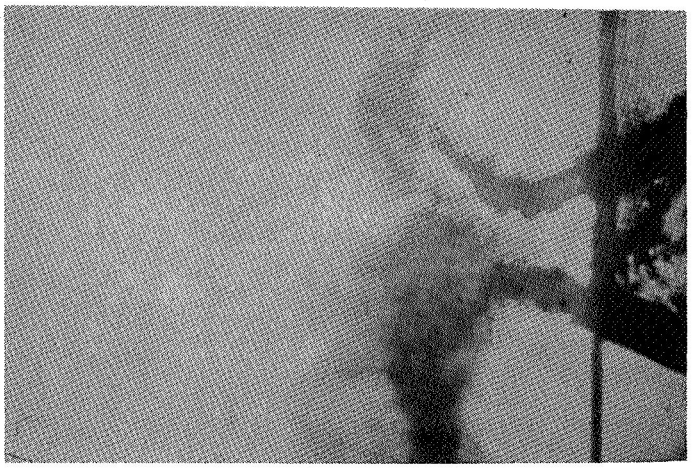

(c) Time = 2.2 milliseconds

Figure 13. Typical Sequence Showing Cyclic Behavior of NTO/Hydrazine Reactive Stream "Blowapart" with 0.173-Inch-Diameter (45° Impingement Angle) Unlike Impinging Stream Orifice Pair Element, Edge View of Spray Fan from Injector Face to 4 Inches Downstream, Run 13

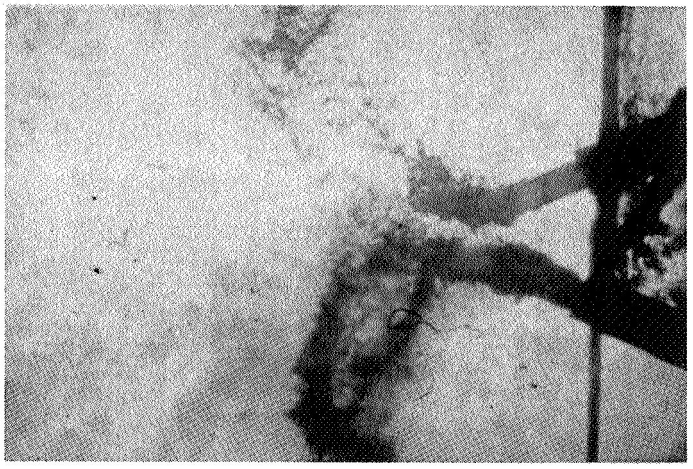

(d) Time = 3.0 milliseconds

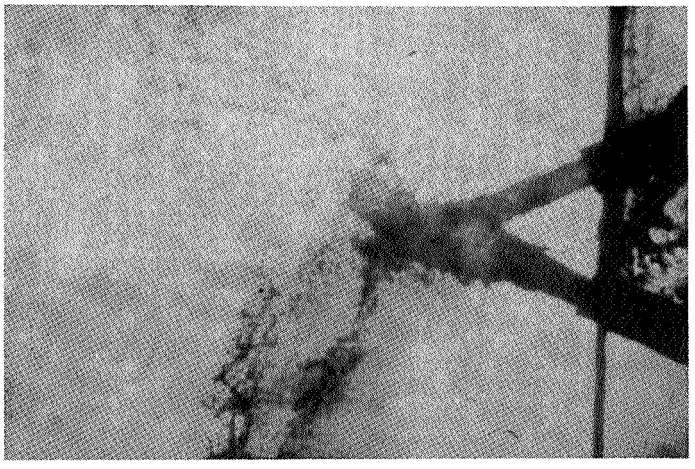

(e) Time = 3.7 milliseconds (Reimpingement)

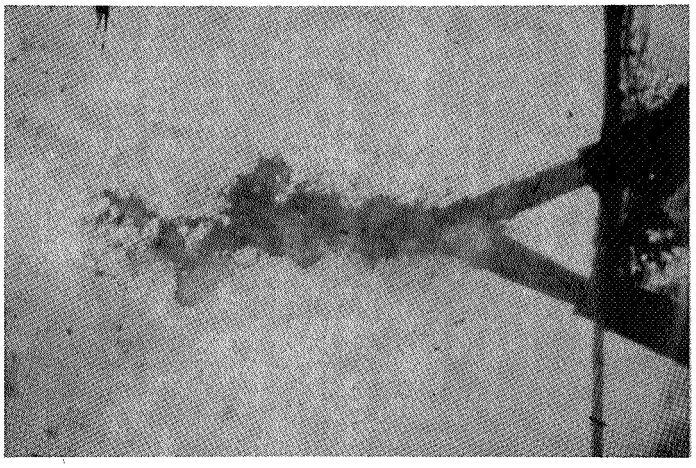

(f) Time = 6.6 milliseconds (Formation of New Spray Fan)

Figure 13. (Concluded)

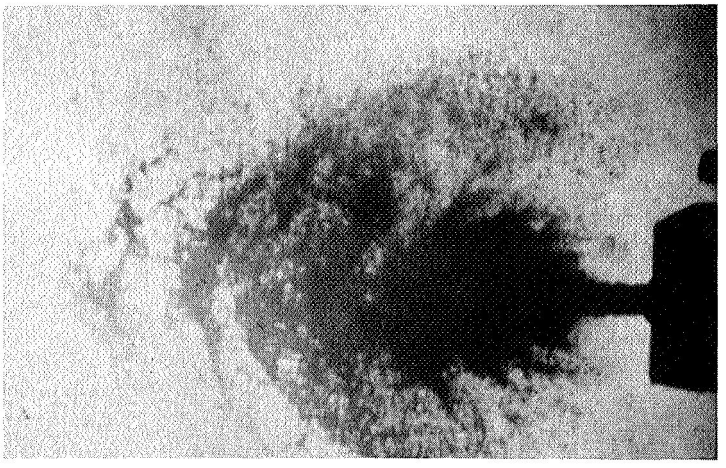

(a) Time = 0 milliseconds
(Fan View of NTO/
Hydrazine Spray Fan)

P_c = 13.7 psia

T_o = 50°

T_F = 60°

ϕ = 0.91

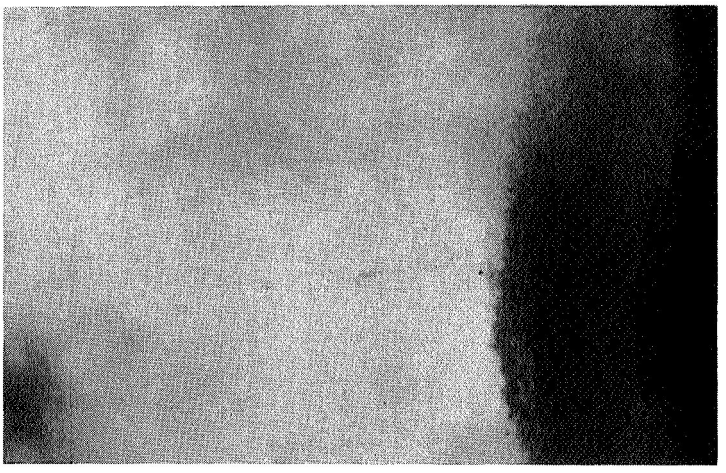

(b) Time = 1.3 milliseconds
(Reactive Stream
Blowapart)

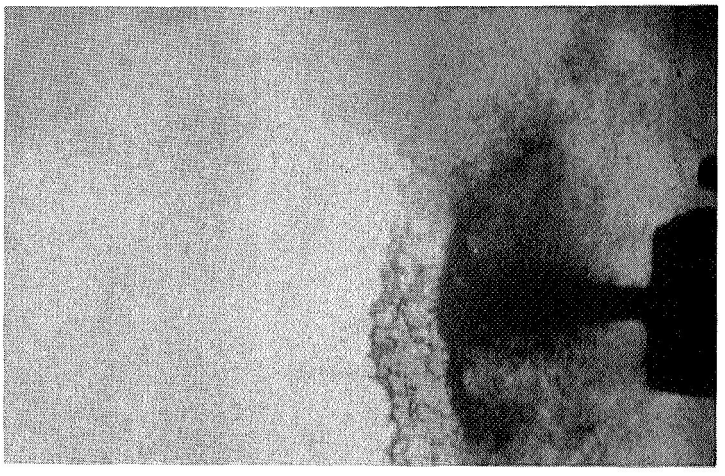

(c) Time = 2.2 milliseconds
(Reimpingement)

Figure 14. Typical Sequence Showing Cyclic Behavior of NTO/Hydrazine Reactive Stream Blowapart with 0.173-Inch-Diameter (45° Impingement Angle) Unlike Impinging Stream Orifice Pair Element, Fan View of Spray Fan From Injector Face to 4 Inches Downstream, Run 20

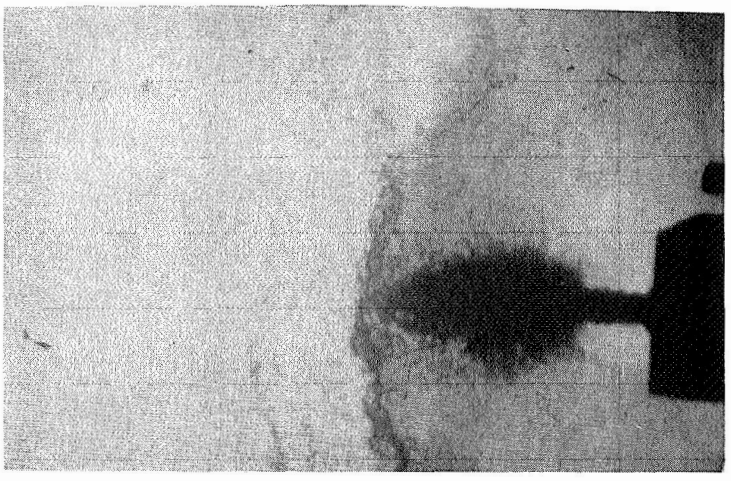

(d) Time = 3.1 milliseconds
(New Fan Begins to Form)

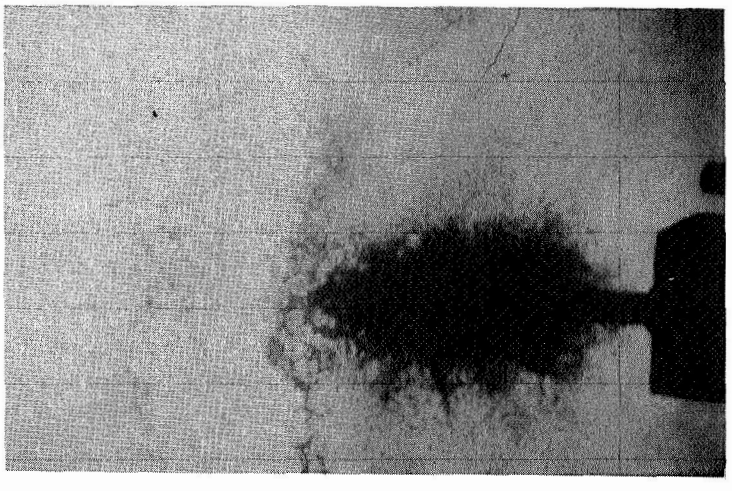

(e) Time = 3.9 milliseconds

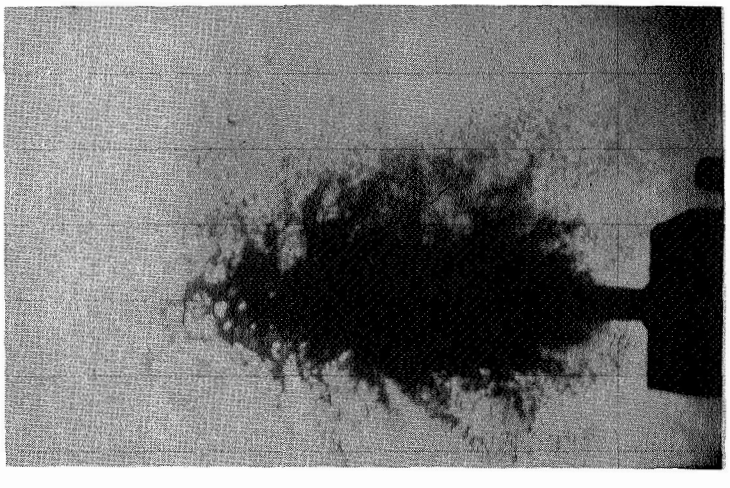

(f) Time = 5.2 milliseconds

Figure 14 (Concluded)

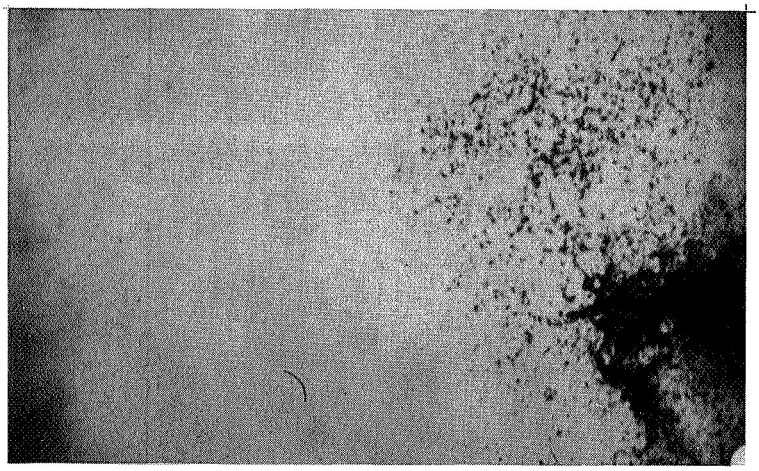

Injector is 2 Inches Beyond Right Border of Photograph

(a) Time = 0 milliseconds (Edge of Spray Fan)

P_c = 13.7 psia

T_o = 50°

T_F = 60°

ϕ = 0.69

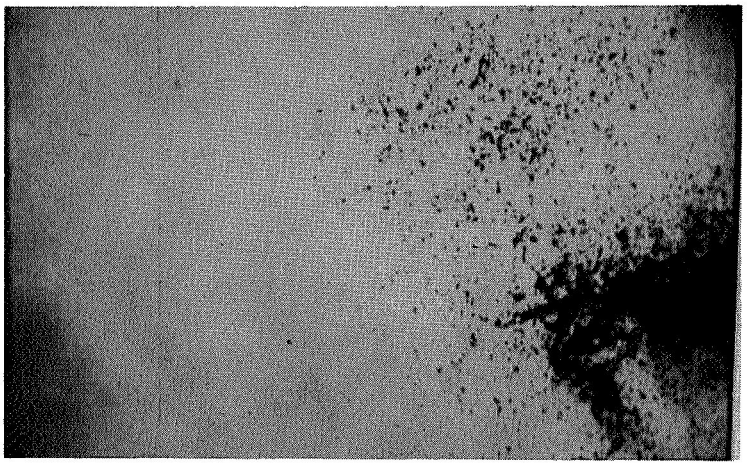

(b) Time = 0.34 millisecond (Condition Prior to Disturbance)

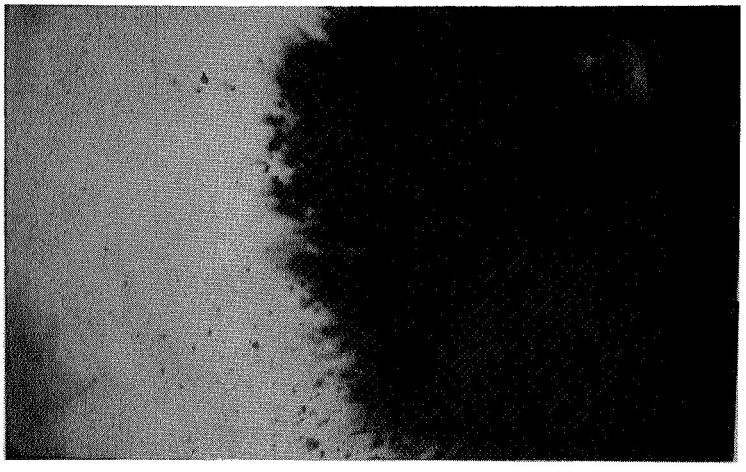

(c) Time = 0.67 millisecond (Reactive Stream Blowapart)

Figure 15. Typical Sequence Showing Cyclic Behavior of NTO/Hydrazine Reactive Stream Blowapart With 0.173-Inch-Diameter (45° Impingement Angle) Unlike Impinging Stream Orifice Pair Element, Edge View of Spray Fan From 2 to 6 Inches Downstream of Injector Face, Run 16

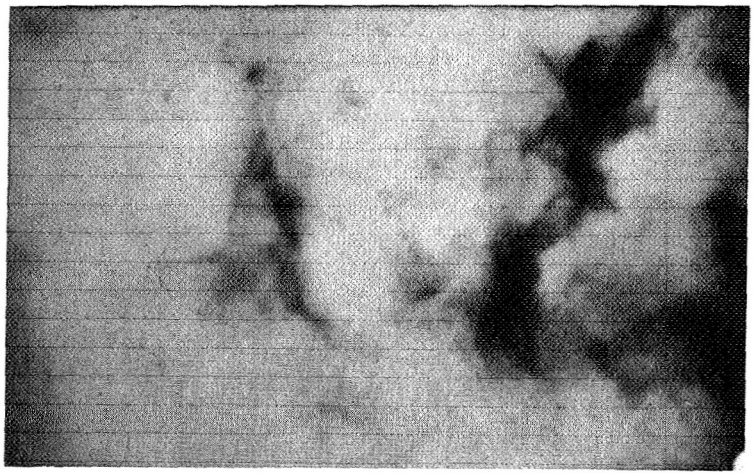

(d) Time = 1.0 milliseconds (Spray Shattered by Disturbance)

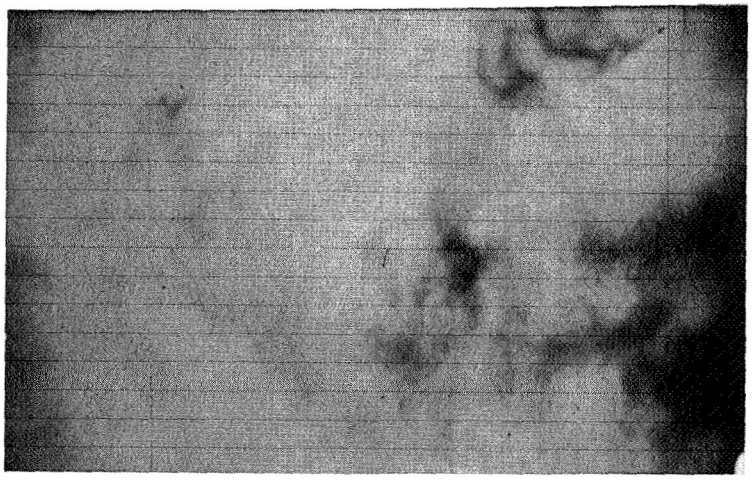

(e) Time = 1.3 milliseconds

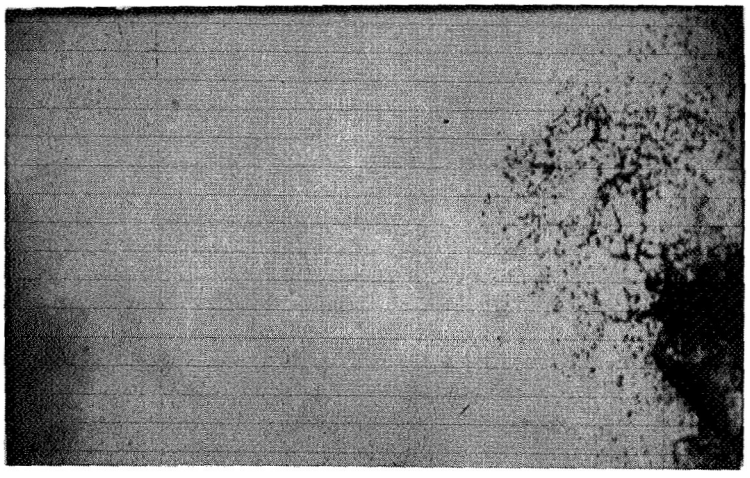

(f) Time = 5.8 milliseconds (Spray From New Fan)

Figure 15 (Concluded)

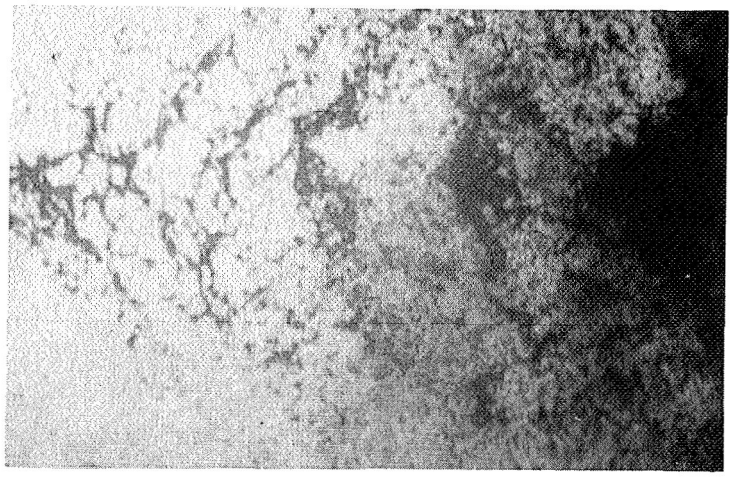

Injector Face 2 Inches
to the Right of Photographs

(a) Time = 0 milliseconds
(Downstream Fan View
of Spray Fan)

P_c = 13.7 psia

T_o = 50°F

T_F = 60°F

ϕ = 0.88

(b) Time = 1.8 milliseconds
(Reactive Stream
Blowapart)

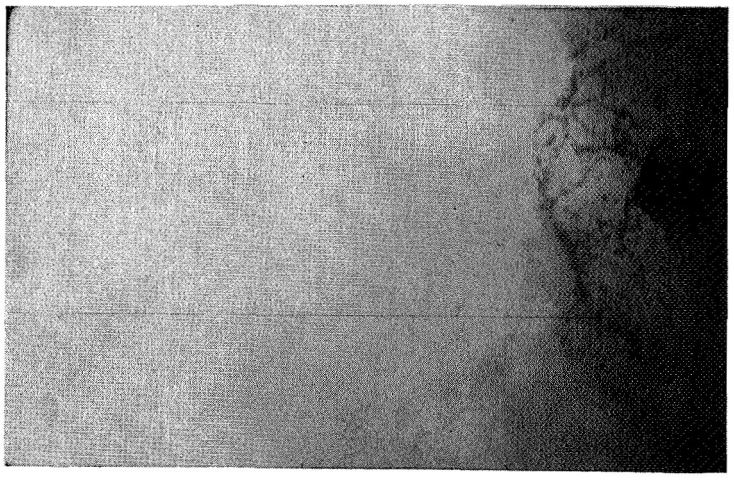

(c) Time = 4.0 milliseconds

Figure 16. Typical Sequence Showing Cyclic Behavior of NTO/Hydrazine Reactive Stream Blowapart With 0.173-Inch-Diameter (45° Impingement Angle) Unlike Impinging Stream Orifice Pair Element, Fan View of Spray Fan From 2 to 6 Inches Downstream of Injector Face, Run 19

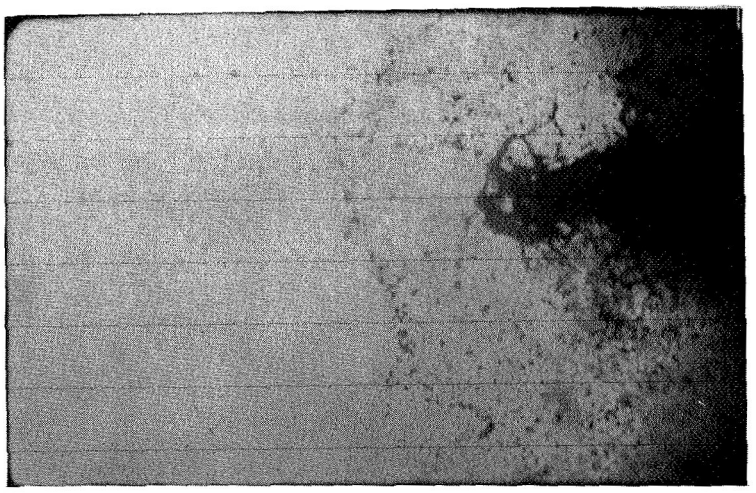

(d) Time = 5.3 milliseconds
(New Spray Fan Appears)

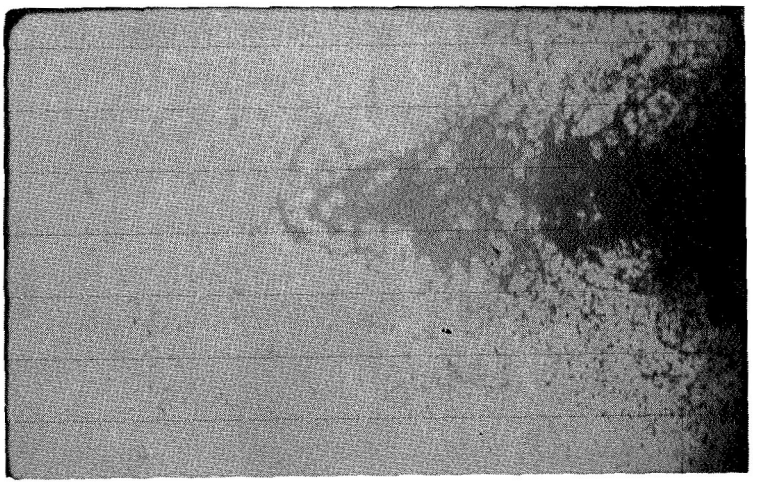

(e) Time = 7.1 milliseconds

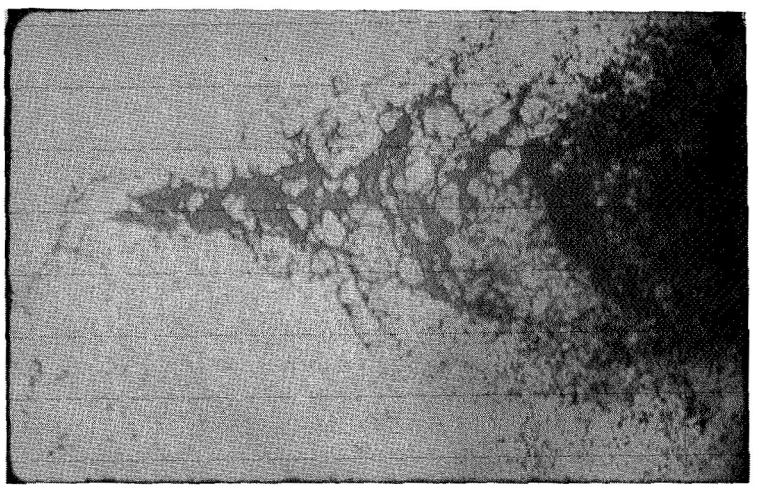

(f) Time = 8.9 milliseconds

Figure 16 (Concluded)

to insure that the rate of popping measured would not be limited by the response time of the feed system, but only by the ability of the disturbance to disrupt the impingement/mixing processes.

A typical sequence showing a disturbance is presented in Fig. 17. These results are very similar to those shown in Fig. 13 for the 45 degree impingement angle. However, while the magnitude of the disturbance was similar, the jets were not blown against the injector face. As shown the jets were "parted" and separation does occur at the impingement point. Flowrate measurements show that the flowrate was constant during the entire test. It should be noted that in the prior tests records show that the flow was temporarily interrupted when the disturbance occurred.

The sporadic disturbances causing temporary separation of the N_2O_4/N_2H_4 liquid streams appear to originate in the liquid phase just downstream of the jet centerline impingement point. The violence of these disturbances can be attested to by shattered plexiglass plates and frequently dislodged camera equipment.

Streak film records of these disturbances place the point of origin about 0.01-inch downstream (jet centerline) impingement. The disturbance propagates at an average speed (approximately equal in both the upstream and downstream directions) of 5150 ft/sec.

Experiments With the 0.072-Inch-Diameter Orifice Pair

Experiments with the 0.072-inch orifice pair (tests 22 and 23) consisted of Fastax photography tests as described in the following paragraphs.

Fastax Photography Tests. As seen in Fig. 18, obtained from run 22, blowapart was also found with the 0.072-inch orifice diameter injector. The sequence of events shown in this figure portray an event analogous to that seen with the large element. More prevalent, however, was what may be termed a "weak blowapart" as illustrated in Fig. 19. This differs qualitatively, in that a segment of the spray fan is obliterated by the

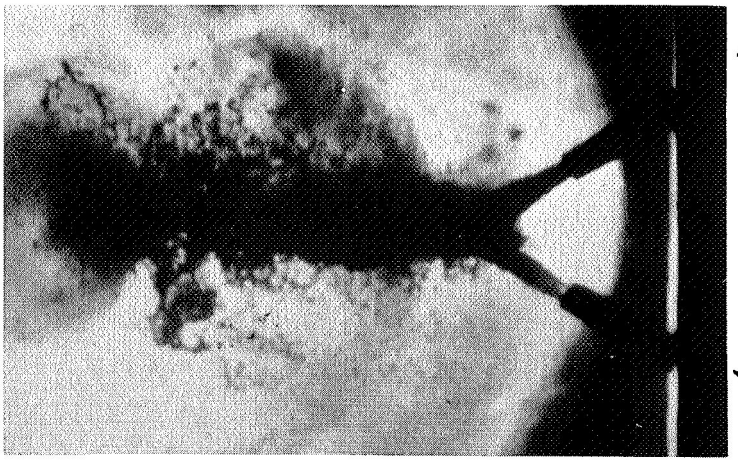

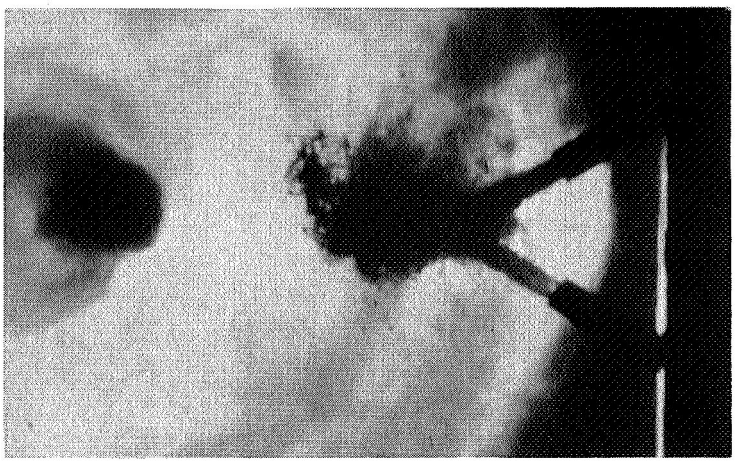

Figure 17. Typical Sequence Showing Cyclic Behavior of NTO/Hz Reactive Stream Blowapart with 0.173-inch (60° Impingement Angle) Diameter Unlike Impinging Stream Orifice Pair Element (Run 30)

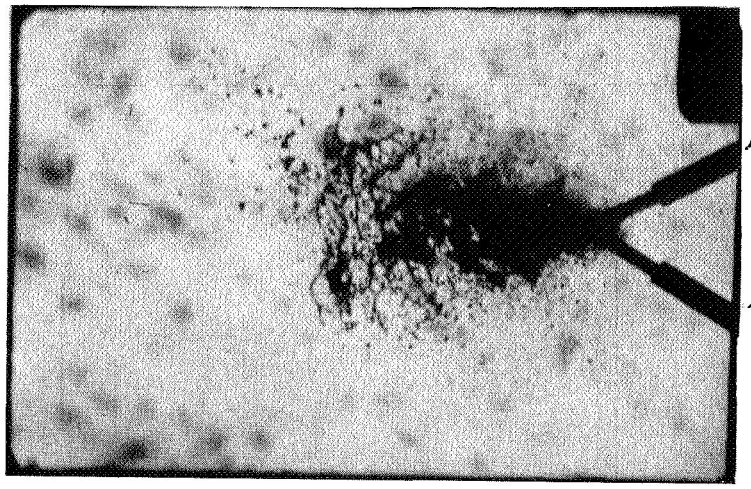

Fuel

(a) Time = 0 milliseconds
(Edge View of Formation
of Spray Fan)

Oxidizer

P_c = 13.7 psia
T_o = 50°F
T_F = 40°F
ϕ = 0.85

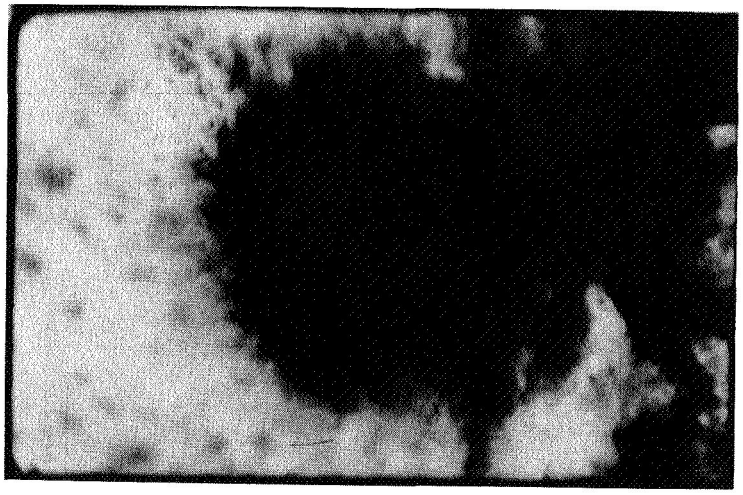

(b) Time = 0.19 milliseconds
(Disturbance Occurs)

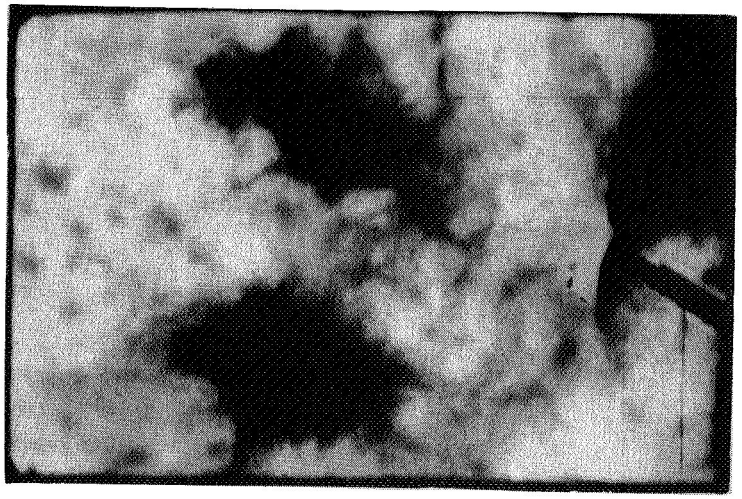

(c) Time = 0.37 milliseconds
(Streams Blown Apart)

Figure 18. Typical Sequence Showing Cyclic Behavior of NTO/Hydrazine Reactive Stream Blowapart With 0.072-Inch-Diameter (60° Impingement Angle) Unlike Impinging Stream Orifice Pair Element, Edge View of Spray Fan From Injector Face to 4 Inches Downstream, Run 22

(d) Time = 0.73 milliseconds (Spray is Consumed)

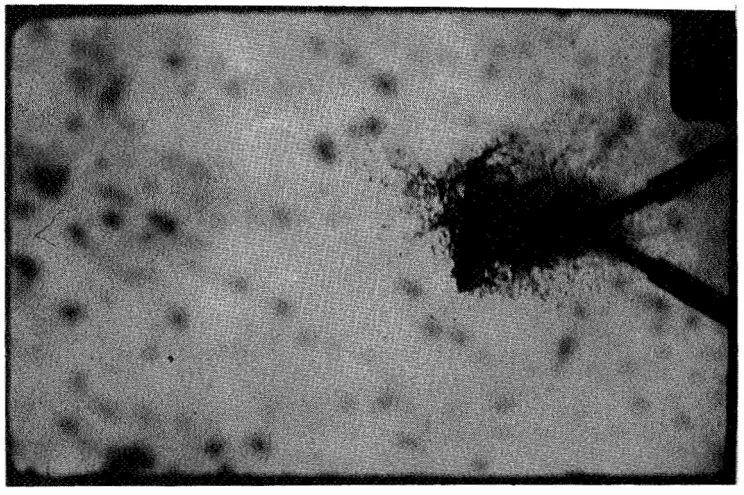

(e) Time = 2.0 milliseconds (Reformation of Spray Fan)

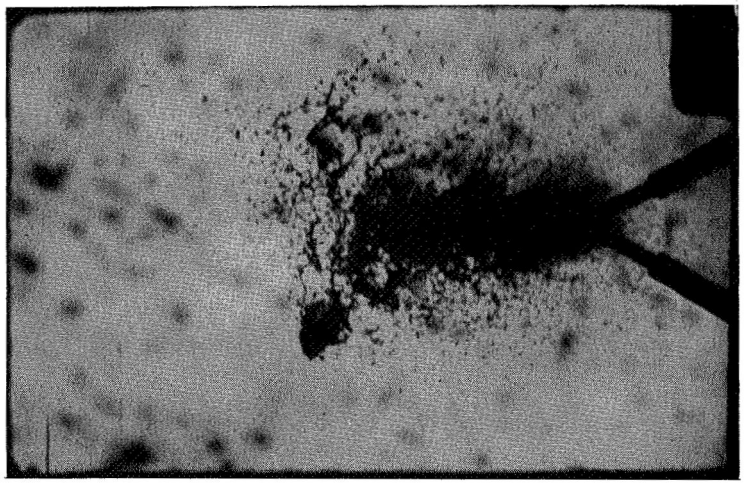

(f) Time = 3.4 milliseconds

Figure 18 (Concluded)

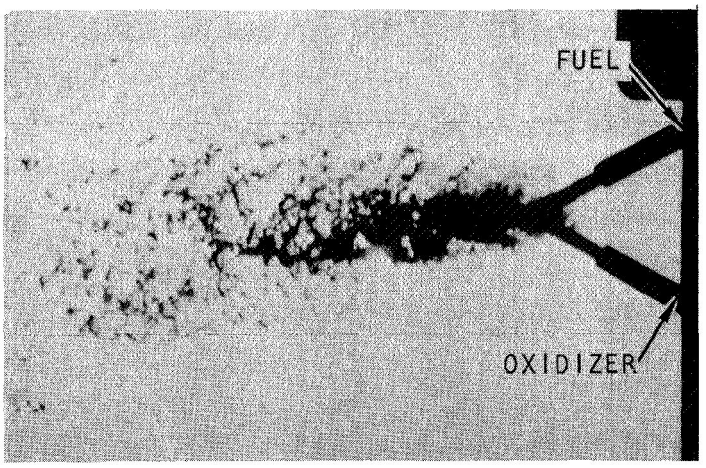

Fuel

(a) Time = 0 milliseconds (Edge View of Spray Fan)

Oxidizer

P_c = 13.7 psia

T_o = 50°F

T_F = 40°F

ϕ = 0.85

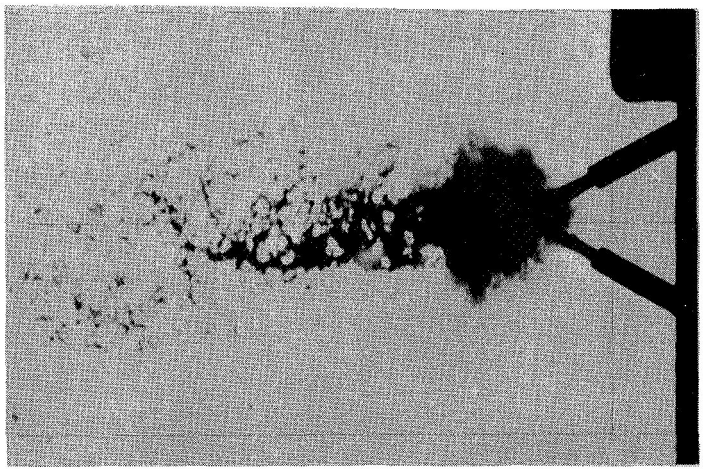

(b) Time = 0.19 milliseconds (Disturbance Appears)

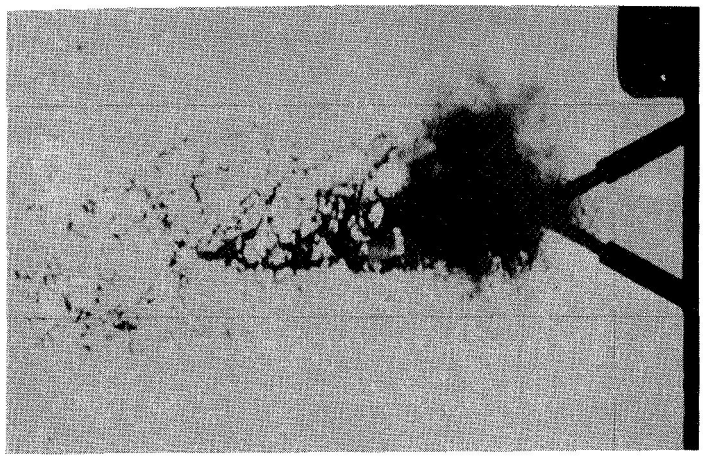

(c) Time = 0.39 milliseconds (Disturbance Grows)

Figure 19. Typical Sequence Showing Cyclic Behavior of NTO/Hydrazine Reactive Stream Weak Blowapart With 0.072-Inch-Diameter (60° Impingement Angle) Unlike Impinging Stream Orifice Pair Element, Edge View of Spray Fan From Injector Face to 4 Inches Downstream, Run 22

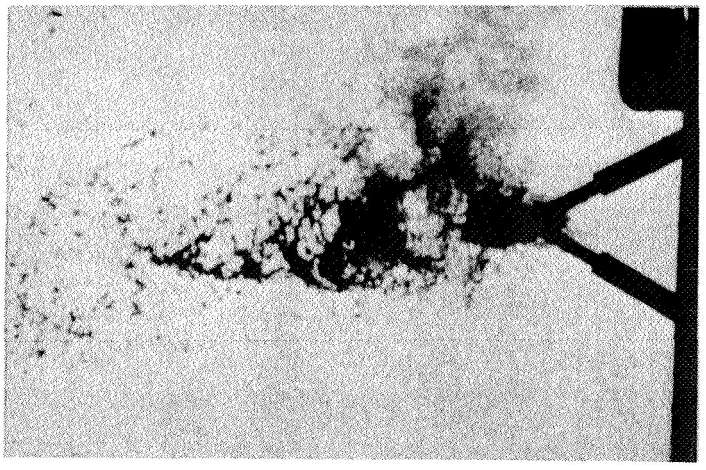

(d) Time = 0.78 milliseconds (Portion of Spray Fan is Consumed by the Disturbance)

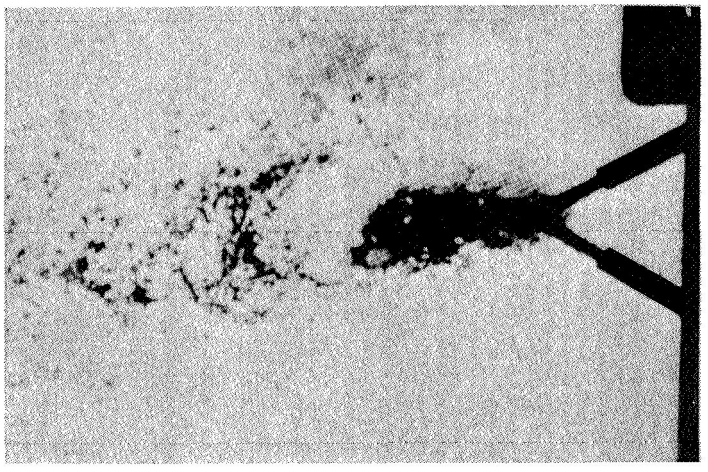

(e) Time = 1.8 milliseconds

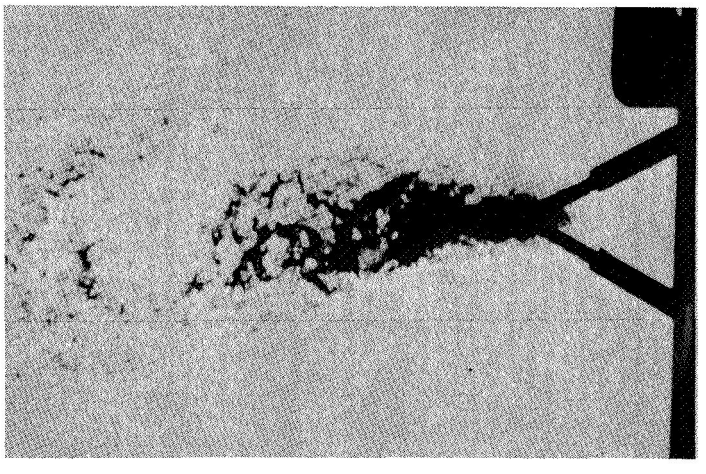

(f) Time = 3.1 milliseconds (Gap in Spray Field Moves Downstream)

Figure 19 (Concluded)

disturbance rather than the entire spray field. Occasional small "puffs" were also seen. These three types of disturbances are sufficiently different to be classed as distinct disturbance types*. There does not appear to be a continuous transition from one type to the other, although the mechanisms must be presumed to be closely related.

The net effect of decreasing injector orifice diameter (from 0.173 to 0.072 inch) at constant injection velocity appears to be that the number of (weak) Class B disturbances greatly increases at the expense of the (strong) Class A blowapart. These changes will be discussed in some detail in the Discussion of Results.

Decreasing the contact time (D/V) from approximately 1.2 to 0.95 sec further reduced the incidence of blowapart (all classes). No photographs are shown of this test condition (run 23) because the physical phenomena qualitatively were similar to those presented in Fig.18 and 19.

*For convenience in subsequent discussion, the disturbance types will be referred to as A, B, and C in order of decreasing magnitude.

NITROGEN TETROXIDE (NTO)/50% HYDRAZINE + 50% UDMH (50-50) RESULTS

Experiments conducted with the propellant combination NTO/50-50 utilized the 60-degree impingement angle 0.173-inch-orifice element. A cavitating venturi was used upstream of the element and the propellants were chilled to insure that flashing would not occur upon injection. Experiments were conducted at constant contact time (i.e., element flow conditions constant) at both atmospheric pressure and at an elevated pressure of 200 psia. High speed Fastax movies were taken during these tests.

Atmospheric Pressure

Three NTO/50-50 tests were conducted using the Fastax camera with strobe back lighting. In the first test (41) two sheets of pyrex glass were mounted on either side of the combustion zone to protect the camera equipment. Splash-back on the glass plate in front of the camera caused some distortion and lack of detail in the coverage. In tests 42 and 43 various setups were tried with similar results, therefore, the pyrex glass plate was removed from in front of the camera in all succeeding tests.

The general observations from the atmospheric pressure movies is that the incidence of strong (Class A) blowapart is much less than that which occurred with the 0.173-inch element using NTO/Hz propellants. There were a significant number of Class B type blowapart disturbances and some Class C weak blowaparts. A typical sequence of photographs showing a Class A blowapart at atmospheric pressure is presented in Fig. 20. Note that the jets are separated at the impingement point and all of the propellants downstream are consumed.

Shown in Fig. 21 is an example of a type B blowapart which occurred at atmospheric pressure wherein the disturbance causes a "puff" or pulsation in the impingement/mixing process. These results are quite similar to those of the 0.072-inch diameter element using NTO/Hz propellants.

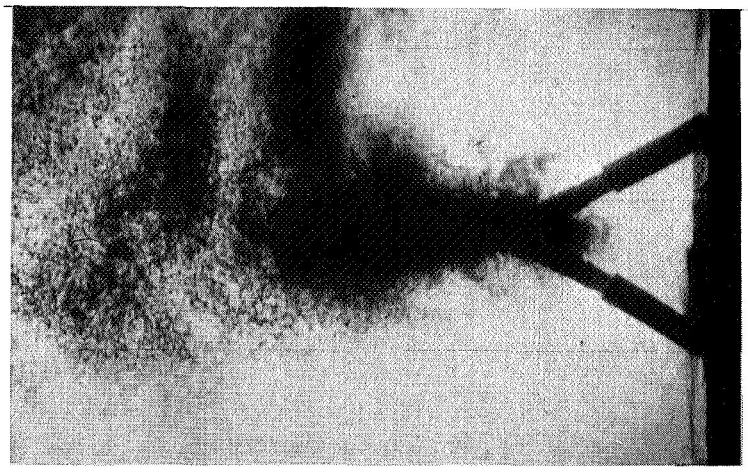

Time = 0 m sec (edge view of spray fan)
P_L = 13.7 psia
T_o = 40°F
T_f = 50°F
ϕ = 1.0

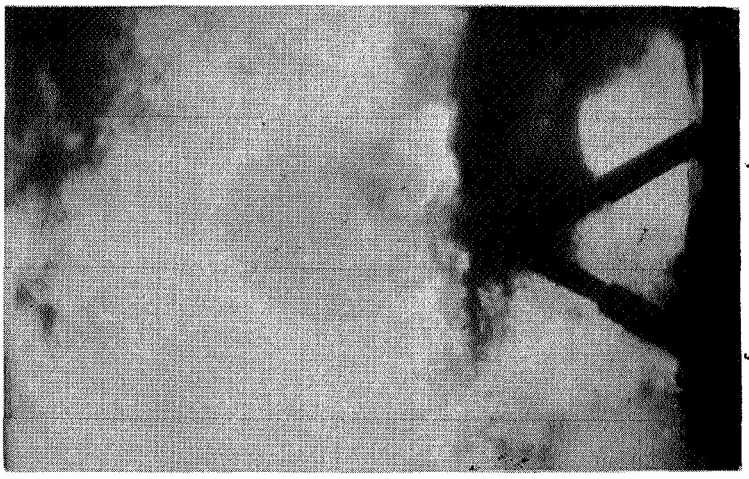

Time = 3.8 m sec
(stream blown apart)
←Oxidizer
←Fuel

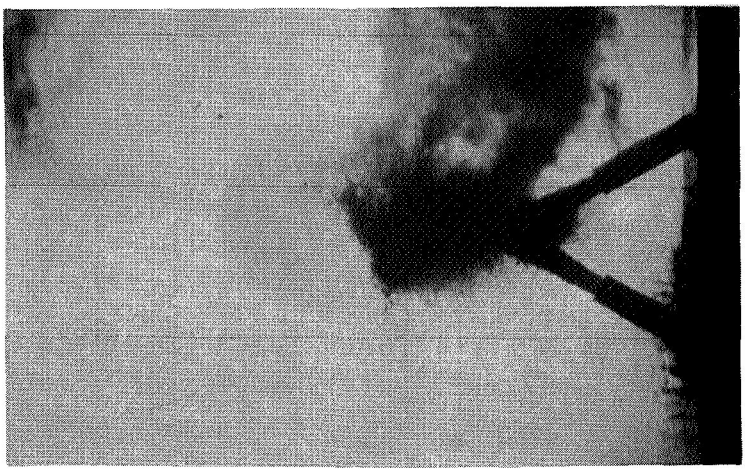

Time = 7.7 m sec
(stream reattaching)

Figure 20. Typical Sequence Showing Cyclic Behavior of NTO/50-50 (Class A Blowapart) Reactive Stream Blowapart with 0.173-inch (60° Impinging Behavior) Diameter Unlike Stream Orifice Pair Element (Run 45)

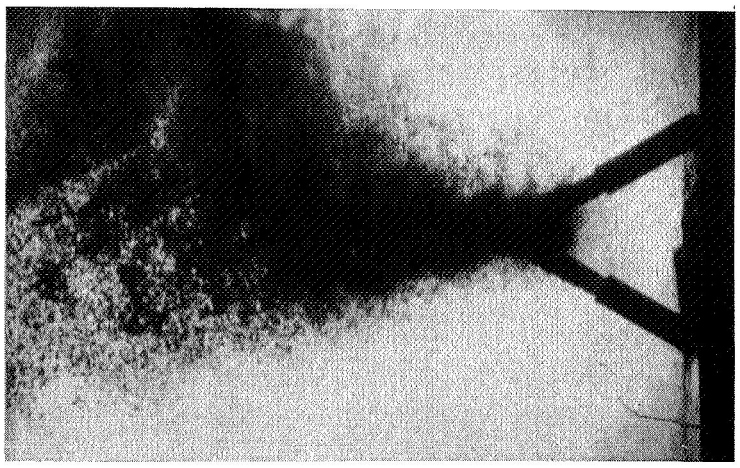

Time = 0 m sec (edge view of spray fan)
P_c = 13.7 psia
T_o = 40°F
T_f = 50°F
ϕ = 1.0

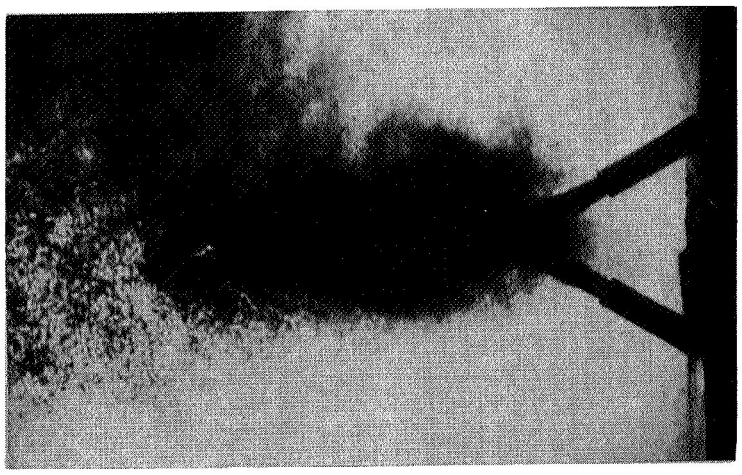

Time = 5.4 m sec
(disturbance)
Oxidizer
Fuel

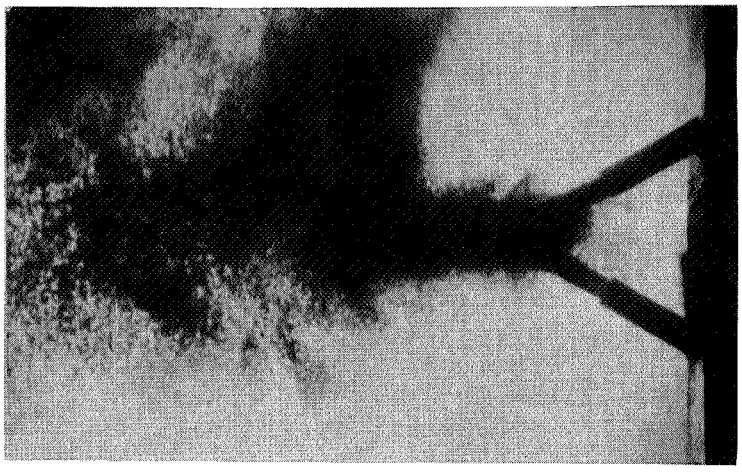

Time = 11.5 m sec
(spray fan reformation)

Figure 21. Typical Sequence Showing Cyclic Behavior of NTO/50-50 Class B Reactive Stream Blowapart with 0.173-inch (60° Impingement Angle) Diameter Unlike Impinging Stream Orifice Pair Element (Run 45)

In comparing the overall atmospheric pressure results with those obtained with NTO/Hz it is obvious that the propellant combination had a significant influence on the type of blowapart which occurred. That is, for the 0.173-inch NTO/Hz experiments almost all the explosions were strong (Class A), while relatively few strong Class A blowaparts occurred for the NTO/50-50 propellants. It also appears that the change in propellant combination had the same effect on the levels of blowapart strength as the reduction in orifice size had for the NTO/Hz propellants, since the Class B and C explosions became predominant with NTO/Hz when the orifice size was reduced to 0.072 inch.

The motion pictures provided a good view of the downstream flow field, including individual droplets. Backflow from the point of impingement was also clearly evident. Color distinction could be made only at the edges of the flow field. The reddish oxidizer vapor was easily distinguishable from the darker liquid droplets and fuel vapor.

Elevated Chamber Pressure

Experiments were also run at elevated chamber pressure using the special chamber discussed under "Apparatus". A total of five test firings (runs 52 - 56) were conducted using the 0.173-inch-diameter unlike-doublet injector and the N_2O_4/50-50 propellant combination. A tabulation of the test run conditions is contained in Table II .

Initially, test 52 was conducted as a checkout firing followed by tests 53 - 56, which were run at approximately 230 psia chamber pressure with element dynamic pressure ratios ($\rho_f V_f^2/\rho_o V_o^2$) varying from 0.96 to 1.5. Additionally, window purge pressure was varied to evaluate purge effectiveness in reducing spray deposition on the view windows.

Fastax film records show that excessive N_2O_4 vapor obscured view of the spray throughout the duration of run 52. The typical sequence of events for runs 53 - 56 was characterized by (1) visual initial injection and combustion of the spray, followed by (2) a period (approximately 200

milliseconds) during which the spray was completely obscured by combustion gases and vapors, and (3) subsequent clearing of the gases and vapors to provide a visual record of the reacting spray impingement and combustion. Variable window purge pressures did not significantly change visual clarity on successive runs. Some degree of N_2O_4 vapor recirculation reduced clarity of the stream impingement zone on all tests. However, the mode of stream separation was satisfactorily defined. Typical photographic results are presented in Fig. 22 . These film records show that "stream separation" was characterized by a "cyclic" blowapart which was in the Class B and C range. No Class A type blowapart was observed. These results appear to be quite similar to those observed at atmospheric pressure.

INHIBITED RED FUMING NITRIC ACID (IRFNA)/
UNSYMMETRICAL DIMETHYL HYDRAZINE (UDMH) RESULTS

Experiments with IRFNA/UDMH were conducted with the 60 degree impingement angle 0.173-inch-orifice element. These experiments were conducted in "open air" and the dynamic pressure ratio was approximately 1.0. High speed movies were taken of the impingement/mixing process.

For the IRFNA/UDMH propellant combination very weak Class C type blowapart predominated with some Class B type also occurring. Typical photographs showing the disturbances are presented in Figures 23 and 24. These results again show that at equal values of propellant operating conditions the choice of propellant combination is extremely important, affecting the strength of blowapart which will occur. The magnitude of the explosions decreased in the order NTO/Hz > NTO/50-50 > IRFNA/UDMH.

CHLORINE PENTAFLUORIDE (CPF)/
HYDRAZINE (Hz) RESULTS

Using CPF/Hz propellants, two variables were investigated (1) orifice size, resulting in variation in D/V, and (2) dynamic pressure ratio. Orifice size was varied from 0.173 to 0.026-inch and dynamic pressure ratio was varied from 0.6 to 1.6 ($\rho_f V_f^2/\rho_o V_o^2$). High speed movies were taken during these runs.

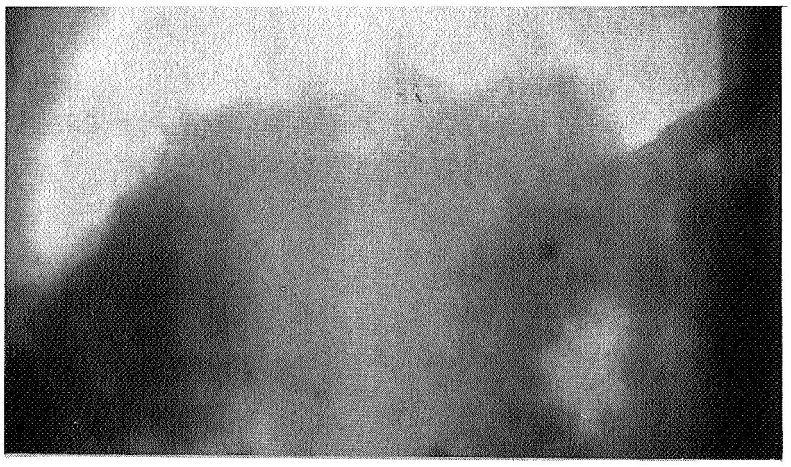

Time = 0 m sec
P_c = 225 psia
T_o = 40°F
T_f = 45°F
ϕ = 1.1

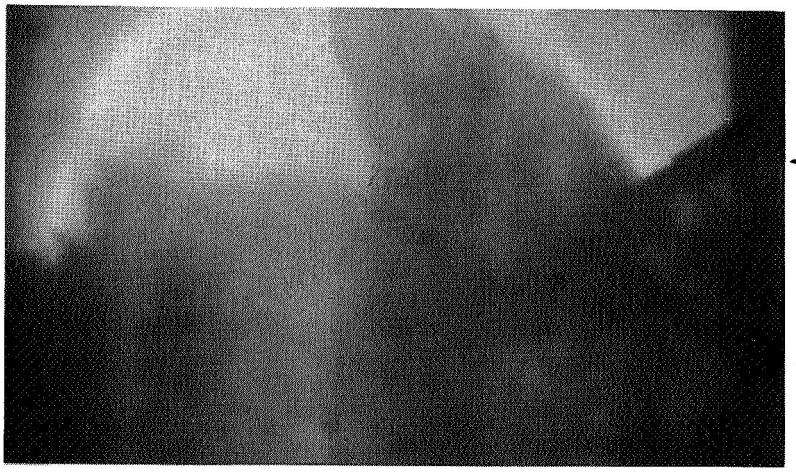

Time = 6.2 m sec
Oxidizer
Fuel

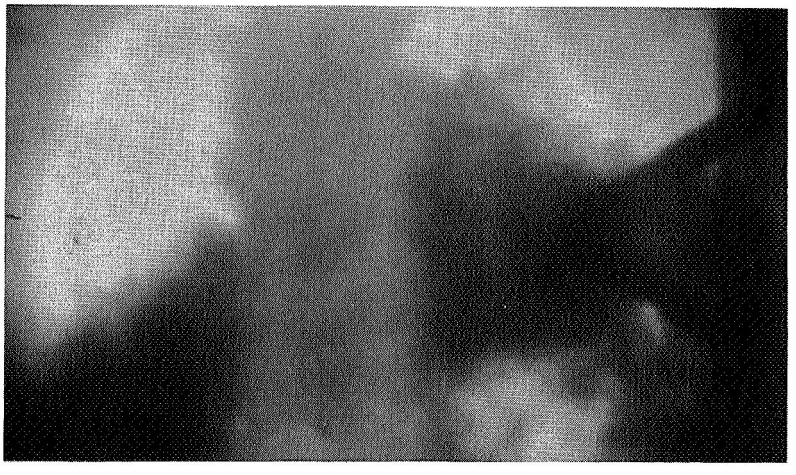

Time = 7.7 m sec

Figure 22. Typical Sequence Showing Cyclic Behavior of NTO/50-50 Class B/C Reactive Stream Blowapart with 0.173-inch (60° Impingement Angle) Diameter Unlike Impinging Stream Orifice Pair Element (Run 54)

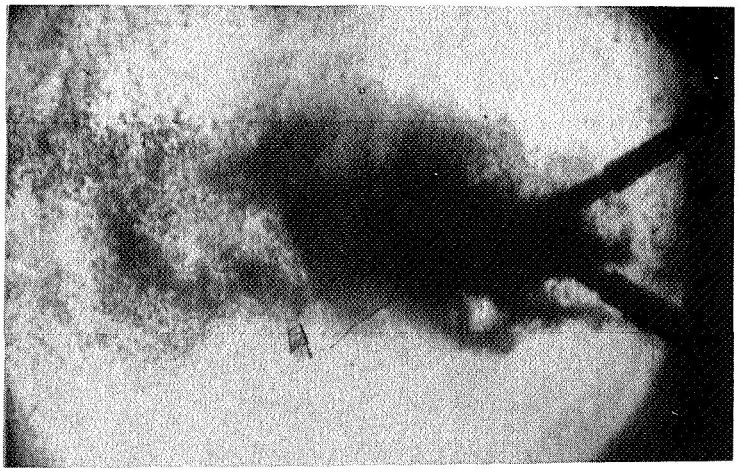

Time = 0 m sec (spray fan)
P_c = 13.7 psia
T_o = 35°F
T_f = 50°F
ϕ = 1.1

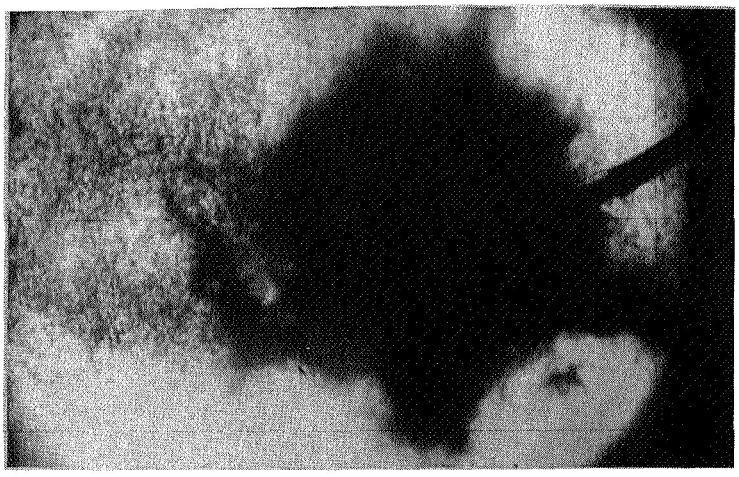

Time = 4.6 m sec
(disturbance)
←Oxidizer
←Fuel

Time = 10 m sec
(spray fan reformation)

Figure 23. Typical Sequence Showing Cyclic Behavior of IRFNA/UDMH (Class B) Reactive Stream Blowapart with 0.173-inch (60° Impingement Angle) Diameter Unlike Impinging Stream Orifice Pair Element (Run 54)

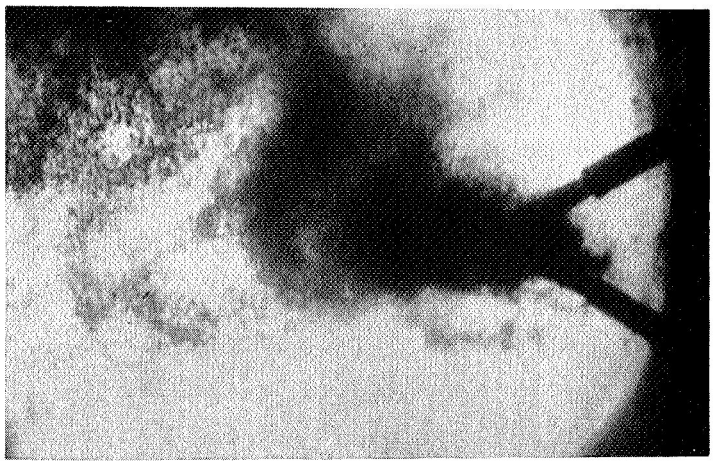

Time = 0 m sec (spray fan)
P_c = 13.7 psia
T_o = 35°F
T_f = 50°F
ϕ = 1.1

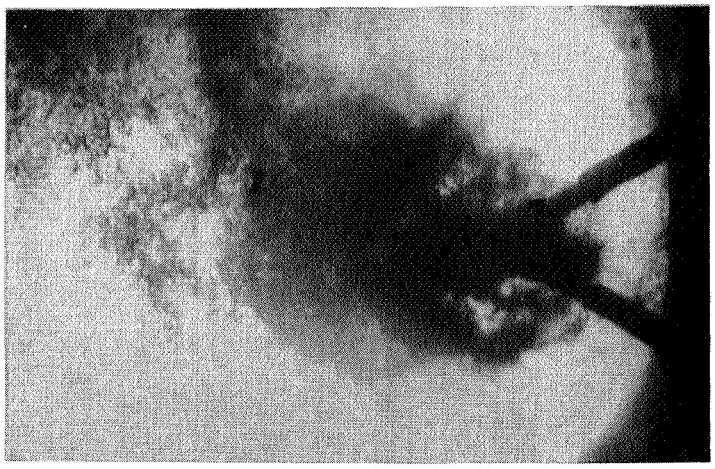

Time = 4.6 m sec
(Disturbance)
Oxidizer
Fuel

Time = 6.9 m sec
(spray fan Reformation)

Figure 24. Typical Sequence Showing Cyclic Behavior of IRFNA/UDMH (Class C) Reactive Stream Blowapart with 0.173-inch (60° impingement angle) Diameter Unlike Impinging Stream Orifice Pair Element (Run 54)

0.173-Inch-Diameter Orifice Tests

The impingement process recorded for CPF/N_2H_4 with the 0.173-inch-orifice doublet is characterized by apparently continuous stream separation. Although distinction between the oxidizer and fuel sprays could not be made downstream of impingement, it appears as though each jet is reflected from the fan centerline as a separate spray at approximately the angle of incidence. As a result, the region directly downstream of impingement is essentially void of propellant. This result is shown in the photograph shown in Fig.25. Note that only one picture is presented due to the steady-state nature of the separation.

Special care was taken during these tests to insure that the CPF was sufficiently chilled (-10°F) so that flashing would not occur after injection. Orifice ΔP and flowrate measurements substantiate that no detectable 2-phasing of propellant occurred within the orifices, and temperature measurement verified the required low temperature propellant condition.

These data represent the first definitive record of continuous hypergolic propellant stream separation.

0.026-Inch-Diameter Orifice Tests

An attempt was made to evaluate the impingement/mixing process at much shorter contact times by utilizing a 0.026-inch-diameter element. This design resulted in an approximate reduction in D/V of 6. In addition, the effect of dynamic pressure ratio at this low contact time was also studied.

Presented in Fig.26 are the results obtained at three different dynamic pressure ratios, 0.85, 1.29 and 1.62. In all cases the flow process at the impingement point was invarient with time. At dynamic pressure ratios of 0.85 and 1.29 the streams separated as was the case for the 0.173-inch orifice.

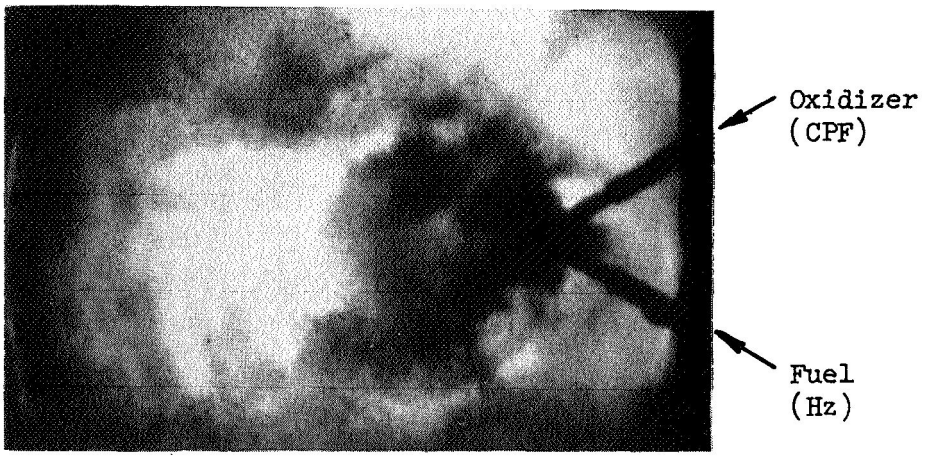

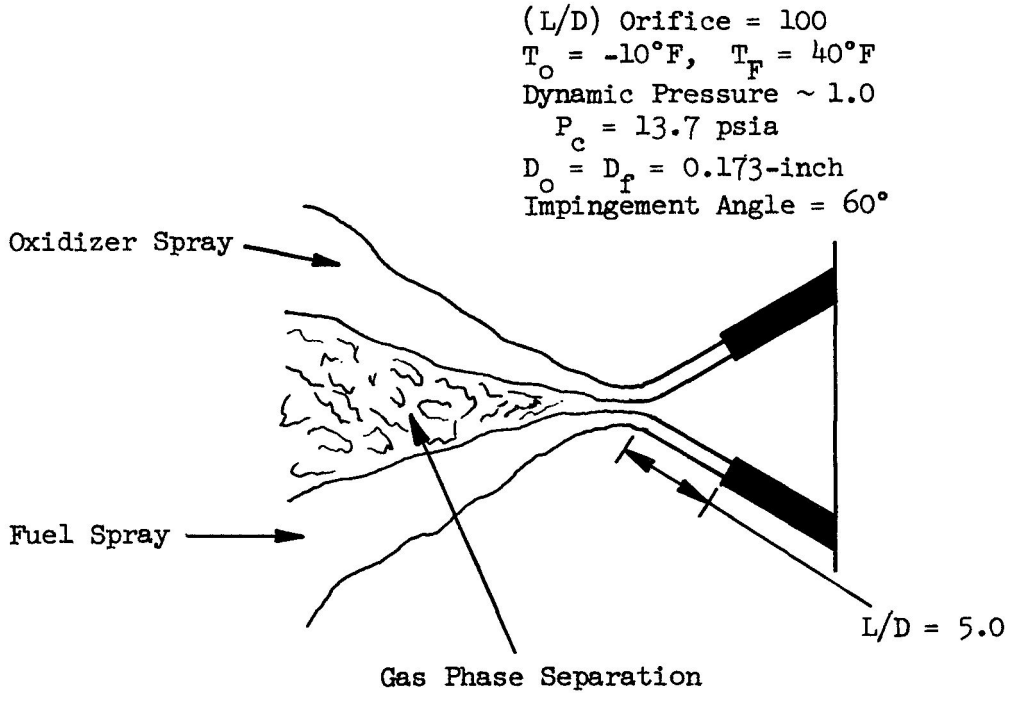

Figure 25. Continuous Blowapart for ClF_5/N_2H_4 with 0.173-inch Diameter Unlike Impinging Stream Orifice Pair (Run 40)

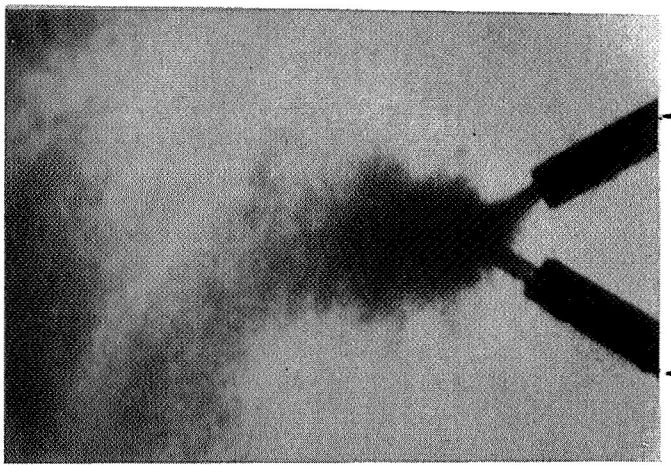

ϕ = 1.62

ϕ = 1.35

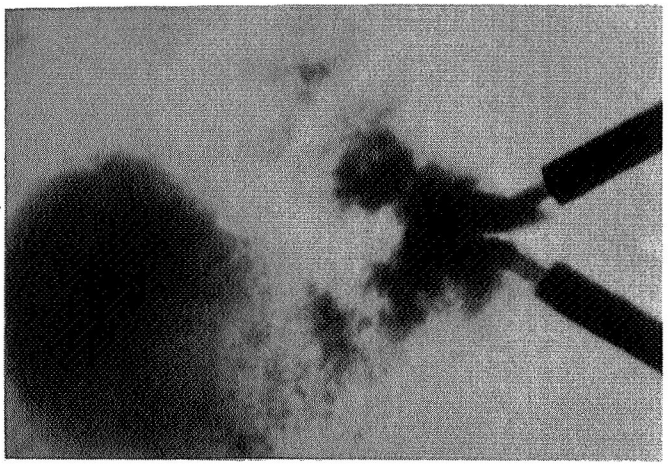

ϕ = 0.80

Figure 26 . Effect of Dynamic Pressure Ratio on Separate/Mix for CPF/Hz Propellants Using a 0.026-inch Diameter Unlike Impinging Stream Orifice Pair Element

It appears from the photographs that the streams are indeed reflected at the impingement point with little or no mixing. Although not cyclic in terms of a disturbance the movies do show that the streams will actually part at the impingement point momentarily then come closer and then repeat this process. This could be the result of the gases building up pressure within the impingement zone until the forces cause a momentary escape of the gases.

At a dynamic pressure ratio of 1.62 the jets appear to mix. This suggests that the mixing is indeed caused by the dynamics of the jets. These results clearly demonstrate that both mixing and separation can occur, depending upon the injector design conditions.

DISCUSSION OF RESULTS

The photographic results were analyzed in terms of the rate of explosion, or "pops", and the classification of the magnitude of the disturbances. These rate measurements with the several propellant combinations used in this program were then compared at equivalent operating conditions. In addition, streak measurements taken during several tests with NTO/Hz were analyzed to determine the speed and initiation point of the disturbance. While the objective of this study was not a detailed determination of the limits of blowapart, the results did yield some information on the effects of several operating parameters on the magnitude and rate of popping. These results are discussed and compared. Unfortunately the scope of the program does not allow a thorough comparison of these results with other data which was generated before and during this study by other investigators, or a detailed analysis including a blowapart model. An attempt is made to discuss several of the more pertinent studies and make overall comparisons of their results with those obtained during this program.

DESCRIPTION OF CYCLIC BLOWAPART PHENOMENA

As observed with the system NTO/hydrazine at 40 to 60°F, injected from unlike-doublet elements with equal diameter (0.173-inch) orifices, blowapart involved the following typical sequence of events.

1. Formation of a spray fan similar in shape to that formed by non-reactive liquids. Downstream of the fan were abundant quantities of propellant droplets. Close examination of the movies suggests that the spray fan may show some lamination with more fuel on the fuel jet side and vice versa. Nevertheless, during this period the propellants remain in contact and are "mixed", at least within the small dimension corresponding to the spray sheet thickness.

2. Apparent detonations or explosive deflagrations occur in which virtually the entire existing sprayfield is gasified. The fuel and oxidizer jets are literally blown apart and back toward the injector face. Following this, separate clouds of fuel and oxidizer spray droplets are seen which move downstream without mixing.

3. The jets gradually reform and again develop a spray fan.

Similar, but weaker, disturbances also occurred in which only portions of the spray fan were consumed by the explosion. These latter disturbances became predominant for NTO/Hz with smaller diameter orifices (0.072 inches).

As observed with the NTO/50-50, or IRFNA/UDMH propellants, the cyclic blowapart is similar to that described for the NTO/Hz propellants. However, for NTO/50-50 and IRFNA/UDMH propellants the typical magnitude of the disturbance was much less. Very few strong explosions occurred and the process was in fact very similar to that observed with NTO/Hz with the 0.072-inch orifice element.

DESCRIPTION OF STEADY-STATE BLOWAPART

Steady-state blowapart was also observed during this program when CPF/Hz were used as the propellants. For this case as the jets approached each other, propellant gasification near the plane of intersection caused sufficient forces between the jets to divert the streams away from the impingement point. The angle of diversion is approximately equal to the impingement angle (included angle 60 degrees). The diversion of the jets resulted in no further mixing of the propellants and unmixed spray was observed to persist several inches downstream of the impingement point.

PROPELLANT SPRAY OBSERVATIONS

Nature of the Disturbance

Throughout this report the word "disturbance" has been used with regard to the cyclic blowapart phenomena because of uncertainty regarding the detailed nature of the phenomenon which blows apart the injected propellant streams

or disrupts the spray fan. For NTO/Hz with the intermediate size injector, spherically shaped bursts of shattered propellant spray are characteristically seen. These can be seen in successive frames, growing relatively slowly. These may represent some type of explosive deflagration, although at this point this is still speculation.

High speed streak movies were taken of the flow from the impingement point to approximately 3-inches downstream. The film was orientated as shown in the sketch below (Fig. 27)

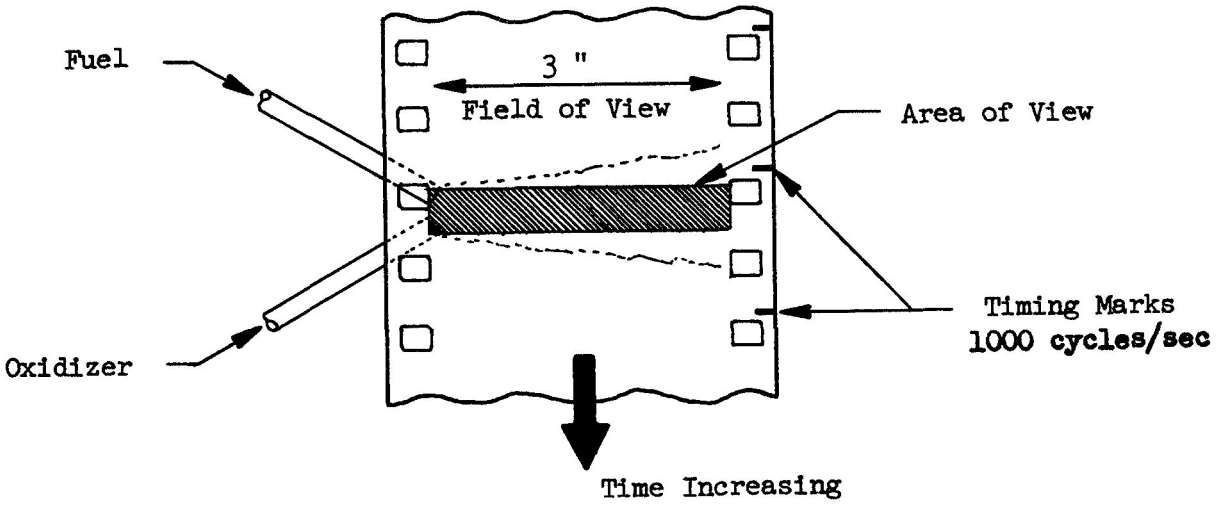

Figure 27. Orientation of Film with Respect to Injector Fan

The average film speed was 4200 frames/sec. An enlarged photograph of a typical disturbance pattern is shown in Fig. 28. Note that the high velocity waves, appear in pairs, noted in the figure as "initial" and "secondary" disturbances. Two such pairs are seen in the photograph. The initial and secondary waves are separated in time by about 0.2 msec. Reduction of the time/distance characteristics recorded on this photograph shows that the initial disturbance originates just slightly downstream of the impingement point. The location of initial disturbance is determined by the minimum slope shown in the photograph. There is a minimum because the disturbance is traveling both upstream and downstream from the point of initiation. This origin of the initial disturbance is about 0.01-inch downstream of the jet impingement point. Analysis from other disturbances also recorded on

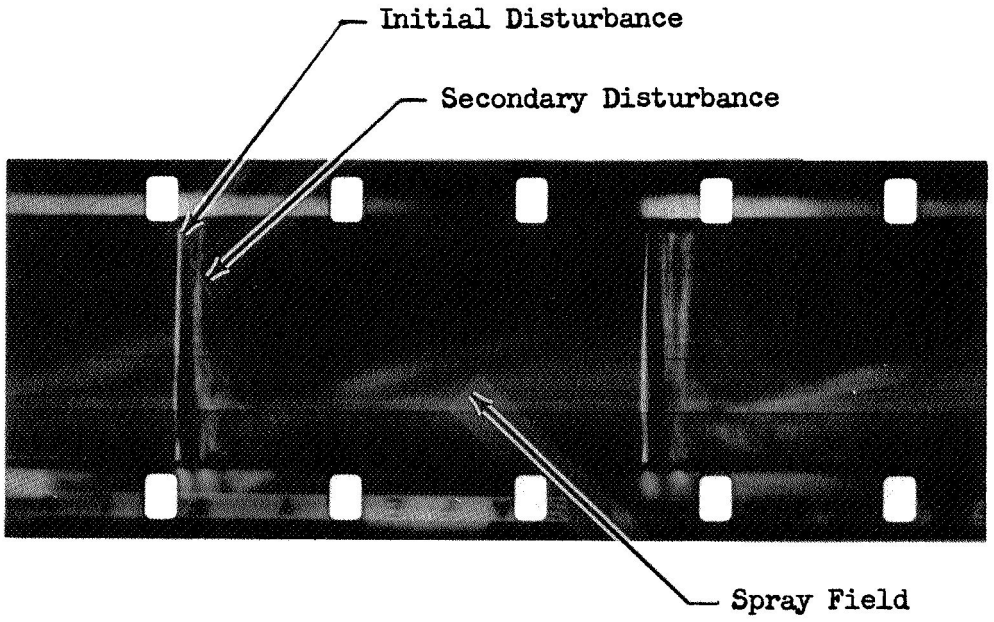

(a) STREAK PHOTOGRAPH

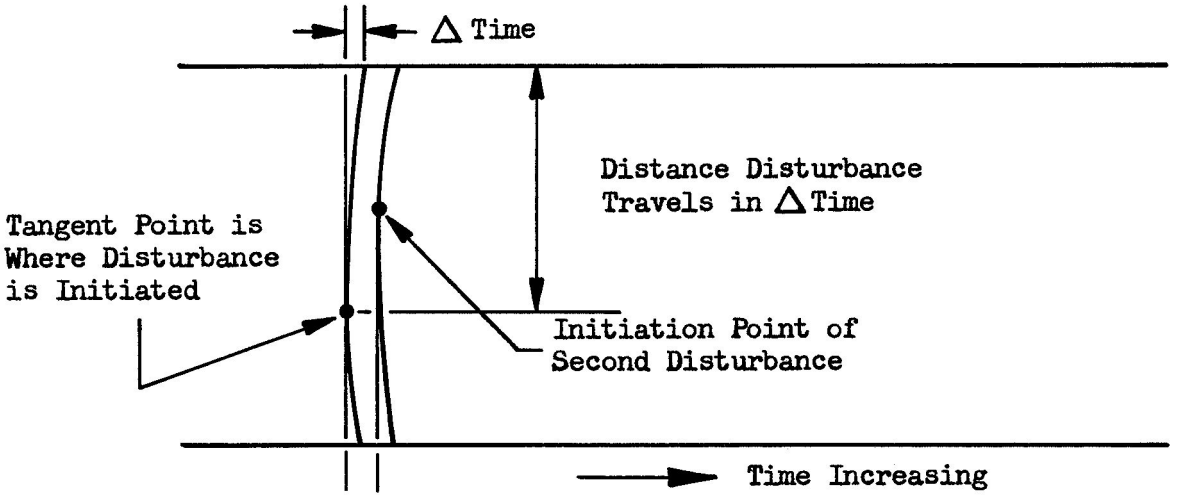

(b) SCHEMATIC OF FILM

$$V = \frac{kD}{\Delta T}$$

where

k = Calibration of film (in. of flow field/in. of film)

D = Film distance

ΔT = Time

Figure 28. Section of Streak Photograph Showing Disturbances and Description of Events.

this film shows that the origin of the initial disturbance varies from 0.01 to 0.1-inch downstream from the jet centerline impingement point. The wave speed was calculated to be 5150 ft/sec. Disturbances of this velocity are generally explosive deflagration waves. Velocities several times that of sonic speeds usually result from detonations.

The origin of the second disturbance varied from about 0.4-inch to 2.7-inches downstream of the impingement point. The location and time of initiation requires that the downstream explosion cannot be caused by the initial wave. However, the results do suggest that the reflected wave from the injector face does intersect the second disturbance at or near the point of its initiation. The fact that there are always two separate disturbances occurring together suggests that the second disturbance is not random but is inextricably tied to the initial disturbance.

Streak photographs were attempted with the other propellants; however, the disturbances did not provide sufficient light for exposure of the film. No other method was attempted to obtain the speed of the Class B or C disturbances.

Presence of Spray Droplets

A secondary goal in the program was to determine the presence or absence of propellant droplets in the downstream combustion zone of the 0.173-inch orifice doublet. Previous holography experiments (Ref. 15) with the identical injector had showed an absence of droplet dispersions in the zone 12-inches downstream of the injector. Results of the holography experiments (Ref. 15) left an uncertainty as to whether the lack of droplet dispersion detail in the downstream region was caused by limited resolution of the holograms or simply the nonexistance of liquid drops at this distance from the injector face.

The identical injector was used in both programs with similar operating conditions. Because the downstream field of view in the present program extended only to 6 inches from the injector face, direct comparison with the

12-inch downstream view (Ref. 15) cannot be made. However, the photographs taken in the subject effort and holograph reproductions reported in Ref. 15 show a great deal of similarity in the spray field view extending 6 inches downstream of the injector. Of particular significance is the correspondence between spray field disturbances noted in both investigations. Still photographs from Ref. 15 show instances where in one case the spray field is uniformily distributed and in another case the spray field is separated into two distinct regions. Such spray field behavior was observed in the subject investigation (13A and 13D). It is possible that the spray field dissimilarities noted in still photographs from the Ref. 15 investigation were random exposures of the cyclic blowapart phenomena characterized by motion picture coverage in the subject effort.

Because the holograph experiments were conducted in a D/V range of 1 to 2 x 10^{-4} sec. these tests would be expected to result in propellant blowapart (Fig. 13). If, in fact, blowapart did occur in holograph experiments (Ref. 15) it would be expected to retard the establishment of a spray field at downstream locations (i.e., without repeated disruption of the spray field by blowapart, the droplet spray dispersion observed at 6 inches downstream might well persist at distances 12 inches downstream of the injector). From these considerations, the absence of droplets in the downstream holographs (12 inches from injector) may have been due in part to upstream spray obliteration resulting from blowapart.

Color Photograph

Early in the program, attempts were made to bring out differential color in the fuel and oxidizer spray droplets formed by the 0.030-inch injection element with NTO/Hz. These attemps were not successful and the colors obtained did not approach those of Ref. 13. This is attributed to a combination of too much back light and insufficient top lighting. No light source as strong as the microflash unit used for top lighting in the referenced investigation was available until virtually the end of the program. In the meanwhile, emphasis was shifted to Fastax coverage and no further serious attempt was made to obtain distinguishable colors.

EFFECT OF PROPELLANT COMBINATION ON BLOWAPART

Experiments were conducted at near identical flow conditions ($\rho_f V_f^2 / \rho_o V_o^2 = 1.0$) using the following propellant combinations:

1. NTO/Hz
2. NTO/50-50
3. IRFNA/UDMH
4. CPF/Hz

As stated in the Results Section of this report, impingement of NTO/Hz, NTO/50-50 and IRFNA/UDMH jets resulted in cyclic blowapart ranging in magnitude from violent (Class A) to rather minor (Class C) disturbances. Impingement of CPF/Hz jets resulted in steady-state separation.

The frequencies of disturbances were determined from the films for each propellant combination. The type (Class A, B or C) and number of disturbances were determined as well as the overall disturbance rate. The results are presented in Table III.

TABLE III. SUMMARY OF DISTURBANCE RATE FOR SEVERAL PROPELLANT COMBINATIONS

Test No.*	Propellant Combination	Dynamic Pressure Ratio, ϕ (F/O)	Blowapart Frequency, pops/sec				Contact Time, D/V $\times 10^{-4}$ sec
			Class A	Class B	Class C	Overall	
32	N_2O_4/N_2H_4	1.02	122			122	2.9
49	IRFNA/UDMH	1.1	0	56	83	139	2.1
45	N_2O_4/50-50	1.04	1	11	100	112	2.7
37	CPF/N_2H_4	1.00	Continuous Stream Separation				2.7

*All tests were conducted at 13.7 psia pressure. The orifice diameters were 0.173-inches and the impingement angle was 60 degrees.

These results show that the specific rate of pops by "class" changed dramatically with propellant combination. It is interesting, however, to note that the overall rate of popping for the first three propellants including all disturbances were quite similar. CPF/Hz; however, resulted in continuous blowapart at these operating conditions.

The results obtained with NTO/Hz, NTO/50-50 and IRFNA/UDMH, and the measured speed of the wave accompanying the disturbance strongly suggests that an explosion is occurring near the initial contact point of the jets. In fact, the streak measurements show that the initial explosion occurs in less than one diameter from the theoretical impingement point of the jet centers. In this

region the propellants are being turbulently mixed and are still acted upon by hydraulic pressure forces. It therefore appears plausible to assume that the explosions are caused by ignition in the mixing region or detonation of explosive intermediates.

In References 18 and 19,it has been established that for NTO and Hz, 50-50, and UDMH, various explosive nitrates are formed. The specific nitrate formed depends upon the fuel. In the Ref. 18 study, shock sensitivity experiments were conducted on various solution strengths of the nitrates to determine detonation strengths and sensitivity. A table listing these results is reproduced in Table IV below.

TABLE IV. EXPLOSIVE CHARACTERISTICS OF NITRATES

Propellant	Nitrate	Impact Sensitivity Ft-lb	TNT Equivalent Wt. Percent
NTO/Hz	HN	4	142
NTO/50-50*	HN(UN)	4(12)**	142(106)
NTO/UDMH*	AN(UN)	119(12)	79(106)

*Those may also have the UDMH Nitrate (UN)
**Numbers in parenthesis refer to UN

These results suggest that the magnitude of the detonations will be greatest for Hz and least with UDMH. This result is of course consistent with those obtained during this program. Other mechanisms causing the observed disturbances are also possible; for example, rapid liquid phase heat release could cause ignition explosions.

In this case it is conceivable that the propellants with the greatest reactivity rate would result in the least amount of mixing, since gas generation inhibits mixing, producing separation as observed for the CPF/Hz propellants. Low reactivity provides large amounts of liquid phase mixing and as a result ignition explosions. The greater the amount of mixed propellant the greater the force of the explosion.

The study by Rodriguez (Ref. 20) suggests that NTO/Hz is relatively less reactive than NTO/UDMH. Based on this observation and the above argument, it would be expected that a greater degree of liquid phase mixing would result with the NTO/Hz propellant combination than with NTO/50-50 or UDMH, and therefore NTO/Hz would produce the greatest explosions. This is also consistent with the results of this study.

A detailed model formulation of either mechanism would be difficult,but certainly quite possible. Evaluation of the models would however, require some studies of the impingement/mixing process in the vicinity of the impingement point.

EFFECTS OF OPERATING CONDITIONS

Variation of Orifice Size

Some limited parametric investigation was conducted employing NTO/Hz propellants to determine the effect of orifice size on blowapart. For this study three different orifice sizes were used, 0.030, 0.072 and 0.173-inch diameter. Significant variation in the character and frequency of blowapart were observed. Cyclic blowapart occurred, for the large orifice (0.173 inch) injector, every 5 to 10 milliseconds, although the frequency was irregular. The disturbances for this element size were Class A in magnitude.

With the intermediate size injector element (orifice diameter 0.072 inch) at approximately the same injection velocities as used with the large element, the overall incidence of explosive disturbances was reduced. In addition the disturbances were approximately equally divided between Class A, B, and C blowapart. For the smallest (0.030 inch) orifice element there was no evidence that any blowapart occurred. Most of this data was with still photographs, however. In the one test where Fastax photographs were obtained with this injector, only about 300 milliseconds of apparent mainstage data was acquired. This showed no blowapart.

The film records for these runs were reduced to determine the rates of pops in all classes and the overall pop rate. The results are presented in Table V.

Since the contact time defined by (D/V) also varies as the diameter is changed, several other tests at differing contact time for the same diameter are also listed in the Table. As shown in Ref. 16 pop rate cannot be correlated with D/V independent of diameter. Consequently the results are not plotted since sufficient data were not taken to define the functional relationship. Comparison of these results (Table V) with Ref. 16 shows reasonable agreement. It should be noted that in the Ref. 16 study the pop rate was determined from

TABLE V. EFFECT OF ORIFICE SIZE AND CONTACT TIME ON BLOWAPART (NTO/Hz PROPELLANTS)

Orifice Size (in.)	ϕ	$(D/V)_f$ 10^{-4} sec	Blowapart Frequency Pops/sec				V_F ft/sec
			Class A	Class B	Class C	Overall	
0.030	1.0	0.45	0	0	0	0	56
0.072	0.85	1.2	35	45	26	106	50
0.072	0.94	0.95	5	15	0	20	63
0.173	1.0	2.9	122	0	0	122	50

pressure traces and may not include all of the disturbances (Class B and C). These low order disturbances probably do not have sufficient strength by the time they have traveled to the measurement location to be distinguishable.

It is obvious from the results listed in Table V that the overall pop rate as well as the proportion of Class A, B, or C disturbances varies when orifice diameter and/or contact time varies.

Consideration of the cyclic nature of the blowapart leads to the realization that the percentage of the time that the propellants form a normal spray fan, i.e., the "mixed" time, varies continuously with the operating conditions. In Fig. 29, the "percent mixed" time for the series of tests is plotted schematically against D/V. Such plots can provide a useful measure of "how much" separation occurs.

In analyzing the film records, the interval between each successive disturbance was also recorded. These data for two test runs are presented in Fig. 30 as a function of the sequential event. This period fluctuated for both runs in apparently random fashion within a bandwidth of 3 to 12 milliseconds.

Variation in Chamber Pressure

Several experiments were conducted at a chamber pressure of about 200 psia. This was accomplished by enclosing the element within a chamber capable of being pressurized by ambient nitrogen gas flowing through the chamber nozzle. In this manner the element flowrate can be maintained constant and increases in chamber pressure are accomplished by variation of the GN_2 flowrate. The objective of the tests was to determine if increasing the chamber pressure would result in steady-state separation as predicted by the blowapart model of Ref. 14. Analysis of the pop rate obtained during the ambient pressure (13.7 psia) and elevated pressure experiments are presented in Table VI.

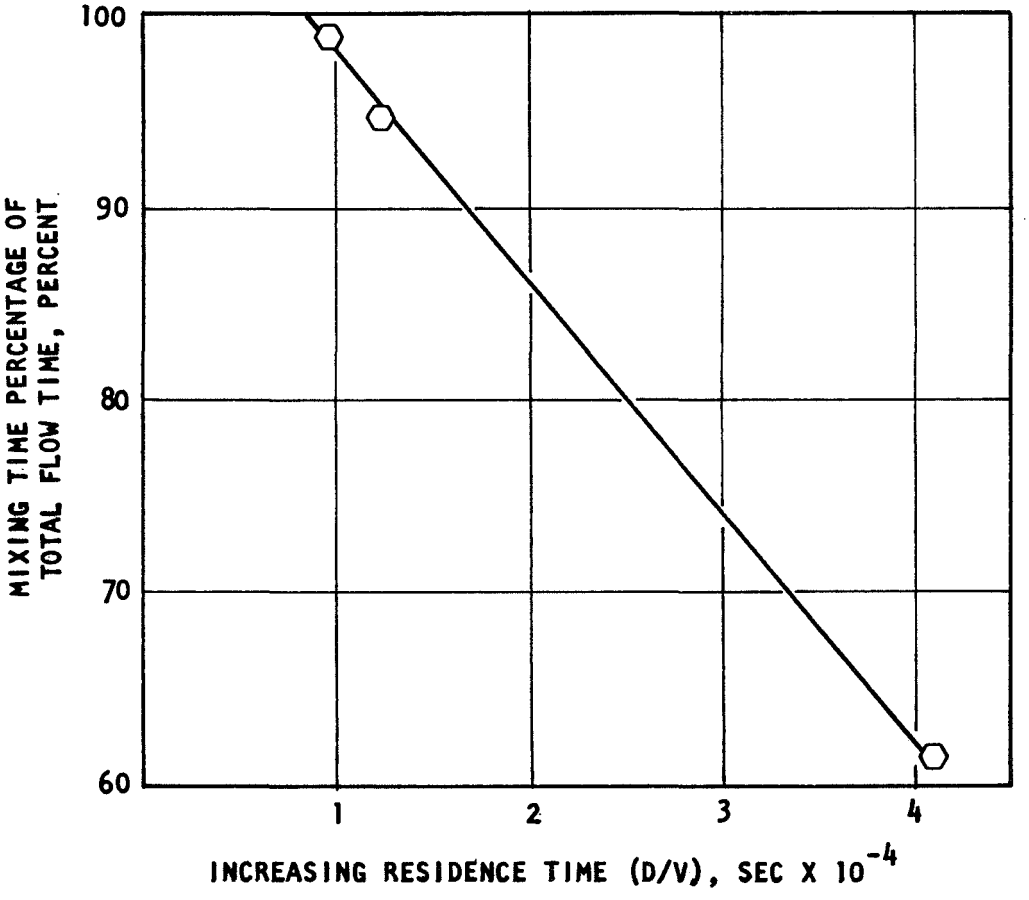

Figure 29. Correlation of Percentage of Time Propellants Mix as a Function of Residence Time (D/V)

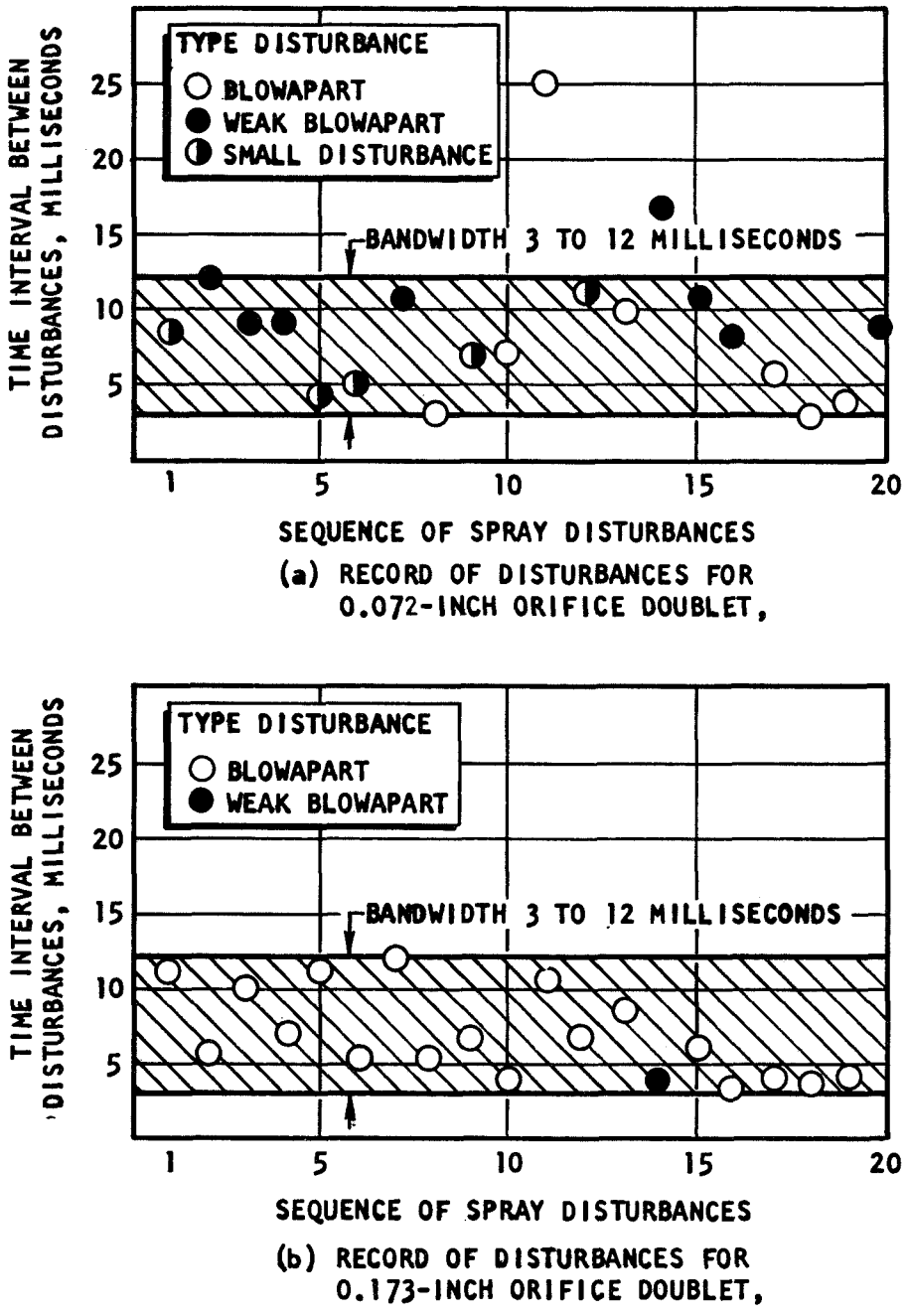

Figure 30. Comparison of Time Interval Between Spray Disturbances for 0.173- and 0.072-Inch Orifice Elements

TABLE VI. CYCLIC BLOWAPART RATES FOR NTO/50-50 IN A PRESSURIZED CHAMBER AND OPEN AIR TEST (D_{ORF} = 0.173 IN.)

Test	Pressure, psia	PR.Ratio(Ø)	Overall Blowapart Rate (Disturbances/Sec)	D/V x 10^{-4} sec
55	225	0.99	124[1]	2.7
46	13.7	1.05	112[2]	2.7

[1] Overall blowapart rate includes Type B and Type C disturbances. No Type A disturbances observed.

[2] Previous "Open Air" data. Overall blowapart rate includes Type A, Type B, and Type C disturbances but with only one (A) type disturbance observed.

As shown in the table, increasing the chamber pressure from 13.7 to 225 psia had only a minor effect on the rate of disturbance increasing from 112 pops/sec at 13.7 psia to 124 pops/sec at 225 psia. These results show that increasing the chamber pressure to 225 psia did not product steady-state separation. It is not known whether further increases in chamber pressure would result in stream separation caused by gas phase reactions, nor what occurs at intermediate pressures.

Variations in Dynamic Pressure Ratio

The impingement/mixing process near the impingement point should influence blowapart. The study of Ref.17 has shown that popping in liquid rocket engines using NTO/50-50 propellants is influenced by the stagnation dynamics of the injection impingement. Clayton's model assumes that two jets impinging at equal dynamic pressures are inherently unstable and that large variations in the impingement characteristics occur near $\rho_F V_F^2 / \rho_o V_o^2 = 1.0$.

In Ref. 17 , it is stated without proof that depending upon the relative dynamic pressures of the two streams several differing flowfields will result downstream of impingement. For example, at a dynamic pressure ratio of one, a double stagnation point will occur at the impingement point, and for jet dynamic pressures which are unequal, the stream having the lower stagnation pressure will stagnate against the other stream. Schematic representatives of those characteristics taken from Ref.17 are reproduced below.

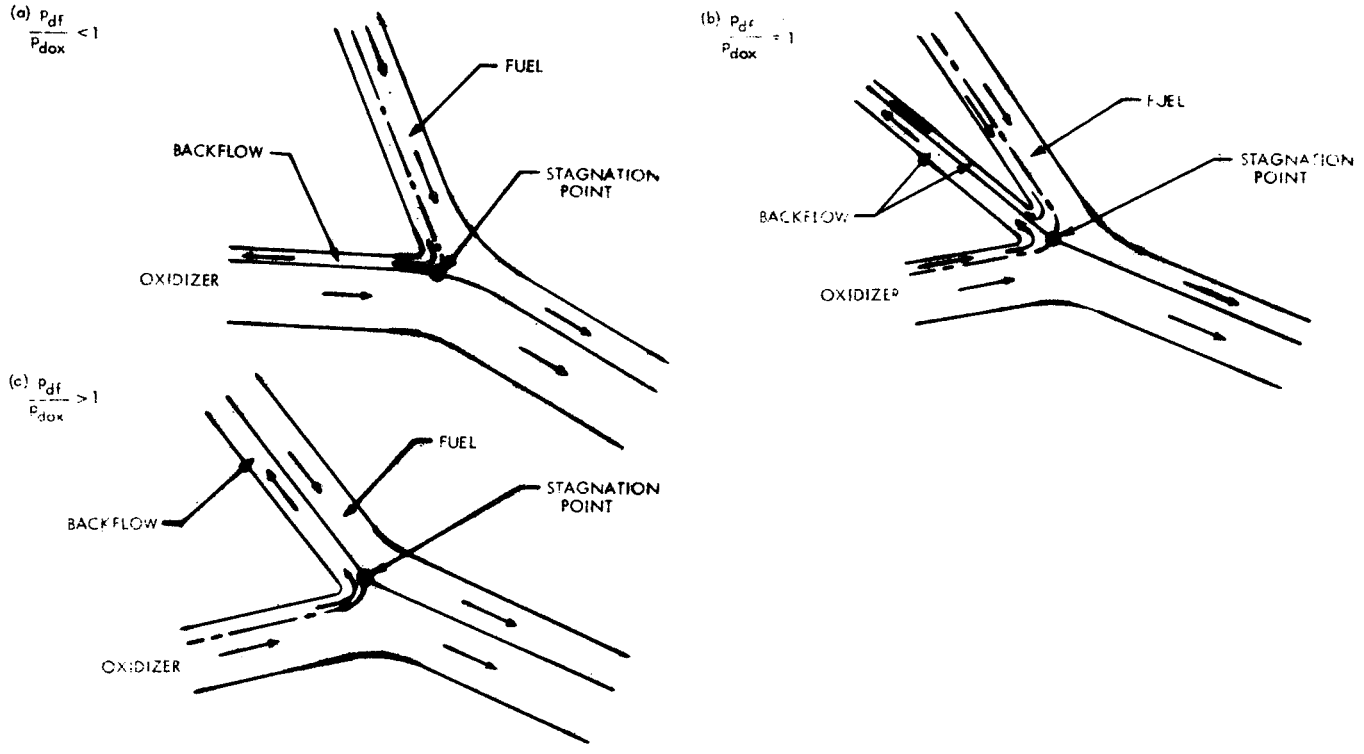

Figure 31 . Schematic Representations of the Impingement Region for Unlike Impinging Free Liquid Jets (Ref. 17)

The results presented in Reference 17, show that, for unlike impinging NTO/50-50 jets, at a unity dynamic pressure ratio the highest rate of pops occurs and that the rate of pops decreases as $\phi \neq 1.0$ (at constant temperature). This study was conducted at 100 psia chamber pressure.

The determination of the effect of dynamic pressure ratio independently of other variables is extremely difficult to ascertain. This is due to dynamic pressure being dependent upon, contact time, geometry, and mixing uniformity. For example, the dynamic pressure ratio is related to contact time as shown in equation (1).

$$\phi = \rho_F V_F^2 / \rho_o V_o^2 = \left[\left(\frac{D}{\bar{V}}_{ox} \right)^2 \Big/ \left(\frac{D}{\bar{V}}_{F} \right)^2 \right] \frac{\rho_F}{\rho_o} \quad ; \quad \text{if } D_o \equiv D_F \tag{1}$$

Dynamic pressure is related to mixing uniformity by:

$$N = \frac{1}{1 + \phi \, D_F / D_o} \tag{2}$$

N = mixing uniformity criteria defined by Rupe.

To maximize mixing N is equal to 0.5. At this condition ϕ is equal to 1.0 (if $D_F = D_o$) and consequently maximum mixing occurs at the identical point where dynamic pressure ratio is unity. It is, therefore, extremely difficult to separate these variables.

During the experiments, variations in dynamic pressure ratio were accomplished for all propellant combinations investigated. This variation was not intended in all cases but occurred due to slight system pressure drop differences

with each propellant combination. A list of the tests and the overall pop rates measured from the high speed movies are presented in Table VII. Note that variations in dynamic pressure ratio, depending upon propellant combination, ranged from about 0.8 to 1.6. In addition, tests were conducted with NTO/50-50 propellants at both ambient (13.7 psia) pressure and at about 200 psia. All tests with the other propellants were conducted at 13.7 psia pressure. Since, unlike the other propellant combination, CPF/Hz exhibited steady-state processes, it is discussed separately.

TABLE VII. EFFECT OF DYNAMIC PRESSURE RATIO ON BLOWAPART

Propellant	ϕ	P_c psia	$(D/V)_F$ 10^{-4} sec	Overall Pop Rate Pop/sec
NTO/50-50 D_j = 0.173	1.5	235	2.2	197
	1.1	225	2.6	133
	0.995	225	2.7	124
	0.96	220	2.7	126
NTO/Hz D_j = 0.173	1.1	13.7	2.8	156
	0.90		3.0	100
	1.26		2.6	124
NTO/50-50 D_j = 0.173	1.04	13.7	2.7	112
IRFNA/UDMH D_j = 0.173	1.1	13.7	2.1	168
	0.97		2.6	115
CPF/Hz D_j = 0.173	1.62	13.7	0.24	Mixing
	0.805		0.23	Continuous Blowapart
	1.35		0.18	

NTO/Hz, NTO/50-50 and IRFNA/UDMH Blowapart Characteristics. The results obtained for the above listed propellant combinations are insufficient to assess the effect of dynamic pressure ratio on blowapart. Although the results are quite limited, they do show, however, that dynamic pressure ratio does influence the resulting pop rate.

CPF/Hz Blowapart Characteristics. The CPF/Hz results are extremely interesting in that as was shown in the photographs of Fig. 26, continuous separation occurred at a dynamic pressure ratio of 0.8 and 1.35 while at ϕ = 1.62 steady-state propellant mixing occurred. The exact value for ϕ where mixing first occurs is not known.

As mentioned above, variations in dynamic pressure ratio cannot be made independently of contact time. The fuel contact times for each test are listed in Table VII. Note that the contact time for the 1.62 dynamic pressure ratio test was no longer than for the other tests. Consequently, if $(D/V)_F$ is the appropriate characteristic contact time then these results would suggest that mixing could not have resulted because of differences in contact time (i.e., longer contact time should result in a greater propensity to separate the jets because of gas phase reactions).

CONCLUSIONS

Prior to this investigation, the prevalent view of reactive stream separation was that it was a quasi-steady process. This is reflected in the experimental approach used by essentially all previous experimenters, e.g., still photography. The same view is evident also in all published attempts at analytical modeling. The data obtained in this program present a break-through in investigation of reactive stream separation phenomena in that the cyclic nature of the blowapart process is so clearly illustrated for the propellants NTO/Hz, NTO/50-50, and IRFNA/UDMH. In addition, a continuous, or quasi-steady separation was observed with the propellants CPF/Hz. Both cyclic and steady-state blowapart can result in significant physical separation of fuel and oxidizer spray.

Cyclic blowapart was not observed with CPF/Hz at all. It was encountered with each of the other three propellant combinations tested. The phenomenon may be described in general to result from repeated explosions which disrupt the spray fan and drive the jets apart, thereby producing temporary physical separation of fuel and oxidizer. In between these explosions a normal spray fan forms in which the propellants are not separated. The strength of the cyclic blowapart was variable ranging from cases where the explosion obliterated the entire spray fan (Class A), or portions of the spray (Class B), to mere "puffs" (Class C).

Among those propellants which produced cyclic blowapart, propellant combination was found to have a strong effect on the average blowapart strength. For example, at equivalent operating conditions (dynamic pressure ratio 1.0, orifice diameters = 0.173 inch) NTO/Hz, experienced almost exclusively the violent (Class A) blowapart while NTO/50-50 and IRFNA/UDMH produced primarily Class B and C blowapart. The average frequency of explosion of all types was however, approximately constant.

Operating conditions influenced both the frequency and strength of cyclic blowapart. With NTO/Hz reduction of the orifice diameter from 0.173 inch to 0.072 inch reduced both the strength and frequency of the explosions. With 0.030-inch diameter orifices no blowapart was seen under the conditions tested. Increased injection velocity (for 0.072-inch orifices) substantially reduced the occurrence of blowapart. Increase of the operating pressure from 13.7 psia to about 200 psia with the system NTO/50-50 had little effect on the cyclic blowapart. Changes in dynamic pressure ratio over the limited range tested (0.9 to 1.5) produced some variation in the number of explosions per unit time, but did not alter the character of blowapart. Under no test conditions was a quasi-steady stream separation encountered with NTO/Hz, NTO/50-50, or IRFNA/UDMH.

The results with NTO/Hz, NTO/50-50, and IRFNA/UDMH indicate that a new and different mechanism may be needed to explain the cyclic explosions which occur with the N_2O_4 type oxidizer. Both the existence of explosive intermediates (e.g., hydrazine nitrate) and ignition of pockets of pre-mixed liquid propellants offer possible explanations of cyclic blowapart.

With CPF/Hz, a distinct continuous stream separation was found to exist and the forces generated by propellant reaction and gasification at the impingement region were sufficient to cause the individual downstream propellant sprays to diverge by about 60 degrees. These results were seen with both 0.173-inch and .026-inch orifice injectors. With the smaller orifice sizes, however, it was found possible to eliminate stream separation by increasing the dynamic pressure ratio ($\rho_f V_f^2/\rho_o V_o^2$) from near unity to 1.62.

In light of these results it is quite possible that the gas phase separation blowapart mechanisms suggested by Kushida and Houseman may apply to CPF/Hz. Physically the type of blowapart seen with these propellants conforms with that envisioned on the basis of that model. Furthermore, the apparent increased tendency to separate at near unity dynamic pressure ratio is consistent with such a mechanism.

A final conclusion is that high-speed motion picture photography as applied in the subject program with appropriate back lighting, top lighting, and other photographic techniques is an extremely valuable method for experimental investigation of blowapart.

RECOMMENDATIONS

Experimental studies conducted during the subject program provided a more complete understanding regarding the manner in which the phenomena termed blowapart occurs. Continued use of this experimental technique to further elucidate blowapart is strongly recommended. The following areas of investigation are recommended for near future effort:

1. An effort should be made to define the mechanisms causing cyclic blowapart. Results of the subject program showed that the interpretation of blowapart with hydrazine type fuels and N_2O_4 or IRFNA oxidizers as only a quasi-steady state phenomena is invalid. Therefore, a need exists to define and describe a new model for blowapart.

2. Together with the definition of the cyclic blowapart mechanisms, a concurrent effort to describe the pertinent parametric effects of test conditions on cyclic blowapart in a detailed manner should be undertaken. The study should be broad enough to clearly show the validity of any proposed blowapart model.

3. Further experimental tests should be conducted with CPF/Hz to determine the influence of operating pressure, temperature and dynamic pressure ratio over a range of orifice diameter to injection velocity ratios (D/V) in order to more conclusively confirm the applicability of the gas phase reaction mechanism of reactive stream separation proposed by Kushida and Houseman.

REFERENCES

1. Elverum, G. W., Jr. and P. Standhammer: The Effect of Rapid Liquid-Phase Reactions on Injector Design and Combustion in Rocket Motors, Progress Report 30-4, Jet Propulsion Laboratory, Pasadena, California, August 1959.

2. Johnson, B. H.: An Experimental Investigation of the Effects of Combustion on the Mixing of Highly Reactive Liquid Propellants, Technical Report 32-689, Jet Propulsion Laboratory, Pasadena, California, July 1965.

3. Stanford, H. B. and W. H. Tyler: "Injector Development" Supporting Research and Advanced Development, Space Programs Summary 37-51, Vol. IV, Jet Propulsion Laboratory, Pasadena, California, February 1965, p. 192.

4. Stanford, H. B.: "Injector Development," Supporting Research and Advanced Development, Space Programs Summary 37-36, Vol. IV, Jet Propulsion Laboratory, Pasadena, California, December 1965, p. 174.

5. Riebling, R. W.: "Injector Development: Impinging Sheet Injector," Supporting Research and Advanced Development, Space Program Summary 37-45, Vol. IV, Jet Propulsion Laboratory, Pasadena, California, 30 June 1967.

6. Riebling, R. W.: "Injector Development; Stream Separation Experiments," Supporting Research and Advanced Development, Space Program Summary 37-45, Vol. 4, Jet Propulsion Laboratory, Pasadena, California, 30 June 1967.

7. Woodward, J. W.: "Combustion Effects in Sprays," Supporting Research and Advanced Development, Space Programs Summary 37-36, Vol. IV, Jet Propulsion Laboratory, Pasadena, California, December 1965.

8. Burrows, M. C. (NASA-Lewis Research Center): Mixing and Reaction Studies of Hydrazine and Nitrogen Tetroxide Using Photographic and Spectral Techniques, AIAA Paper No. 67-107, presented at the AIAA 5th Aerospace Science Meeting, New York, N. Y., January 1967.

9. Lawver, B. R. and B. P. Breen: Hypergolic Stream Impingement Phenomena-Nitrogen Tetroxide/Hydrazine, NAS-CR-72444, Dynamic Science Division, Marshall Industries, Monrovia, California, October 1968.

10. Zung, L. B. (Dynamic Science Corporation, Monrovia, California): Hypergolic Impingement Mechanisms and Criteria for Jet Mixing or Separation, presented at the 6th ICRPG Liquid Propellant Combustion Instability Conference, 9-11 September 1969.

11. R-7223: Reactive Stream Impingement, Rocketdyne, a Division of North American Rockwell Corporation, 29 September 1967.

12. Houseman, J. (Jet Propulsion Laboratory, Pasadena, California): Jet Separation and Optimum Mixing for an Unlike Doublet, presented at the 6th ICRPG Liquid Propellant Combustion Instability Conference, 9-11 September 1969.

13. Campbell, D. T., "Photographic Study of Hypergolic Propellant Stream Blowapart," Presented at AIAA Joint Specialists Conf., San Diego, Calif. 1970.

14. Kushida, R. and J. Houseman: Criteria for Separation of Impinging Streams of Hypergolic Propellants, JPL Report WSCI-67-38, 1967.

15. Wuerker, R. F., B. J. Matthews and R. A. Briones (TRW Systems Group): Producing Holograms of Reacting Sprays in Liquid Propellant Rocket Engines, TRW Report 68.4712.2-024, 31 July 1968.

16. Lee, A., and J. Houseman: Popping Phenomena with N_2O_4/N_2H_4 Injectors, presented at the Western States Section meeting of the Combustion Institute on Stable Combustion of Liquid Propellants, JPL, October 26 - 27, 1970.

17. Clayton, R.: Experimental Observations Relating the Inception of Liquid Rocket Engine Popping and Resonant Combustion to the Stagnation Dynamics of Injection Impingement, TR 32-1479, JPL, 15 Dec. 1970.

18. Perlee, H., et al: Hypergolic Ignition and Combustion Phenomena in the Propellant System Aerozine - 50/N_2O_4, Final Report No. 4019, Bureau of Mines, Pittsburgh, Pa., April 1, 1965 to March 31, 1967.

19. Friedman, R., et al: A Study of Explosions Induced by Contact of Hydrazine-type Fuels with Nitrogen Tetroxide, Tech. Doc. Rpt. ASD-TDR-62-685, Atlantic Research Corp. September 1962.

20. Rodriguez, S., A. Axworthy: Liquid Phase Reactions of Hypergolic Propellants, R-8374, Rocketdyne, a Division of North American Rockwell, Canoga Park, California, December 1970.

APPENDIX A

FILM RECORD OF BLOWAPART PROCESS

Selected fastax tests of the 0.173-inch orifice injector firings were assembled in a film strip to provide a movie depicting the propellant blowapart process. A description of the test hardware and test conditions is also presented in the film. Sequence of tests shown in the film clip is listed below:

1. Overall view of spray field viewed 30 degrees off axis and 15 feet downstream of injector shown pulsating flame light (Run 9-25-13)
2. Fan view of spray fan, view from injector face to 4 inches downstream (Run 10-21-5, Fig. 10)
3. Edge view of spray fan, view from injector face to 4 inches downstream (Run 9-25-13, Fig. 9)
4. Edge view of spray fan, view from 2 to 6 inches downstream of injector face (Run 10-21-1, Fig. 11)
5. Fan view of spray fan, view from 2 to 6 inches downstream of injector face (Run 10-21-4, Fig. 12)

In addition a film sequence showing the effect of propellant combination on blowapart for the 0.173-inch-diameter element was assembled.

The films may be obtained, on a loan basis, by contacting the Jet Propulsion Laboratory, Pasadena, California, Attention of the Project Manager, J. H. Rupe.

APPENDIX B

DISTRIBUTION LIST FOR FINAL REPORT

Copies	Recipient	Designee
	NASA Headquarters Washington, D. C. 20546	
1	Contracting Officer	
1	Patent Office	
	NASA Lewis Research Center 21000 Brookpark Rd. Cleveland, Ohio 44135	
1	Office of Technical Information	
1	Dr. R. J. Priem	
	NASA Manned Spacecraft Center Houston, Texas 77001	
1	Office of Technical Information	
	NASA Marshall Space Flight Center Huntsville, Alabama 35812	
1	Technical Library	
1	Keith Chandler, R-P+VP-PA	
	NASA Pasadena Office 4800 Oak Grove Drive Pasadena, California 91103	
1	Patents and Contracts Management	
	Jet Propulsion Laboratory 4800 Oak Grove Drive Pasadena, California 91103	
2	Jack H. Rupe	
3	Chief, Liquid Propulsion Technology RPL Office of Advanced Research and Technology NASA Headquarters Washington, D. C. 20546	
1	Director, Technology Utilization Division Office of Technology Utilization NASA Headquarters Washington, D. C. 20546	
25	NASA Scientific and Technical Information Facility P.O. Box 33 College Park, Maryland 20740	

Copies	Recipient	Designee
1	Director, Launch Vehicles and Propulsion, SV Office of Space Science and Applications NASA Headquarters Washington, D. C. 20546	
1	Director, Advanced Manned Missions, MT Office of Manned Space Flight NASA Headquarters Washington, D. C. 20546	
1	Mission Analysis Division NASA Ames Research Center Moffett Field, California 24035	

NASA FIELD CENTERS

1	Ames Research Center Moffett Field, California 24035	Alberta Alksne N-203-9
2	Lewis Research Center 21000 Brookpark Road Cleveland, Ohio 44135	E. W. Conrad Allen J. Metzler
1	Goddard Space Flight Center Greenbelt, Maryland 20771	Merland L. Moseson Code 620
2	Jet Propulsion Laboratory California Institute of Technology 4800 Oak Grove Drive Pasadena, California 91103	Henry Burlage, Jr. Propulsion Div. 38
3	Langley Research Center Langley Station Hampton, Virginia 23365	Ed Cortwright Director
2	Lewis Research Center 21000 Brookpark Road Cleveland, Ohio 44135	Dr. Abe Silverstein Director
2	Manned Spacecraft Center Houston, Texas 77001	J. G. Thibodaux, Jr. Chief, Prop. + Power Div.
2	John F. Kennedy Space Center, NASA Cocoa Beach, Florida 32031	Dr. Kurt. H. Debus

GOVERNMENT INSTALLATIONS

Copies	Recipient	Designee
1	Aeronautical Systems Division Air Force Systems Command Wright-Patterson Air Force Base Dayton, Ohio 45433	D. L. Schmidt Code ASRCNC-2
1	Arnold Engineering Development Center Arnold Air Force Station Tullahoma, Tennessee 37388	Dr. H. K. Doetsch
1	Bureau of Naval Weapons Department of the Navy Washington, D. C. 20546	J. Kay RTMS-41
1	Defense Documentation Center Headquarters Cameron Station, Building 5 5010 Duke Street Alexandria, Virginia 22314 Attn: LIGIA	
1	Picatinny Arsenal Dover, New Jersey 87851	I. Forsten, Chief Liquid Propulsion Laboratory
2	Air Force Rocket Propulsion Laboratory Research and Technology Division Air Force Systems Command Edwards, California 93523	RPRPO/Mr. H. Main
1	U. S. Army Missile Command Redstone Arsenal 35809	Mr. Walter Wharton
1	U. S. Bureau of Mines 4200 Forbes Ave. Pittsburgh, Penn. 15213	Mr. Henry Perlee
1	U. S. Naval Ordnance Test Station China Lake California 93557	D. Couch
1	Air Force Office of Scientific Research 1400 Wilson Blvd. Arlington, Virginia 22208	B. T. Wolfson

CPIA

Copies	Recipient	Designee
1	Chemical Propulsion Information Agency Applied Physics Laboratory 9821 Georgia Avenue Silver Spring, Maryland 20810	Tom Reedy

INDUSTRY CONTRACTORS

1	Aerojet-General Corporation P.O. Box 285 Azusa, California 91703	W. L. Rogers
1	Space Division Aerojet-General Corporation 9200 East Blair Dr. El Monte, California 91734	S. Machlawski
1	Aerospace Corporation 2400 East El Segundo Boulevard P.O. Box 95095 Los Angeles, California 90045	O. W. Dykema
1	Atlantic Research Corporation Edsall Road and Shirley Highway Alexandria, Virginia 22314	Dr. Ray Friedman
1	Bell Aerosystems Company P.O. Box 1 Buffalo, New York 14240	W. M. Smith
1	Boeing Company P.O. Box 3707 Seattle, Washington 93124	J. D. Alexander
1	Wright Aeronautical Division Curtiss-Wright Corporation Wood-Ridge, New Jersey 07075	G. Kelley
1	Research Center Fairchild Hiller Corporation Germantown, Maryland	Ralph Hall
1	Missile and Space Systems Center General Electric Company Valley Forge Space Technology Center P.O. Box 8555 Philadelphia, Pa.	F. Mezger F. E. Schultz

Copies	Recipient	Designee
1	Grumman Aircraft Engineering Corp. Bethsage, Long Island New York 11714	Joseph Gavin
1	Honeywell, Inc. Aerospace Div. 2300 Ridgway Rd. Minneapolis, Minn.	Mr. Gordon Harms
1	Hughes Aircraft Co. Aerospace Group Centinela and Teale Streets Culver City, California 90230	E. H. Meier V.P. and Div. Mgr., Research Dev. Div.
1	Arthur D. Little, Inc. 20 Acorn Park Cambridge, Massachusetts 02140	Library
1	Lockheed Propulsion Company P.O. Box 111 Redlands, California 92374	H. L. Thackwell
1	The Marquardt Corporation 19555 Saticoy Street Van Nuys, California 91403	Howard McFarland
1	Denver Division Martin Marietta Corporation P.O. Box 179 Denver, Colorado 20201	Dr. Morganthaler A. J. Kullas
1	Astropower Laboratory McDonnell-Douglas Aircraft Company 2121 Paularino Newport Beach, California 92063	Dr. George Moo Director, Research
1	Missile and Space Systems Division McDonnell-Douglas Aircraft Company 3000 Ocean Park Boulevard Santa Monica, California 90406	Mr. R. W. Hallet Chief Engineer Adv. Space Tech.
1	Space & Information Systems Division North American Rockwell 12214 Lakewood Boulevard Downey, California 90241	Library

Copies	Recipient	Designee
1	Rocketdyne Library 596-308 6633 Canoga Avenue Canoga Park, California 91304	Dr. R. J. Thompson S. F. Iacobellis
1	Northrop Space Laboratories 3401 West Broadway Hawthorne, California 90250	Dr. William Howard
1	Stanford Research Institute 333 Ravenswood Avenue Menlo Park, California 94025	Dr. Gerald Marksman
1	TRW Systems Group TRW Incorporated One Space Park Redondo Beach, California 90278	G. W. Elverum
1	Reaction Motors Division Thiokol Chemical Corporation Denville, New Jersey 07832	Dwight S. Smith
1	Research Laboratories 400 Main Street East Hartford, Conn. 06106	Erle Martin
1	United Technology Center 537 Methilda Avenue P.O. Box 358 Sunnyvale, California 94068	Dr. David Altman
1	Rocketdyne A Div. of North American Rockwell 6633 Canoga Avenue Canoga Park, California 91304	R. B. Lawhead
1	Pratt & Whitney Aircraft Florida Research & Development Ctr. P.O. Box 3891 West Palm Beach, Florida 33402	G. D. Lewis
1	Defense Research Corporation P.O. Box 3587 Santa Barbara, California 93105	J. Gray
1	Airesearch Mfg. Co. 8351 Sepulveda Blvd. Los Angeles, California 90002	Dr. George Sotter

Copies	Recipient	Designee
1	Aerojet-General Corporation P.O. Box 1947 Sacramento, California 95808	R. S. Valentine
1	Dynamic Science 2400 Micheleon Drive Irvine, California 92584	Dr. B. P. Breen
1	Mathematical Applications Group, Inc. 138 So. Broadway White Plains, New York 10805	Dr. S. Z. Burnstein

UNIVERSITIES

1	Ohio State University Dept. of Aeronautical Eng. Columbus, Ohio 43210	R. Edse
1	Pennsylvania State Univ. Mech. Engineering Dept. 207 Mechanical Engineering Blvd. University Park, Pa 18902	G. M. Faeth
1	University of Southern California Dept. of Mech. Eng. University Park Los Angeles, California 98007	M. Gerstein
1	Princeton University Forrestal Campus Guggenheim Laboratories Princeton, New Jersey 08540	D. Harrje
1	University of Wisconsin Mechanical Eng. Dept. 1513 University Ave. Madison, Wisconsin 53705	P. S. Myers
1	University of Michigan Aerospace Engineering Ann Arbor, Michigan 43104	J. A. Nicholls
1	University of California Dept. of Chem. Eng. 8181 Eicheverry Hall Berkeley, California 94720	A. K. Oppenhiem R. Sawyer

Copies	Recipient	Designee
1	Purdue University School of Mech. Eng. LaFayette, Indiana 47907	J. R. Osborn
1	Sacramento State College Engineering Division 60000 J. Street Sacramento, California 95619	E. H. Reardon
1	Illinois Institute of Tech Rm. 200 M. H. 3300 S. Federal Street Chicago, Illinois 50618	T. P. Torda
1	Polytechnic Institute of Brooklyn Graduate Center Route 110 Farmingdale, New York	V. D. Agosta
1	Georgia Inst. of Tech. Atlanta, Georgia 30332	B. T. Zinn
1	University of Denver Research Institute Denver, Colorado	W. H. McLain
1	New York University Dept. of Chem. Eng. University Heights New York 53, New York	Leonard Dauerman
1	The Johns Hopkins University Applied Physics Laboratory 2821 Georgia Avenue Silver Spring, Maryland 20910	W. G. Beel
1	Dartmouth University Hanover, New Hampshire 03755	P. D. McCormack
1	Princeton University Forrestal Campus Guggenheim Laboratories Princeton, New Jersey 08540	I. Glassman

FOREIGN UNIVERSITIES

Copies	Recipient	Designee
1	The University of Sheffield Dept. of Fuel Technology St. George's Square Sheffield 1, Yorks, England	Mr. J. Swithenbank
1	Motorlar Enstitusu Professor Zubeyir Demirque Director of Engine Institute Istanbul - Gumussuyu	
1	Instituto Nacional De Teorica Aeroespacial Carlos Sanchez-Yarifa Serrano 43 Madrid, Spain	